

**NAM**

# **Groningen Field Review 2015 Subsurface Dynamic Modelling Report**

---

**NAM Reservoir Engineering Team: Ulan Burkotov, Henk van Oeveren &  
Per Valvatne**

Datum June 2016

Editors Jan van Elk & Dirk Doornhof



## General Introduction

The subsurface model of the Groningen field was built and is used to model the first step in the causal chain from gas production to induced earthquake risk. In essence, it models the pressure response in the gas bearing formations to the extraction of gas and water.

The reservoir model of the Groningen field was built in 2011 and 2012 and has a very detailed model of the fault zones in the field, to support studies into induced earthquakes in the field. The model has been used to support Winningsplan 2013 and has since then been continuously improved. This report describes these improvements and in particular the effort to obtain the history match.

The pressure in the field is an important driver for compaction and therefore subsidence. Compaction in turn affects stress and strain and is therefore of importance for mechanism inducing earthquakes. The model therefore has an important role in the optimization of the gas withdrawal from the reservoir to reduce seismicity.

The reservoir model has been reviewed by an independent consultant SGS Horizon. An extensive assurance review with opinion letter have been prepared by SGS Horizon. Both of these are available on:

[www.namplatform.nl/feiten-en-cijfers/onderzoeksrapporten](http://www.namplatform.nl/feiten-en-cijfers/onderzoeksrapporten)





**NAM**

<b>Title</b>	<b>Groningen Field Review 2015 Subsurface Dynamic Modelling Report</b>		<b>Date</b>	June 2016
			<b>Initiator</b>	NAM
<b>Author(s)</b>	NAM Reservoir Engineering Team: Ulan Burkitov, Henk van Oeveren & Per Valvatne	<b>Editors</b>	Jan van Elk Dirk Doornhof	
<b>Organisation</b>	NAM	<b>Organisation</b>	NAM	
<b>Place in the Study and Data Acquisition Plan</b>	<p><u>Study Theme: Prediction Reservoir Pressure based on gas withdrawal</u></p> <p><u>Comment:</u> The subsurface model of the Groningen field was built and is used to model the first step in the causal chain from gas production to induced earthquake risk. It models the pressure response in the gas bearing formations to the extraction of gas and water. The reservoir model of the Groningen field was built in 2011 and 2012 and has a very detailed model of the fault zone in the field to support studies into induced earthquakes in the field. The model has been used to support Winningsplan 2013 and has since then been continuously improved. This report describes these improvements and in particular the effort to obtain the history match.</p> <p>The pressure in the field is an important driver for compaction and therefore subsidence. Compaction in turn affects stress and strain and is therefore of importance for mechanism inducing earthquakes. The model therefore has an important role in the optimization of the gas withdrawal from the reservoir to reduce seismicity.</p>			
<b>Directly linked research</b>	<ol style="list-style-type: none"> <li>1. Technical Addendum to Winningsplan 2013.</li> <li>2. Opinion Letter: "Independent Review of Groningen Subsurface Modeling" by SGS Horizon.</li> <li>3. Report; "Independent Review of Groningen Subsurface Modelling – Update for Winningsplan 2016" by SGS Horizon.</li> </ol>			
<b>Used data</b>	Sub-surface data from the Groningen field; open-hole logs, core data, pressure data, production data etc.			
<b>Associated organisation</b>	Independent consultant SGS Horizon			
<b>Assurance</b>	The model has been reviewed by an independent consultant SGS Horizon.			

Restricted

EP201603238100

**Groningen Field Review 2015**  
**Subsurface Dynamic Modelling Report**  
by  
**Burkitov, Ulan (NAM-UPO/T/DL)**  
**Van Oeveren, Henk (NAM-UPO/T/DL)**  
**Valvatne, Per (NAM-UPO/T/DL)**

<b>Name</b>	<b>Ref. Indicator</b>	<b>Role</b>	<b>Date</b>	<b>Signature</b>
Jelgersma, Frank	NAM-UPO/T/DL	Discipline Lead Reservoir Engineering Onshore NL		
Pardoel, Frank	NAM-UPO/T/DG	Discipline Lead Production Geology Onshore NL		
Kelder, Oscar	NAM-UPO/T/DL	Discipline Lead Petrophysics Onshore NL		
Van Boom, Ruud	NAM-UPO/T/DL	Discipline Lead Geophysics Onshore NL		
Svendsen, Grete	NAM-UPO/T/GW	Discipline Lead Production Technology Groningen		
Doornhof, Dirk	NAM-PTU/E/Q	Discipline Lead Geomechanics		

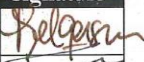
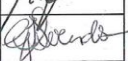
This document is classified as Restricted. Access is allowed to Shell personnel, designated Associate Companies and Contractors working on Shell projects who have signed a confidentiality agreement with a Shell Group Company. 'Shell Personnel' includes all staff with a personal contract with a Shell Group Company. Issuance of this document is restricted to staff employed by a Shell Group Company. Neither the whole nor any part of this document may be disclosed to Non-Shell Personnel without the prior written consent of the copyright owners.

Further electronic copies can be obtained from the Global Information Centre.

EP201603238100

Restricted

**Groningen Field Review 2015**  
**Subsurface Dynamic Modelling Report**  
 by  
**Burkitov, Ulan (NAM-UPO/T/DL)**  
**Van Oeveren, Henk (NAM-UPO/T/DL)**  
**Valvatne, Per (NAM-UPO/T/DL)**

Name	Ref. Indicator	Role	Date	Signature
Jelgersma, Frank	NAM-UPO/T/DL	Discipline Lead Reservoir Engineering Onshore NL	30-3-16	
Pardoel, Frank	NAM-UPO/T/DG	Discipline Lead Production Geology Onshore NL	30/3/16	
Kelder, Oscar	NAM-UPO/T/DL	Discipline Lead Petrophysics Onshore NL	30-3-16	
Van Boom, Ruud	NAM-UPO/T/DL	Discipline Lead Geophysics Onshore NL	30-3-16	
Svendsen, Grete	NAM-UPO/T/GW	Discipline Lead Production Technology Groningen	30-3-16	
Doornhof, Dirk	NAM-PTU/E/Q	Discipline Lead Geomechanics	30-3-16	

This document is classified as Restricted. Access is allowed to Shell personnel, designated Associate Companies and Contractors working on Shell projects who have signed a confidentiality agreement with a Shell Group Company. 'Shell Personnel' includes all staff with a personal contract with a Shell Group Company. Issuance of this document is restricted to staff employed by a Shell Group Company. Neither the whole nor any part of this document may be disclosed to Non-Shell Personnel without the prior written consent of the copyright owners.

Further electronic copies can be obtained from the Global Information Centre.

## Executive summary

### Study objectives

Static and dynamic modelling of 2015 is driven by the Groningen 2016 revised production plan (nl. Winningsplan), which is to be submitted on 1<sup>st</sup> April 2016. The high level diagram below shows the time schedule as well as the main work streams associated with this Winningsplan, see Figure 1. The new model will directly contribute to the Groningen Seismic Hazard and Risk Assessment (HRA) by providing historical and predicted reservoir pressures for different production scenarios. In addition the model will continue to be used for the business forecasts.

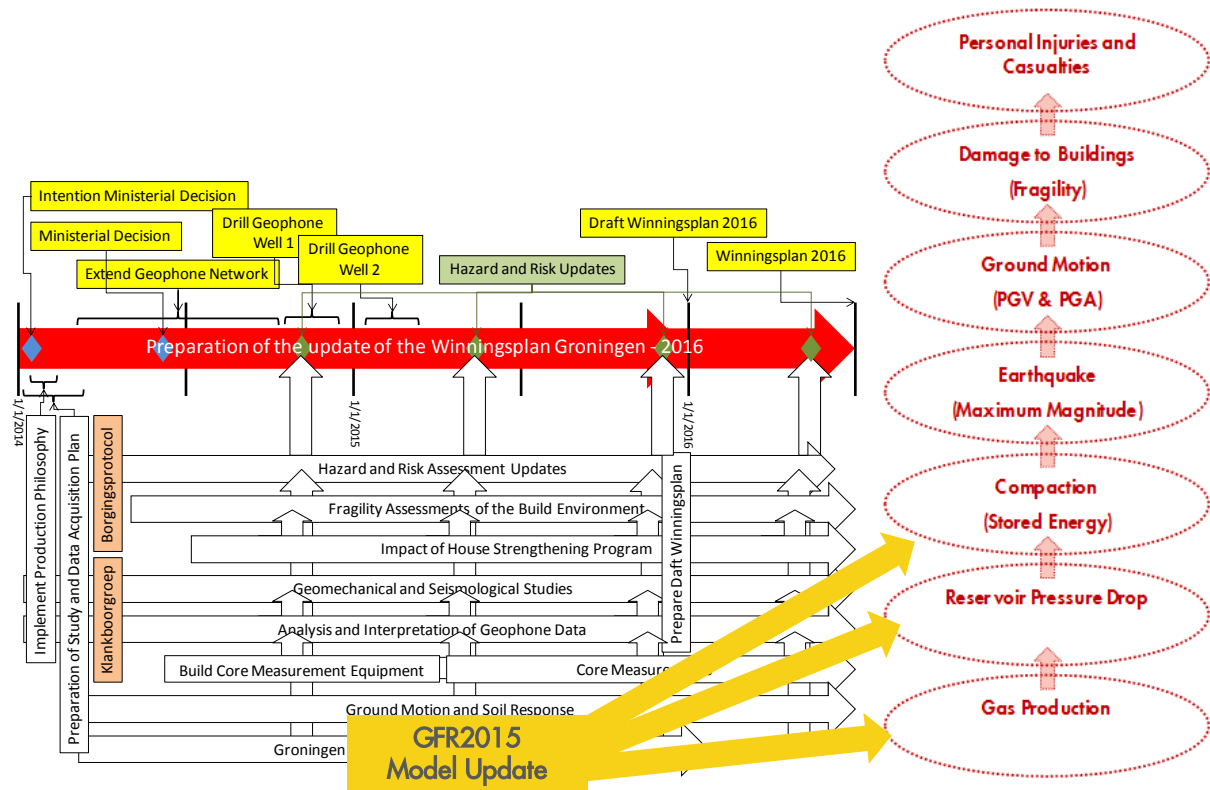


**Figure 1 High level workflow diagram. Workstreams which lead to the preparation of Groningen Winningsplan 2016.**

For the Technical Addendum to the Winningsplan Groningen 2013 two subsurface realisations of the Groningen field were used. These models were labelled as G1 and G2:

- The G2 model was the best history matched dynamic model with respect to the reservoir pressure data (SPTIG and RFI) and gas-water contact movement (PNL logs). An update of this G2 model (GFR2013) has been used for business planning and reserves reporting purposes. The G2 model assumed weak aquifer support to the north and had a mismatch with subsidence data in the north-western part of the model area.
- An alternative G1 realization had moderately strong aquifer support to the north and showed improved subsidence match but with less good match to gas-water contact movement.

The main objectives of 2015 static and dynamic modelling efforts are as follows:

- To use the dynamic model in Winningsplan 2016
- To use the dynamic model in the Seismic Hazard and Risk Assessment process

And the secondary objectives are:

- Business planning purposes
- Annual Reporting of Petroleum Resources (ARPR)
- Development Opportunities

The main reasons for initiating the Groningen Field Review 2015 (GFR2015) and replacing the existing model are:

- The need for a single dynamic model that not only matches pressure and water contact movement, but also existing Groningen subsidence data.
- Larger model area to allow for improved pressure and subsidence prediction to the west of the field, including the city of Groningen.
- Local reservoir pressure matches (at the cluster level) should be improved to ensure good well capacity prediction (gas rate vs. tubing-head pressure).
- Aquifer behaviour resulting in water rise was not adequately well matched.
- New data have been acquired since the last model update.

In addition to the reasons above, there were a number of comments on the previous static and dynamic model from external reviewers like TNO and SGS Horizon, that have now been incorporated in the new model.

### **Main features of the study**

In collaboration with the geomechanics team it was decided to extend the existing grid boundaries approximately 8-10 km to the West and 5 km to the South, with the main reasons being:

- The previous model was focused mostly on the Groningen closure since the objectives of the model were different. However, for geomechanical studies like prediction of subsidence, the area outside of the Groningen closure is also of great importance.
- Subsidence in the greater Groningen area, including under the city of Groningen, is not only affected by pressure depletion in the main Groningen gas field, but also that in adjacent aquifers and surrounding Land asset fields. To improve the forecast of subsidence in this greater area, an expanded model of the subsurface is required.
- Having historical and forecasted pressure values available on an extended numerical grid that includes the surrounding aquifers, allows for more flexibility in geomechanical calculations. This is in contrast to a model where pressure in the aquifer is modelled using analytical correlations.

The new extended grid thus includes the following Land Asset fields:

1. Annerveen-Veendam
2. Bedum
3. Bedum South
4. Midlaren
5. Rodewolt
6. Usquert
7. Zuidwending East
8. Feerwerd
9. Warffum
10. Rodewolt
11. Kiel-Windeweer

All available data for those fields were included in the history matching process in same way as those from the main Groningen field. In addition to these additional historical data, newly drilled Groningen wells like Borgesweer-5 and Zeerijp-2 and 3 and old non-Groningen well, Sauweerd-

1, were included in the extended model. The 2012 and 2015 models are compared in Figure 2, with initial distribution of gas shown in blue. All available data (pressure, production, PNL etc.) for those fields were included in the history matching process in same way as those from the main Groningen field. In addition to updated historical data, new well data have been included. This includes not only newly drilled Groningen wells like Borgeweer-5 and Zeerijp-2 and 3, but also data from the abandoned non-Groningen well Sauweerd-1. The 2012 and 2015 models are compared in Figure 2, with initial gas distribution shown in blue.

While the same modelling package is used for GFR2015 (Shell software; MoReS and Reduce++) all input has been revised – tuning parameters have been removed, scripts have been cleaned-up and standard functionality used where possible. Input to GFR2015 that is new or substantially modified includes:

- GFR2015 extended area static model
- New subsidence proxy calculation and match quality indicator (normalised RMSE for subsidence) in MoReS
- Modified assignment of analytical aquifers, combined with different approach to tuning their parameters for history matching and uncertainty evaluation
- Revised set of saturation functions including Brooks-Corey based capillary pressure correlation and improved relative permeability model
- Revised fluid (PVT) properties including implicit modelling of condensed water in the gas phase based on Wehe-McKetta
- More constrained history-matching workflow, with 3 mismatch objective functions instead of 2.

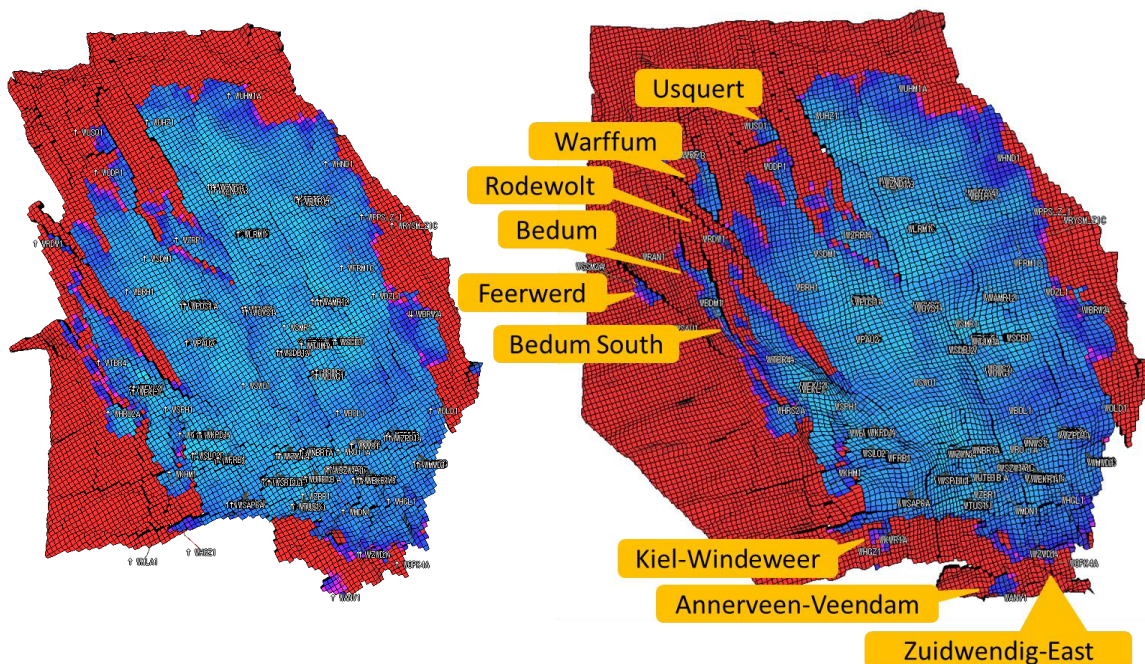


**Figure 2 GFR2012 (left) and GFR2015 (right) grid boundary comparison.**

One of the main objectives of the new dynamic model update is to achieve a history match to measured subsidence data, in addition to the more conventional match on reservoir pressure and

gas-water contact movement. The approach chosen is to build an approximate, fast and integrated subsidence proxy in Mores. The proxy guides the history matching and is used in the uncertainty management workflow. It is important to note that the history match of subsidence is mostly used to improve our prediction of reservoir pressure, especially where we don't have measured well data like for example in the aquifer. The final prediction of subsidence will be done using a separate full-physics geomechanical model, taking predicted reservoir pressure as input. The detailed description and the theory of this proxy are shown in chapter 5.

### History matching workflow

GFR 2015 dynamic model is constrained by the following historical data:

- Production and injection data as controlling parameters
- Pressure data including SP(T)Gs, CITHPs, BUs and RFT's
- PNL data (water rise)
- Subsidence data

Fluid composition data is not directly used in the history-matching process, however the changing gas composition in certain wells was evaluated during the analysis of the reservoir behaviour.

The subsidence data was matched using the subsidence proxy calculation and match quality indicator (normalised RMSE for subsidence) using MoReS (Shell's internal dynamic simulator). An example of the proxy results is shown in Figure 3.

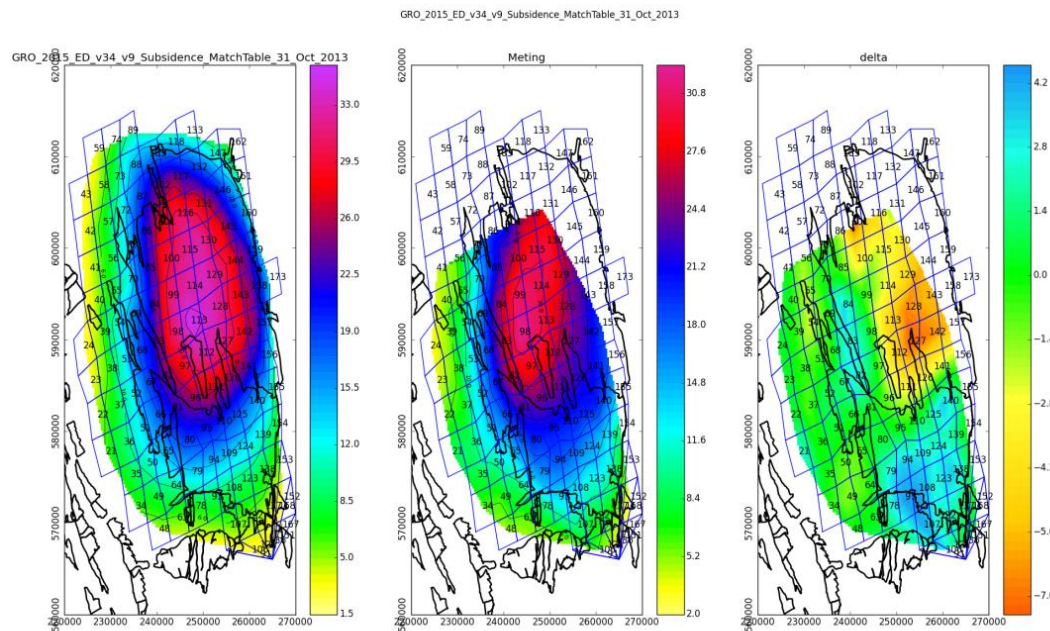


**Figure 3 Example of the simulator output(left) the measured data (middle) and the difference between the two. All in cm.**

An initial “reference” model was manually tuned based on the general understanding of the reservoir behaviour and results from the previous Groningen field reviews. A preliminary understanding of the behaviour of the surrounding Land asset fields had to be created, ensuring that no pressure communication exists with main Groningen field. Then the reference model was used as an input to the Assisted History Matching (AHM) workflow. This workflow serves to investigate many realisations with different variables and hence gives an insight into the various history matching possibilities. The following matching parameters were used to tune the model:

- 24 global and local Gross Block Volume (GBV) and permeability multipliers
- 36 fault grouping sealing factors
- Other tuning parameters like aquifer properties, well inflow properties (skin) etc.

More details on the history matching workflow and results are in chapter 6.

### **Production forecast**

The best matched dynamic model is used for the production and pressure forecasting. The resulting pressure maps are used by geomechanics group for the reservoir compaction and subsidence estimation and further for the hazard and risk assessment. Various production forecast scenarios were considered for the HRA and for the Winningsplan which includes:

- different annual offtake volumes
- different regional caps
- optimization of the annual offtake rates in order to decrease the pressure fluctuations

Also this model will be used for the development opportunities and optimisation e.g. 2<sup>nd</sup> and 3<sup>rd</sup> stage compression and pop-up blocks.

Integrated Production System Modelling (IPSM) is not discussed in this report and more details can be found in the reference (1).

## Table of contents

<b><u>Executive summary</u></b>	<b>I</b>
Study objectives	II
Main features of the study	III
History matching workflow	V
Production forecast	VI
<b><u>Table of contents</u></b>	<b>VII</b>
<b><u>1. Dynamic Model Upscaling</u></b>	<b>1</b>
1.1. Static Model	1
1.2. Grid extension	1
1.3. Properties upscaling	1
<b><u>2. Rock Properties</u></b>	<b>5</b>
2.1. Introduction	5
2.2. Summary of changes with respect to GFR2012	5
2.3. Available data	5
2.4. Saturation height function	6
2.5. Relative Permeability model	13
<b><u>3. Fluid Properties</u></b>	<b>17</b>
3.1. Introduction	17
3.2. Available data	17
3.3. Reservoir Temperature	17
3.4. Pressure table range	21
3.5. Gas Formation Volume Factor	21
3.6. Gas Deviation factor	21
3.7. Gas Viscosity	22
3.8. Formation Water properties	23
3.9. Volume Correction for Bg	23
3.10. Condensate Gas Ratio	25
3.11. Water Gas Ratio	28
<b><u>4. Reservoir Initialisation</u></b>	<b>30</b>
4.1. Hydrostatic Initialisation	30
4.2. Stability of Initialisation	32
<b><u>5. Subsidence proxy</u></b>	<b>35</b>

<b>5.1. Theory</b>	<b>36</b>
<b>5.2. Assumptions and Compressibility</b>	<b>38</b>
<b>6. History Matching and Forecast Uncertainty Analysis</b>	<b>42</b>
<b>6.1. Summary</b>	<b>42</b>
<b>6.2. Reservoir Behaviour</b>	<b>43</b>
<b>6.3. Simulator constraints</b>	<b>47</b>
<b>6.4. Historical data</b>	<b>48</b>
6.4.1. SPTG	48
6.4.2. Subsidence data	48
6.4.3. RFT	49
6.4.4. PNL	49
<b>6.5. Model output</b>	<b>50</b>
6.5.1. SP(I)G	50
6.5.2. Subsidence proxy	51
6.5.3. RFT	52
6.5.4. PNL	53
<b>6.6. Mismatch functions</b>	<b>53</b>
6.6.1. SPG mismatch	54
6.6.2. Subsidence mismatch	54
6.6.3. RFT	55
6.6.4. PNL mismatch	56
<b>6.7. History matching workflow</b>	<b>56</b>
6.7.1. Space filling	57
6.7.2. Adjoint	57
6.7.3. Workflow	58
6.7.4. Model extension	59
<b>6.8. Globally best matched model selection</b>	<b>59</b>
<b>6.9. Regional model improvements</b>	<b>59</b>
<b>6.10. Types of Matching Parameters</b>	<b>61</b>
6.10.1. Gross bulk volume	62
6.10.2. Permeability multipliers	62
6.10.3. Fault seal factors	62
6.10.4. Aquifers	63
6.10.5. Subsidence	64
6.10.6. Saturation functions	65
6.10.7. Free water levels	65
<b>6.11. Set-up of field-wide parameters</b>	<b>65</b>
6.11.1. Slochteren	65
6.11.2. Ten Boer Claystone	66
6.11.3. Ameland Claystone	66
6.11.4. Heterolitics lower and upper Slochteren	66
<b>6.12. Set-up of regional parameters</b>	<b>67</b>
6.12.1. North West	69
6.12.2. Zeerijp	70
6.12.3. North East	70
6.12.4. Bierum, Borgsweer and the Ryssum Aquifer	70
6.12.5. Central Region	71

6.12.6.	South West	72
6.12.7.	Eemskanaal region	72
6.12.8.	Harkstede	72
6.12.9.	Lauwerszee Aquifer	73
6.12.10.	Kolham	74
6.12.11.	The Land Asset fields	74
6.12.12.	Feerwerd	74
6.12.13.	Usquert and Oldorp	75
6.12.14.	Kiel-Windeweer	75
6.12.15.	Warffum	76
6.12.16.	Bedum	76
6.12.17.	Midlaren	77
6.12.18.	Zuidwending and Annerveen	77
6.12.19.	Zuidwending East (OPK-4)	77
<b>6.13.</b>	<b>History matching results</b>	<b>78</b>
<b>6.14.</b>	<b>Uncertainty analysis workflow</b>	<b>79</b>
<b>6.15.</b>	<b>Simple forecast</b>	<b>80</b>
<b>6.16.</b>	<b>Assess parameters effecting the HM and not the FC</b>	<b>80</b>
<b>6.17.</b>	<b>Results of the uncertainty analysis</b>	<b>82</b>
<b>7.</b>	<b><u>Surface Pressure and Flowrate Matching</u></b>	<b>85</b>
7.1.	Capacity matching	85
7.2.	Matching Methodology	87
7.3.	Historic Capacity Matching Results	90
7.4.	Capacity Match Forecasting	93
7.5.	Areas for Improvement	95
<b>8.</b>	<b><u>Recommendations for further work</u></b>	<b>96</b>
8.1.	Investigate gas saturation in the Aquifer	96
8.2.	THP history matching	99
8.3.	Apply “closed-loop” to Cm porosity relationship	100
8.4.	CMI history matching	100
8.5.	Central area high permeability investigation	100
8.6.	Apply Gravity survey into AHM workflow	100
8.7.	Additional pressure point on model area only constrained by Subsidence	101
	<b><u>References</u></b>	<b>102</b>
	<b><u>Bibliographic information</u></b>	<b>105</b>
	<b><u>Report distribution</u></b>	<b>106</b>
	<b><u>Appendix 1. Model repository</u></b>	<b>107</b>
A1.1.	00_Petrel	107

<b>A1.2. 10_RPP</b>	<b>107</b>
<b>A1.3. 20_HM</b>	<b>108</b>
20_HM/01_ReferenceModel	109
20_HM/02_TestUpscaling	109
20_HM/03_CleanSheetModel	109
20_HM/04_ExperimentalDesign_AHM	109
<b>A1.4. 30_FC</b>	<b>112</b>
<b>A1.5. 60_DataExports</b>	<b>112</b>
<b>A1.6. Include</b>	<b>113</b>
<b><u>Appendix 2. Matching Parameter ranges</u></b>	<b><u>114</u></b>

---

## 1. Dynamic Model Upscaling

### 1.1. Static Model

The current version of the dynamic model was built based on the fine scale Petrel grid version 2.5. This version of the static model contains the following updates compared with the GFR 2012 static model:

- Updated property models
- Extended model area
- Slightly revised model grid, top reservoir surface
- Revised layering scheme

The Promise acoustic impedance model from 2003 was used to steer the porosity distribution away from well locations. Also, the new input data and revised input logs were included in the static modelling workflow, like VCL, POR and PERM.

Prior to the version 2.5 model there were 2 versions of the static model realisations, which were used in the dynamic modelling workflow. The feedback from reservoir engineering was considered and modifications were incorporated in the next versions of the static models. For example, missing faults, dynamic compartments, porosity and saturation distribution were discussed as a “closed loop” exercise.

### 1.2. Grid extension

Same model boundary as used by GFR 2003 and 2012 was initially used to build the new static and dynamic models. However after discussions with the NAM Geomechanics team it was decided to extend the existing grid boundaries approximately 8-10 km to the West and 5 km to the South. The main reasons for this decision were as follows:

- The area outside of the Groningen closure has become increasingly important
- Subsidence in the greater Groningen area, including under the city of Groningen is affected by pressure depletion in adjacent aquifers and surrounding Land asset fields
- More flexibility for the geomechanics team for subsidence calculations on the numerical grid

The extended area of the static grid was upscaled in the same way as the main Groningen field.

### 1.3. Properties upscaling

Reduce ++ software of the Dynamo package was used in the upscaling process.

Table 1 illustrates the comparison between the GFR2012 and GFR2015 upscaling in vertical direction.

Reservoir Zones	2012 Model		2015 Model		
	Fine Model	Coarse Model	Fine Model	Coarse Model	
Ten Boer	TBS-3	10	1	10	1
	TBS-2	10	1	10	1
	TBS-1	20	1	20	1
Upper Slochteren	USS-3res	15	2	15	3
	USS-2het	4	1	4	1
	USS-2res	20	2	20	6
	USS-1het	4	1	4	1
	USS-1res	20	2	20	5
Ameland Claystone	LSS-2het	6	1	4	1
Lower Slochteren	LSS-2res	30	10	30	7
	LSS-1het	6	1	4	1
	LSS-1res	59	20	30	6

**Table 1 Upscaling parameters in Z direction in GFR2012 and GFR2015 models**

The number of layers in the Lower Slochteren Sandstone was reduced in comparison with the 2012 model. Fewer layers in the Lower Slochteren improve the simulation performance in terms of speed while preserving the relatively homogeneous reservoir features.

In the Upper Slochteren Sandstone the number of upscaled layers increased to better represent formation heterogeneity.

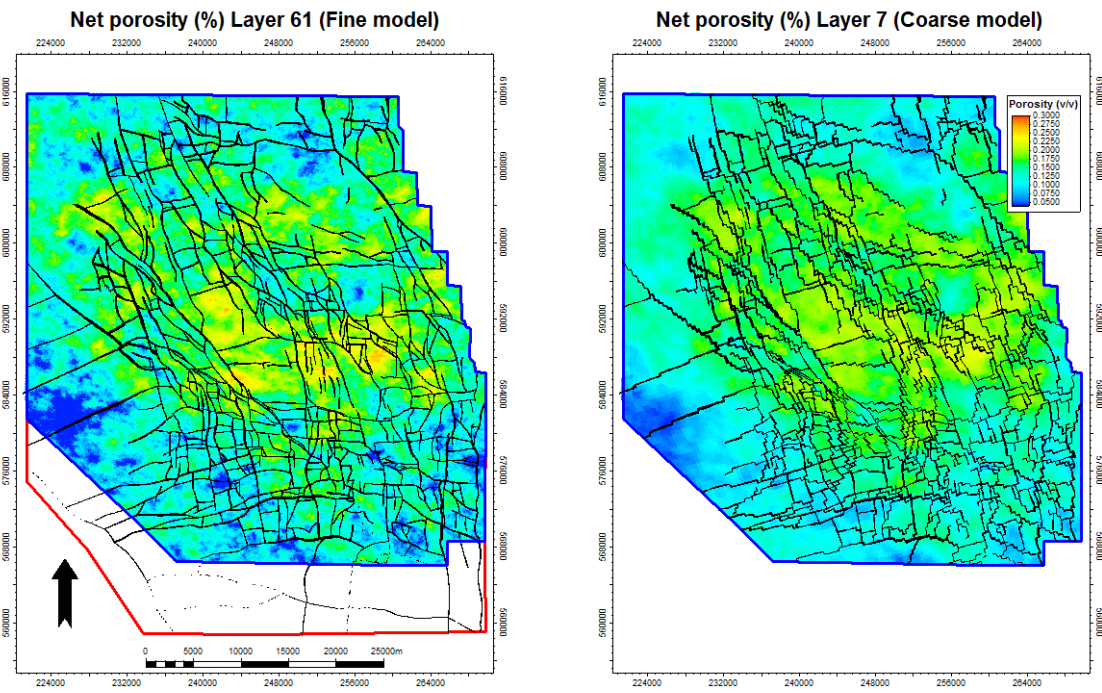


**Figure 4 Porosity map comparison between the fine and coarse grids (Upper Slochteren).**

Figure 4 and Figure 6 show the comparison between the fine Petrel and coarse Mores grids at the same Upper Slochteren layer. Porosity and permeability maps are illustrated respectively.

Extreme high and low porosity and permeability values are smeared out in the upscaled model, however the main trend and the general features are preserved. The threshold was applied to filter the cells with porosity of less than 4 porosity units. The example with the cross-section is shown in Figure 5. The resulting histogram shows that the property distribution in both grids is the same and only low and high ends, i.e. extreme values are missing in the coarse grid (Figure 7).

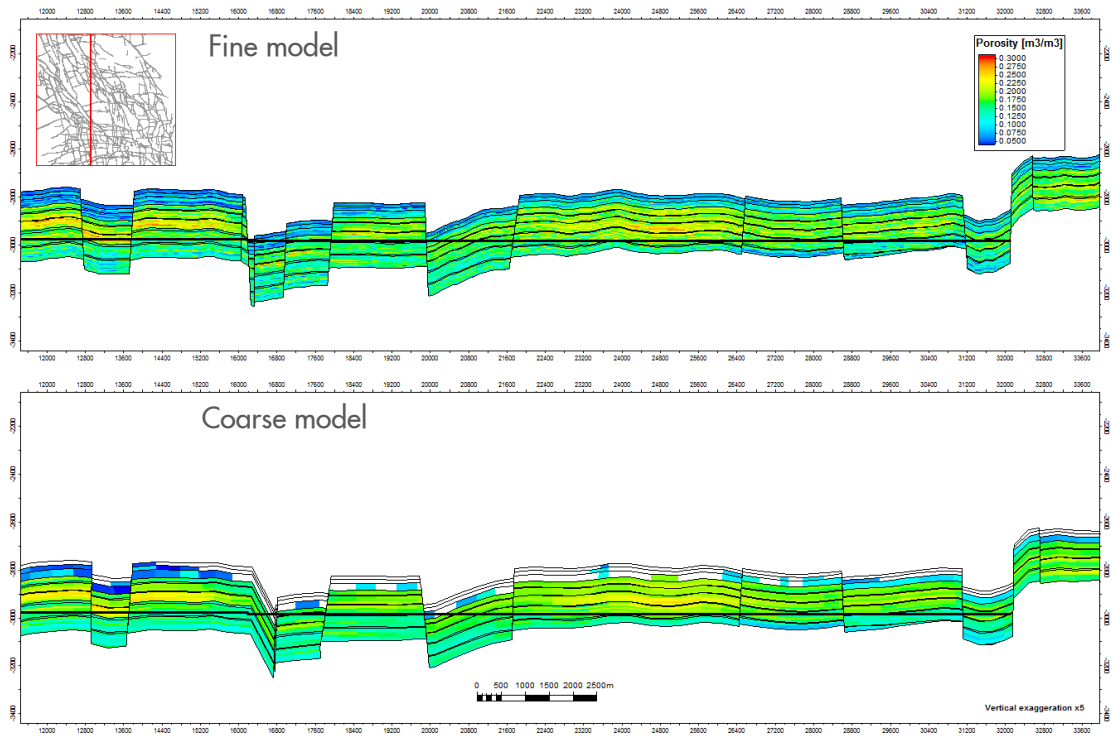


Figure 5 Porosity cross section comparison between the fine and coarse grids. The cells with porosity less than 4 PU are voided.

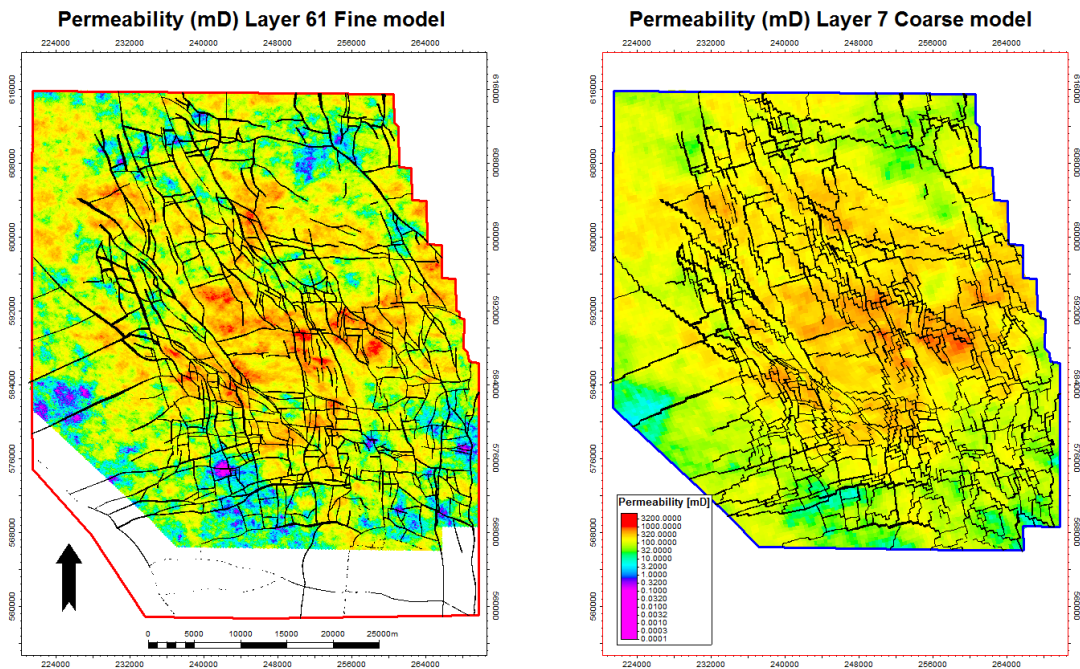
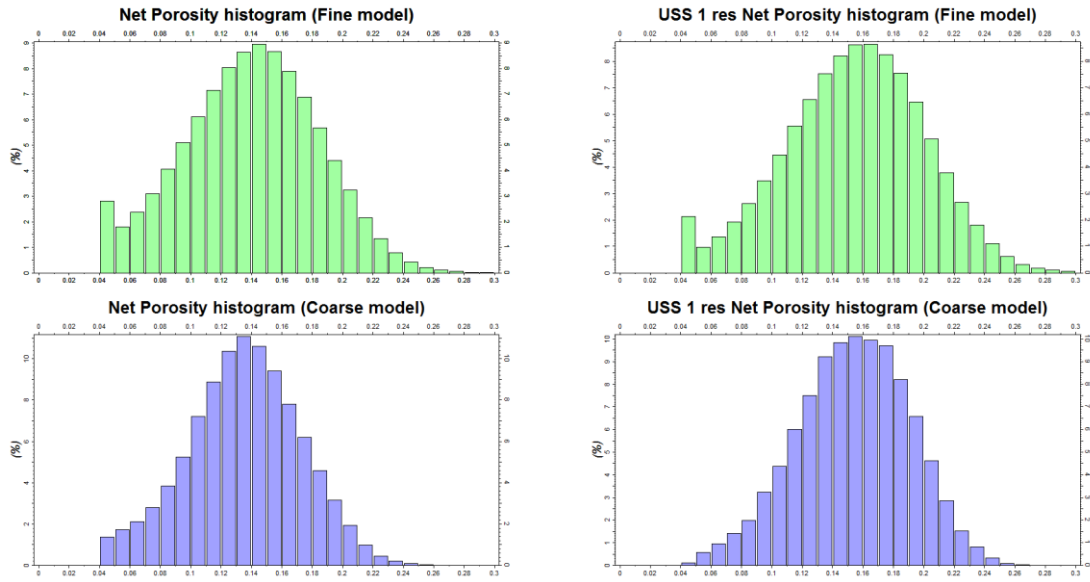


Figure 6 Permeability map comparison between the fine and coarse grids (Upper Slochteren).



**Figure 7 Upper Slochteren and the whole grid net porosity histogram comparison for the fine and coarse grid models.**

## 2. Rock Properties

### 2.1. Introduction

The initial distribution of the water and gas phase in the Groningen dynamic reservoir model is governed by a porosity dependent Brooks-Corey saturation-height function. The function is converted to capillary pressure models, binned to porosity, and the model is then hydrostatically initialized with gas being the reference phase. Drainage capillary pressure functions in the Groningen reservoir model have been derived from saturation logs and capillary pressure is modeled with the Brooks-Corey function. Relative permeability models are generated using the Corey functions. Components of the Corey model are determined by special core analysis (SCAL). Drainage capillary pressure curves are used for initialization and defining the connate water saturation component of the relative permeability model. Imbibition capillary pressure curves are not used. A relative permeability model and a capillary pressure model are created for porosities ranging from 6 p.u. to the maximum porosity, with a bin size of 2 p.u. This bin size is the same bin size used to determine the horizontal permeability in the static reservoir model (1).

### 2.2. Summary of changes with respect to GFR2012

An independent review of the GFR2012 model was carried out by SGS Horizon in 2013 (2). Based on their observations, GFR2015 has adopted the following changes to the saturation functions compared to the GFR2012 work:

- The Lambda function used for saturation height modelling is replaced by a Brooks-Corey function
- The uncertainty band on the saturation height function is increased.
- A correction is made to the saturation height function to achieve a better match to available log data.
- A relation for residual gas saturation uncertainty is introduced as function of porosity
- The saturation-height function cut-off value (determining connate water saturation) is now determined by a derivative cut-off instead of a fixed height

### 2.3. Available data

Log data has been used to derive saturation height functions. For the Groningen Field Review 2012 a saturation height function was calculated based on 11 wells with a high confidence porosity log representing a sufficient coverage over the Groningen field (3). For GFR2015 the same saturation height function is used with a correction suggested by SGS Horizon based on their review of the previous model (2), this is further discussed in the text below. This function has been compared to results from available core experiments (4).

The relative permeability model used is based on both steady state and unsteady state experiments. One steady state experiment has been performed on a core sample from well ZPD-12 (5). Relative permeability end points have been determined by centrifuge and displacement (unsteady state) experiments performed on multiple cores and the results have been gathered in overview reports (6) (7). The Shell in-house relative permeability database RELATE has been used to obtain analogue data on the Corey exponents.

## 2.4. Saturation height function

In the Groningen model capillary and gravitational forces are assumed to be initially in equilibrium. Under this assumption capillary pressure can be written as function of height above the free water level, using Equation 1:

$$P_c = \frac{2\sigma \cos(\theta)}{r} = -(\rho_w - \rho_g)gH$$

### Equation 1: Equilibrium of capillary pressure and gravity

where

- P<sub>c</sub> capillary pressure
- σ interfacial tension
- θ contact angle
- r pore throat size
- g gravitational constant
- ρ<sub>w</sub> water density at reservoir conditions
- ρ<sub>g</sub> gas density at reservoir conditions
- H height above the free water level in m

with ρ<sub>w</sub> and ρ<sub>g</sub> as per Table 2:

Densities at reservoir conditions 346.8 barA, 103 °C		
ρ <sub>w</sub>	1172 (8)	kg/m <sup>3</sup>
ρ <sub>g</sub>	197.0 (9)	kg/m <sup>3</sup>

**Table 2: Water and gas densities at initial reservoir conditions**

The saturation height function from GFR2012 is compared to capillary pressure curves from available core flooding experiments from 7 wells in the Groningen field: ZPD-12, ZND-12, KPD-12, EKL-12 (4), PPS-Z1, RYS-Z1B and FRM-1B (10). Results from centrifuge and mercury injection capillary pressure measurements are available. Only the Hg-air capillary pressure experiments on plugs obtained above the GWC which did not fail during experiments, are compared to the saturation function.

In order to compare results from mercury injection experiments to the capillary pressure as function of height as described above, the capillary pressure is converted from the Groningen rock/fluid system to a mercury/air according to Equation 2 (11),

$$P_{c,R} = P_{c,L} \frac{\sigma_R \cos(\theta)_R}{\sigma_L \cos(\theta)_L}$$

**Equation 2: conversion of laboratory capillary pressure results to reservoir conditions**

where

- L Laboratory conditions
- R Reservoir conditions
- θ<sub>L</sub> contact angle for mercury/air = 140°
- θ<sub>R</sub> contact angle for water/gas = 0°
- σ<sub>L</sub> interfacial tension for mercury/air = 480 mN/m (11)
- σ<sub>R</sub> interfacial tension for water/Groningen gas = 43.4 mN/m (12)

The saturation height function matches well to the experimental data from the KPD-12, ZPD-12 and ZND-12 cores. A less satisfactory match is obtained for the EKL-12 wells. Two examples of the fit are presented in Figure 8. Based on uncertainties in connate saturations, porosity-permeability relations and experimental procedures (3) the consistency between log and core data is deemed acceptable.

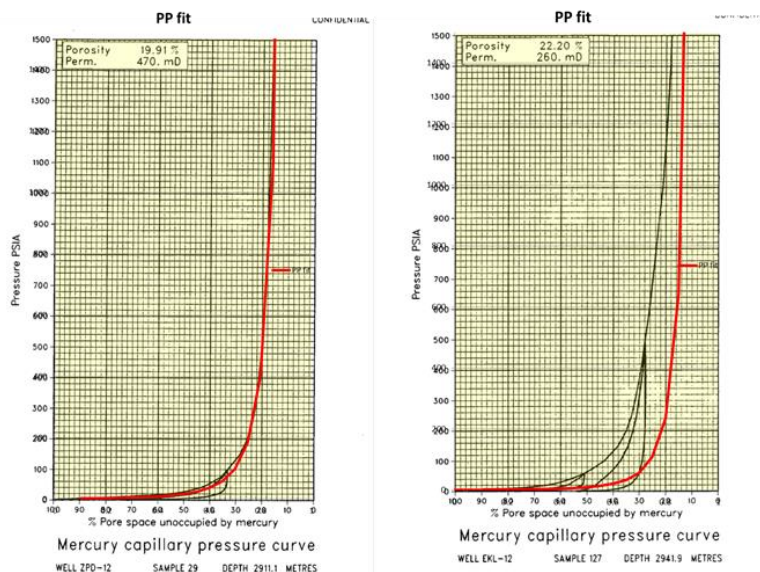


**Figure 8 Fit of the saturation height function to mercury capillary pressure curves on Groningen core samples**

Three suggestions were made by SGS Horizon in their review of the GFR2012 concerning the saturation height function (2). Firstly they suggested investigating a possible depth dependency in the saturation height function. Because the relationship between porosity and permeability is depth dependent, one could expect an additional dependency on either depth or permeability. However, when plotting the difference between the measured log saturation and the saturation height function there seems to be no apparent mismatch dependency with depth, see Figure 9, hence the function was not changed to include depth dependency.

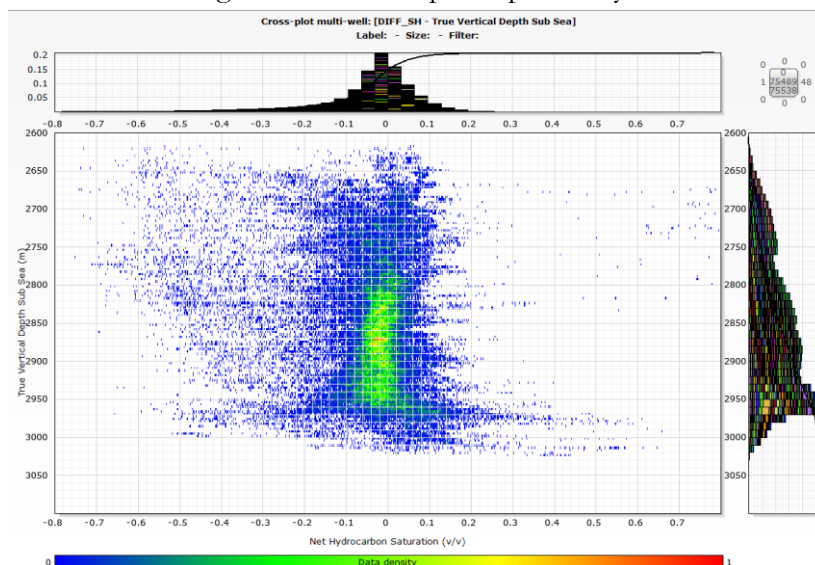


**Figure 9: Difference between the saturation function and the log saturation (x-axis) as a function of TVNAP. No clear trend can be seen (symmetrical histogram, no trends in the data density) A slight difference in general between log saturation and saturation height function, with the saturation height function being slightly higher (negative x-values), as seen here and Figure 10.**

Secondly the SGS Horizon review (2) indicated a systematic error on the saturation height function compared to the log saturation of  $0.013797 \cdot Sh$ . Figure 10 shows the comparison of the log derived saturations of all the wells in Groningen plotted against the saturation height function used in GFR2012. The red line is the uncorrected function assuming a one-to-one comparison. In Figure 10 this model seems to be missing the highest density of data points in the plot. When applying the suggested correction in the saturation function the majority of the data seems to be in better agreement with the model, this is indicated by the blue line in Figure 10. This seems to confirm the SGS horizon statement. The suggested correction factor is thus applied to the saturation function applied in GFR2015.

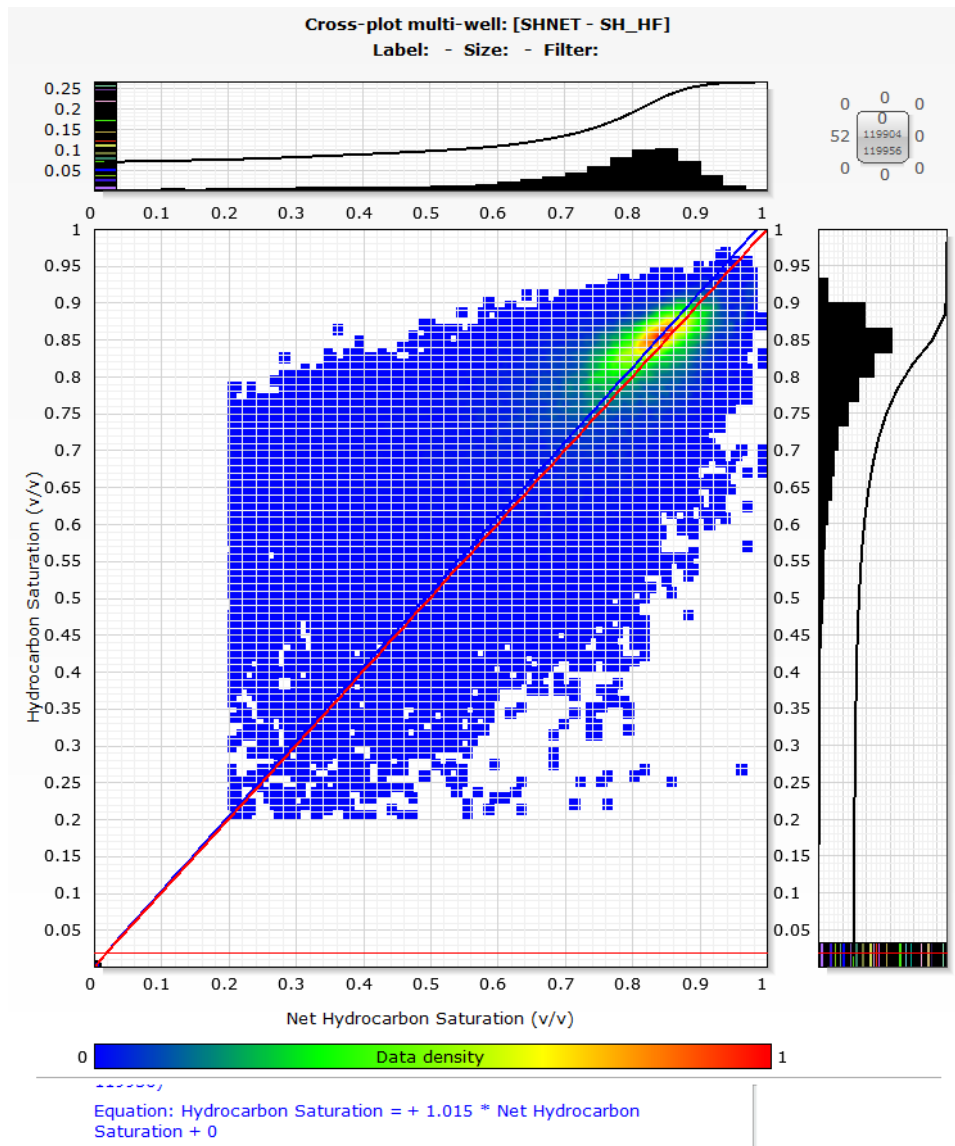


**Figure 10: Saturation data density and fitting function with a correction to the saturation height function (X-axis), as suggested by Horizon review, of 0.015**

Thirdly GFR2012 applied an uncertainty to the saturation measurements in their uncertainty analysis of  $0.11 \cdot Sh$ . Water saturation in logs is based on a water resistivity ( $R_w$ ) which is obtained from Pickett plots. The uncertainty in  $R_w$  is 0.02 and resulting in an uncertainty on the saturation of  $0.13 \cdot Sh$ . This adjusted uncertainty band will be applied in the uncertainty analysis workflow and is in agreement with the suggestion by SGS Horizon (2).

### Saturation as function of capillary pressure

In the updated Groningen model GFR2015 the saturation is modelled as function of capillary pressure governed by the Brooks-Corey equation, see Equation 1:

$$S_w(P_c) = S_{w,irr} + (1 - S_{w,irr}) * \left(\frac{P_{c,entry}}{P_c}\right)^{\frac{1}{n}}$$

### Equation 3: Brooks-Corey water saturation as function of capillary pressure

where

- Sw water saturation
- Sw,irr irreducible water saturation
- Pc,entry capillary entry pressure
- n curvature

with the components of Equation 3 determined from Groningen saturation log data using Techlog. This results in an irreducible water saturation as function of porosity, see Equation 4 and Figure 11.

$$S_{w,irr} = 10^{-0.8-3\phi}$$

### Equation 4: Irreducible water saturation as used in the Brooks-Corey function

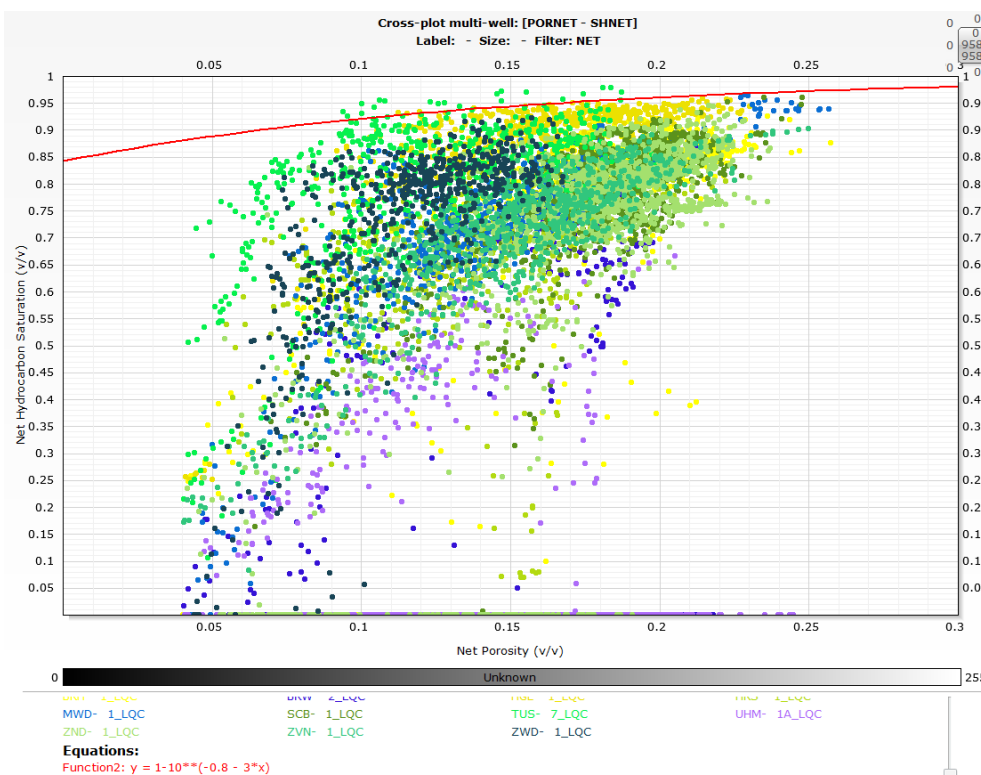


**Figure 11 Irreducible water saturation as function of porosity**

Capillary entry pressure is determined as a function of porosity by constraining the Brooks-Corey model to the saturation logs. These capillary entry pressures are plotted as a function of porosity and the following function is determined, see Equation 5.

$$P_{c,entry} = 10^{0.1354-9.7302*\phi}$$

### Equation 5: Capillary entry pressure as function of porosity used in the Brooks-Corey function

The function is plotted in Figure 13. From available mercury injection core experiments on 17 core samples from 4 wells (4) a capillary entry pressures are estimated, with two examples shown in Figure 12.

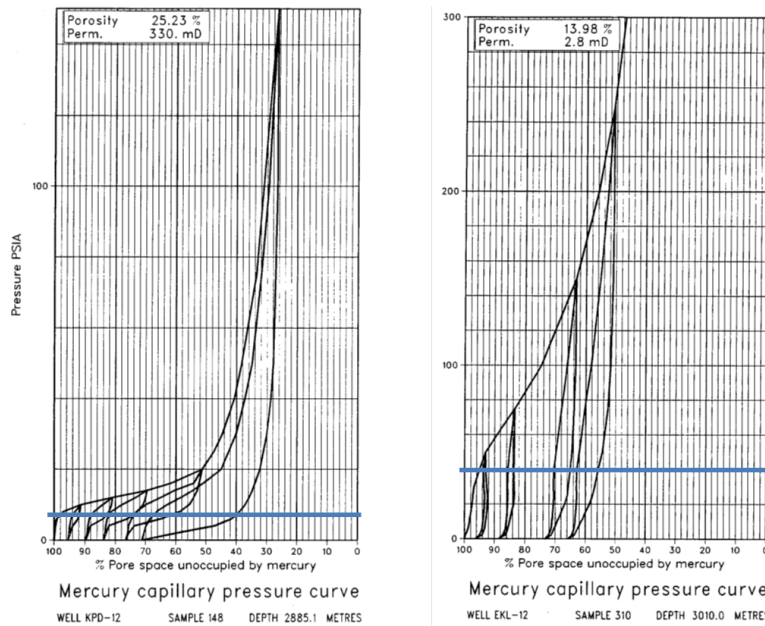


**Figure 12 Capillary entry pressure from mercury-air core flooding experiments, example of well KPD-12**

The capillary entry pressures from these plots are converted to Groningen water-gas reservoir values using Equation 2. A comparison of Equation 5 to the measured entry pressures is shown in Figure 13. Although the amount of data is limited, the model and data do not seem to exclude one another (3).

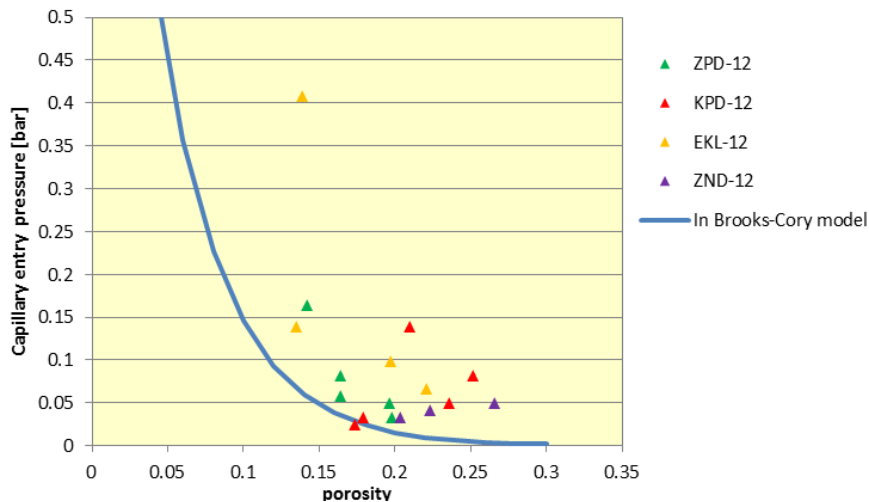


**Figure 13: PC entry from core measurements, as function of porosity, compared to that used in the Brooks Corey model**

Curvature of the Brooks-Corey model shows a slight porosity dependence:  $n = -2.8 * \phi^2 + 2.1 * \phi + 2.6$ . Where n ranges from 2.68 – 2.95 in porosity range 5% - 30%. However, to not overcomplicate the model by adding more dependencies we choose to set  $n = 2.86$  which results in a good agreement with logs (mainly to the porosity range around 18-20%) (3). More dependencies will result in a better fit to the saturation logs but not necessarily in a better description of the saturation.

Combining Equation 4, Equation 5, Equation 6 and the value for n we get a porosity dependent saturation height function, Equation 6:

$$S_w = 10^{-0.8-3*\phi} + (1 - 10^{-0.8-3*\phi}) * \left( \frac{10^{0.1354 - 9.7302 * \phi}}{PC} \right)^{\frac{1}{2.86}}$$

**Equation 6: Saturation as a function of capillary pressure for the Groningen dynamic model.**

The difference between the previously used lambda function and the Brooks Corey function are minimal and shown below, respectively by the blue and red graphs in Figure 14.

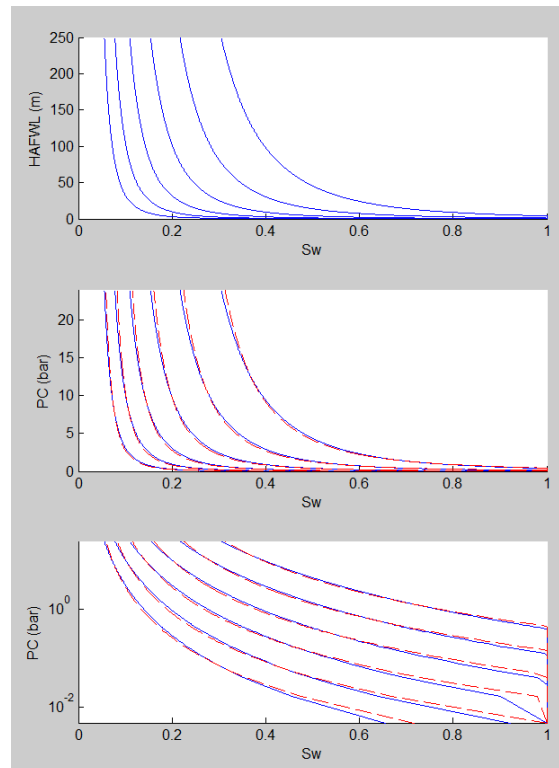


**Figure 14 match of Brooks-Corey (red lines) used in GFR2015 to Lambda functions (blue lines) used in GFR2012 for a range of porosities (5% to 30%).**

### Irreducible water saturation vs. connate water saturation

Irreducible water saturation, Equation 4, is defined to be different from connate water saturation in that irreducible is defined at an infinite capillary pressure, whereas connate is defined as water saturation at a defined maximum capillary pressure slope. The transition zone is thus ranging from fully water saturated to connate water saturation. At connate water saturation the water fraction is said to be irreducible. The choice of the connate water saturation determines the height of the transition zone above the free water level and should be a function of porosity. In the transition zone water saturation is higher than connate saturation and by definition mobile, and the water will flow in the simulator with a flow rate is governed, in part, by the relative permeability model. In GFR2012 the transition zone covered the entire reservoir. Connate water saturation was set at a saturation height of 320m, corresponding to the height difference between the crest of the structure and the lowest measured free water level in the model.

This work applies a maximum slope cut-off of -3000bar/s.u. in the capillary pressure curve to determine the connate water saturation, as suggested by RELATE. The saturation corresponding to this applied maximum curvature is shown for different porosities in Figure 15.

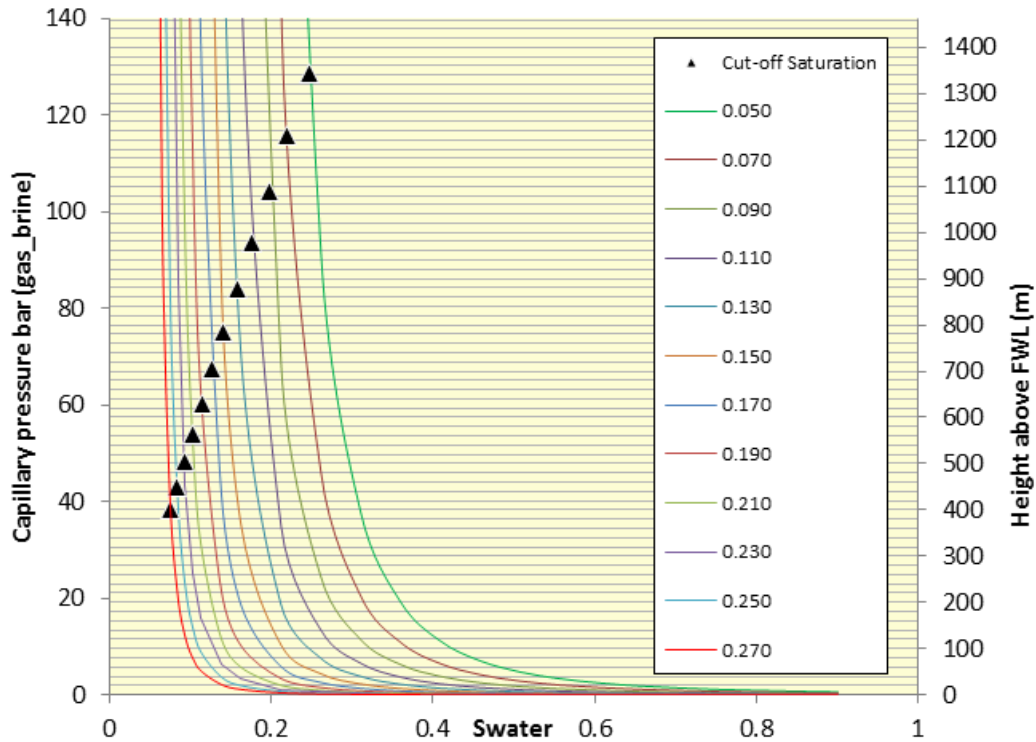


**Figure 15 Connate water saturation based on a capillary pressure derivative cut-off value for different porosity units.**

The connate water saturation is in Figure 16 compared to SCAL data: steady state (SS) experiments, unsteady state experiments (USS) and mercury injection (Hg-air). Figure 16 also compares the connate water saturation to log measurements. Here the p10 water saturation for different porosity bins from all available logs in Groningen is used to represent the connate water saturation from logs. These log derived connate water saturations are in better agreement with the derivative approach compared to the fixed height approach from GFR2012. Additionally the irreducible water saturation as used in Brooks-Corey from Equation 4 is shown.

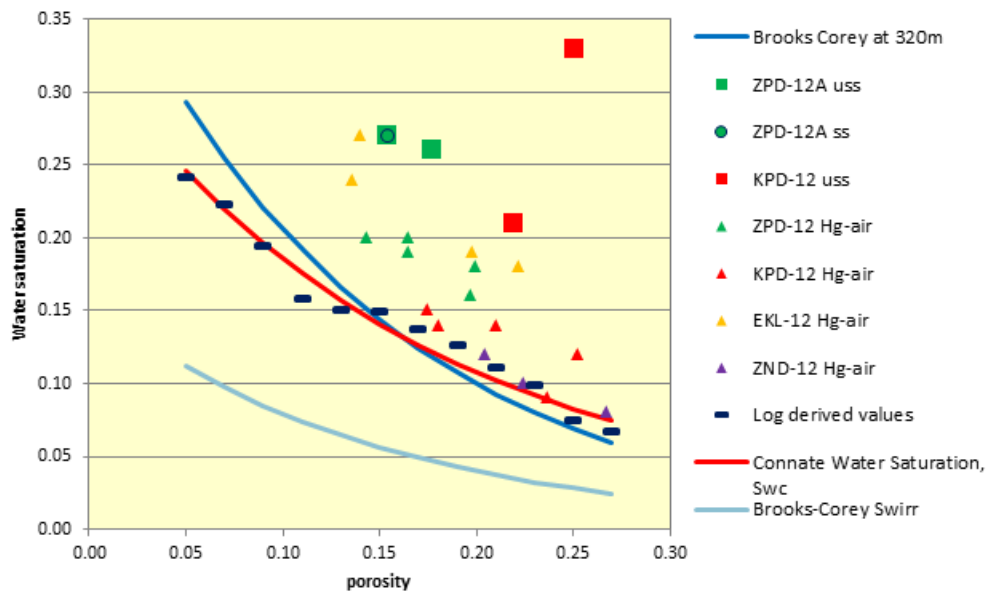


**Figure 16: Connate water saturation for different porosities, along with comparisons to SCAL data and methodology used in GFR2012.**

## 2.5. Relative Permeability model

Relative permeability is modeled with the Corey functions, see Equation 7 and Equation 8.

$$k_{rw} = k_{rw,e} \left( \frac{S_w - S_{wc}}{1 - S_{wc} - S_{gr}} \right)^{N_w}$$

**Equation 7: Corey function for water relative permeability**

$$k_{rg} = k_{rg,e} \left( \frac{1 - S_w - S_{gr}}{1 - S_{wc} - S_{gr}} \right)^{N_g}$$

**Equation 8: Corey function for gas relative permeability**

where

- $k_{rw}$  water relative permeability
- $k_{rg}$  gas relative permeability
- $k_{rw,e}$  water endpoint relative permeability
- $k_{rg,e}$  gas endpoint relative permeability
- $S_w$  water saturation
- $S_{wc}$  connate water saturation
- $S_{gr}$  residual gas saturation
- $N_w$  water Corey exponent
- $N_g$  gas Corey exponent

The connate water saturations are determined from the capillary pressure function described above. The other components and their ranges are obtained from both a single steady state experiment (Van der Gijp (5)), and from 18 unsteady state experiments gathered in a review by Berre (6). Berre compares unsteady state results to Counter current Imbibition (CCI) results, only to indicate that the much cheaper CCI could be an alternative for future experiments because results on core experiments with an initial gas saturation of 50% are in an acceptable agreement with the results of the unsteady state experiments (7), CCI results are not used in for determining model parameters.

In GFR2012 the endpoint residual gas saturation is based on a constant (0.26 base case). Typically one would expect it to be a function of porosity, with  $S_{gr}$  increasing with reduction in porosity. Due to the relative lack of residual gas experimental data from Groningen, USS data from the nearby analogue Norg field is included when determining  $S_{gr}$ . Based on residual gas measurements in Groningen and Norg three functions were fitted to represent the residual gas saturation as a function of porosity and are specified as:

- High Case:  $S_{g,r} = 0.26$   
Similar to GFR 2012 based on Groningen only USS data from 1989 study.
- Base Case:  $S_{g,r} = 0.35 * (0.30 - \phi) + 0.26$   
Linear trend of USS experimental data (including Norg). However, excluding counter-current imbibition data (CCI) data. CCI is not recommended due to too high residual values.
- Low Case:  $S_{g,r} = 0.7 * (0.30 - \phi) + 0.26$   
Including both CCI and USS data from both Groningen and Norg.

These three functions for residual gas saturation are compared to results from core measurement experiments in Figure 17.

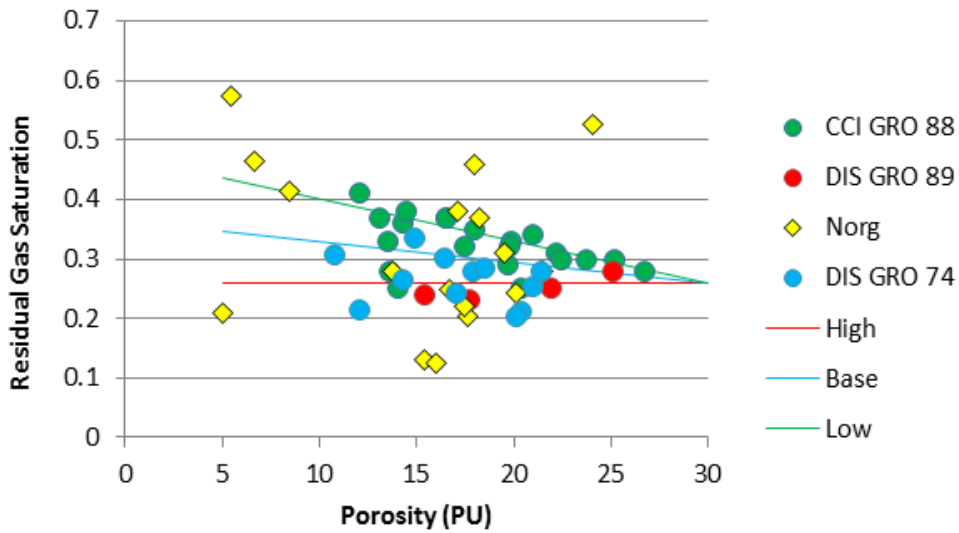


**Figure 17 Residual gas saturation as function of porosity**

Endpoint  $K_{rw}$  values are available from both Groningen and the nearby Norg field. Values obtained from Norg core samples (13)(from USS) are found to be generally low but in agreement with USS data from Groningen studies. All endpoint  $K_{rw}$  values with respect to air, determined from USS experiments are shown in Figure 18. The steady-state experiment suggested a higher endpoint  $K_{rw}$  of 0.19 with respect to air (5). This work applies the following range for the end point relative permeability to water in the uncertainty analysis: 0.03 – 0.13 – 0.25, corresponding to the low, mid and high end of the range respectively.

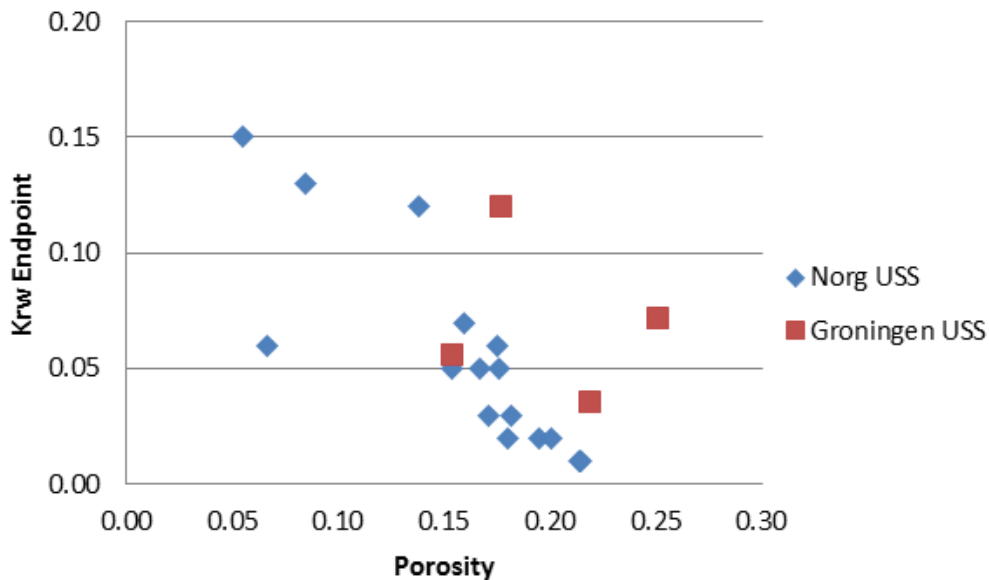


**Figure 18 Relative water permeability at residual gas saturation as a function of porosity**

The uncertainty range for both gas and water Corey exponents, which were measured only once, is based on the available reports and the RELATE analogue fields in the Northern Netherlands. The base case values are based on the steady state data points.

As described above, the uncertainty in the Corey components is based on the spread in values measured in Groningen core samples. Analogue data is available from nearby fields in the Netherlands, but has not been taken into account for this model update since no data quality statements are available for these data. The combined steady state and unsteady state data points are used as base case. Uncertainty in the relative permeability model is captured by a range for all the components. This range is shown in Table 3 and an example for 14% porosity is shown in Figure 20.

**Table 3 range of Corey model parameters**

Parameter	Base case	Low end	High end
$S_{w,c}$	Function	Function	Function
$k_{rw,e}$	0.1283	0.03	0.25
$k_{rg,e}$	0.8583	0.83	0.89
$S_{gr}$	Function	Function	0.26
$N_w$	3	2.7	4
$N_g$	1.7	1.4	2

The box representing the uncertainty for the gas endpoint is based on the measured end point relative permeabilities for gas and the irreducible water saturation shown in Figure 16. Note that the endpoint water saturations of the unsteady state experiments in Figure 19 are the starting water saturations of the experiments, the cores were not at connate water saturation, they are added to Figure 19 for completeness and not to the uncertainty range.

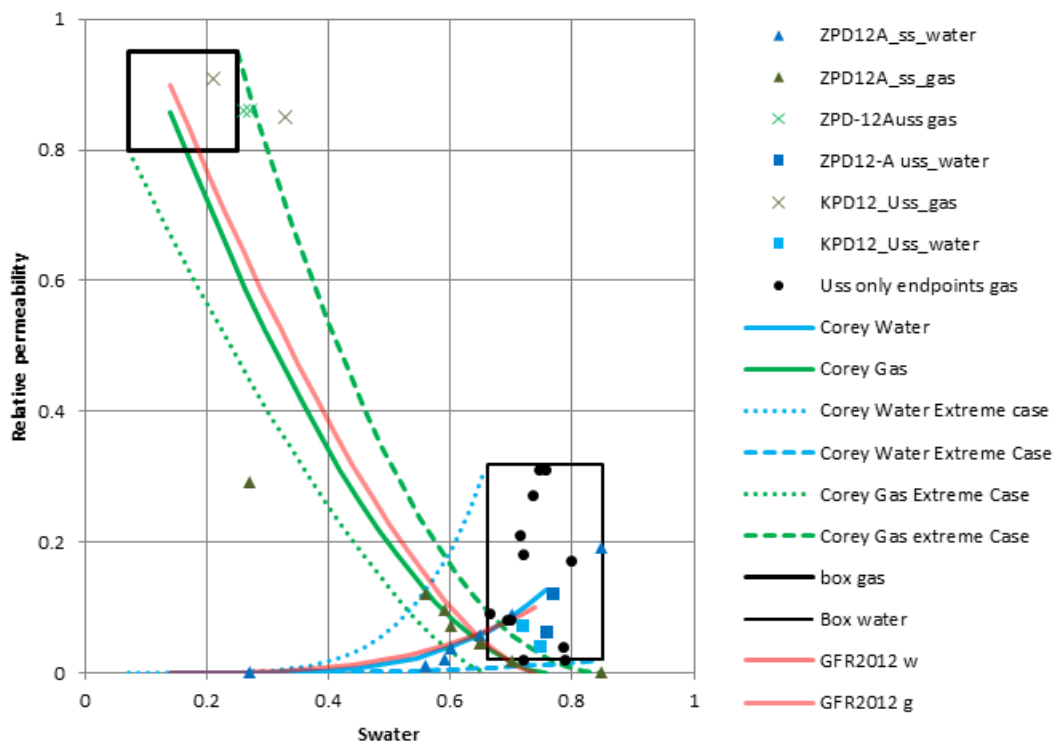


**Figure 19 Corey function fit for 14% porosity Swc (same as SS experiment) to SCAL data on Groningen cores from steady state (SS) and unsteady state (USS) experiments.**

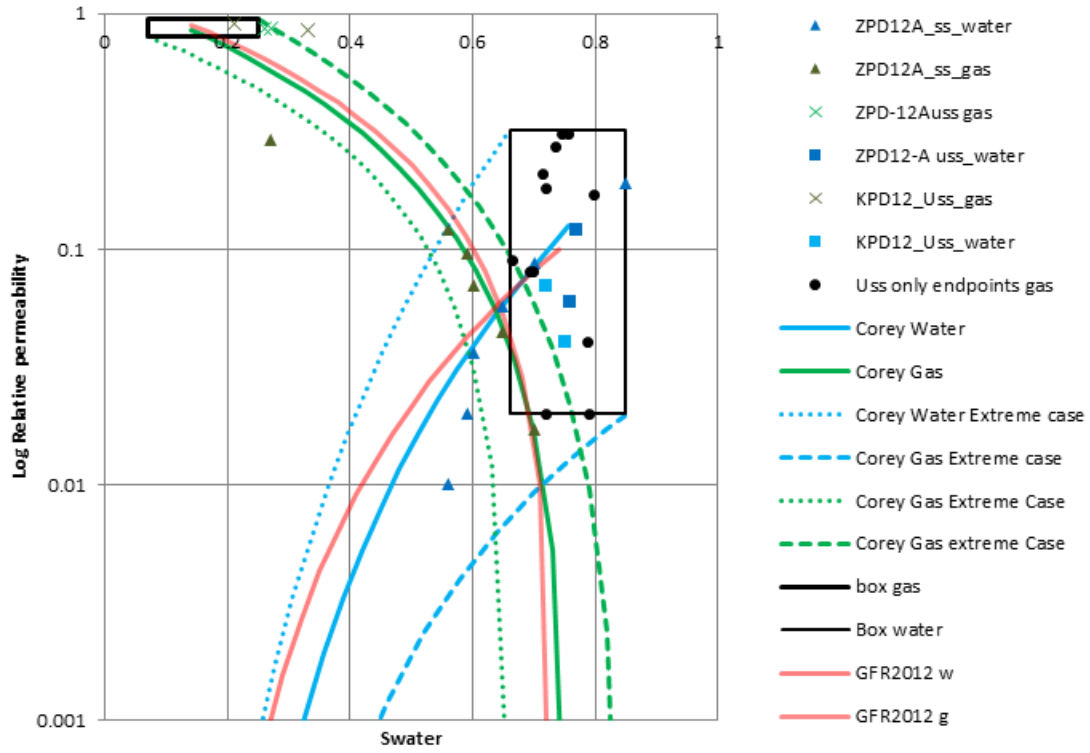


Figure 20: Corey function fit for 14% porosity Swc (same as SS experiment) to SCAL data on Groningen cores from steady state (SS) and unsteady state (USS) experiments on a logarithmic scale for relative permeability.

### **3. Fluid Properties**

#### **3.1. Introduction**

The Groningen PVT model has two mobile phases: gas and water. The gas used to be modeled as a dry gas (GFR2012). As per this model update, the gas is modeled as a wet gas, reflecting condensed water dissolved in the gas implicitly modeled via the gas formation volume factor. The differences of this PVT model with the PVT model used for the GFR2012 are the Condensate Gas Ratio modelling and the Water Gas Ratio modelling.

Lateral gas quality variations are honored by defining 6 PVT regions in the dynamic model using nitrogen content as a differentiator: the main Groningen field and peripheral blocks Harkstede, Usquert, Annerveen, Oude Pekela and Bedum.

#### **3.2. Available data**

##### **Main Groningen**

Groningen gas PVT analysis was performed in 1975 by de Loos (14) on 5 surface samples (Noordbroek 1962, Schaapbulten 1972, Bierum, Ten Boer Stedum 1974). In 2002 a geochemistry report was published, which investigated 358 Groningen surface gas samples up to the year 2000, confirming the de Loos PVT models (15).

##### **Harkstede**

Harkstede gas PVT analysis was performed on one separator sample from HRS-2 and on a surface gas sample combined with a condensate sample to represent the subsurface composition (16).

##### **Usquert**

All PVT information available on Usquert is downloaded from DREAM, no PVT analysis report is available.

##### **Annerveen**

Annerveen PVT analysis has been performed on one separator gas sample and on a combined separator gas sample with a condensate sample (17).

##### **Oude Pekela**

Oude Pekela PVT analysis was performed on 1 separator gas sample (18).

##### **Bedum**

Bedum PVT analysis was performed on two separator gas sample combined with a condensate sample (19).

##### **Oldorp**

Although Oldorp has an outlying gas quality (20) the main Groningen PVT model is assigned because no PVT analysis was performed on Oldorp gas.

#### **3.3. Reservoir Temperature**

The Groningen field is not isothermal. The reservoir temperature varies as a result of the Zechstein thickness, crust thickness and an aerial trend in the temperature distribution. The cap and base rock are assumed heat sources of infinite extent and therefore the reservoir temperature model is assumed to remain constant over the field producing life.

Temperatures have been measured throughout the Groningen field life as part of Static Pressure and Temperature Gradient (SPTG) surveys. All temperature data and analysis for GFR2003 (21) and GFR2012 (22) are collected in attachment 2. The uncertainty in temperature measurements is estimated at 2 degrees Celsius (22).

GFR2003 investigated a relation between temperature and the Zechstein salt layer thickness, but they did not find a clear correlation. Therefore a crust thickness model was used to explain the temperature variations observed from the data (23).

During the work on the GFR2012 a Zechstein thickness correlation was found. It is based on additional information of a temperature anomaly in the North East of the Groningen Field, as proposed by Kettel, referred to as the East Groningen Massif intrusive body (24), see Figure 21-a. This is in line with measured temperatures from SPTG surveys which also show a temperature anomaly in the North of the field, see Figure 21-b. The source of these anomalous high temperatures is uncertain, however a hypothesis is that hot water is circulating through border faults (25).

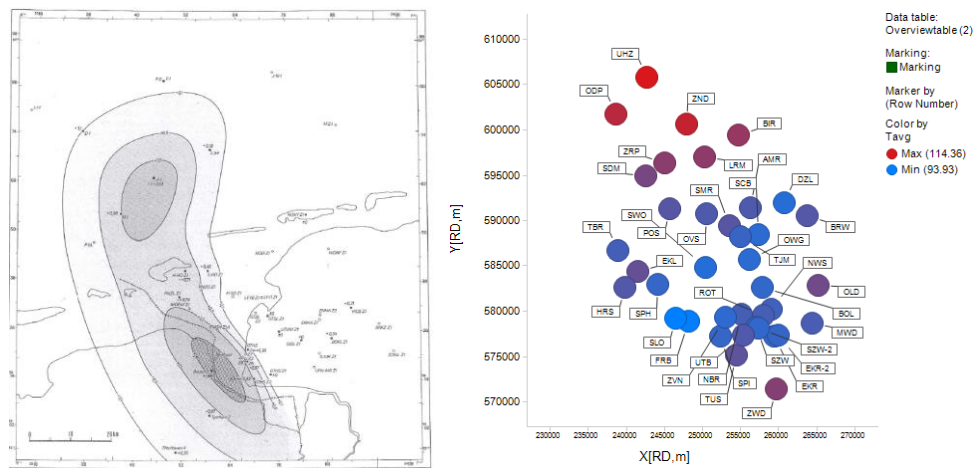


**Figure 21(a-b) a) location of the temperature anomaly according to Kettel, 1983 b) Temperatures at datum level, showing the temperatures on an X-Y grid with the color-warmth representing the reservoir temperature.**

Where Kettel draws the anomaly as a north-west south-east trend (in Figure 21-a) the 2011 updated Groningen basin model study by Stevanovic (26) shows an East-West trend in the temperature high within the field, indicated by a red dotted line in Figure 22.



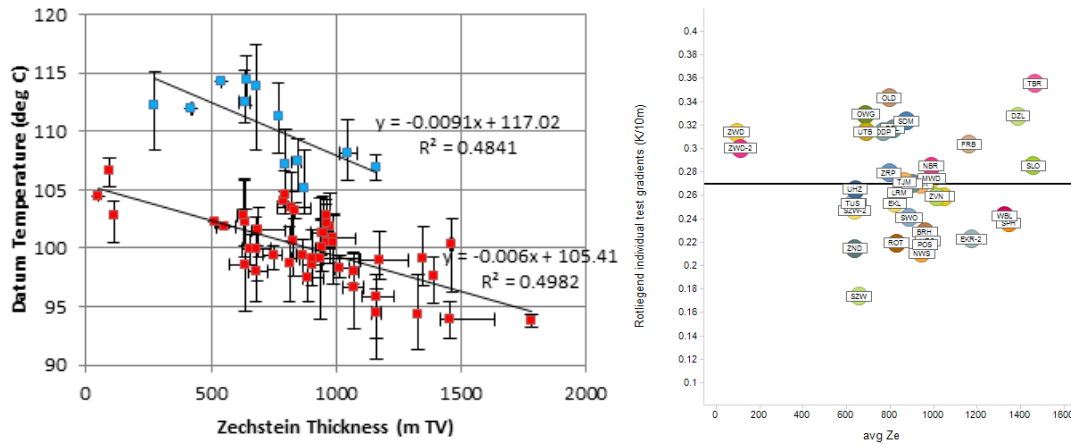


**Figure 24(a-b) a) Temperature correlation to the Zechstein thickness, taking the East Groningen Massif temperature anomaly into account (blue is Northern and red is Southern group). b) No correlation between temperature gradient and Zechstein thickness**

The average temperature gradient was used to convert SPTG temperature measurement to datum level<sup>1</sup> (Figure 21-b). Based on this dataset, a temperature map at datum depth was created by linear interpolation (Figure 25).

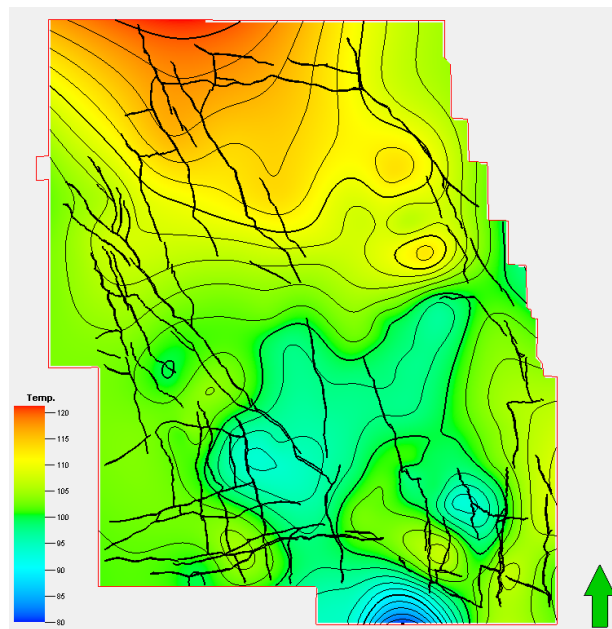


**Figure 25 temperature at datum level by linear extrapolation in Petrel of SPTG temperatures calculated to datum**

Based on the map in Figure 25 and using the average temperature gradient from Figure 24-b, a 3D temperature model was created in Petrel. Temperatures in the reservoir vary from 80°C to 120°C with an average reservoir temperature of 102.2°C (21). This model was exported to Dynamo and upscaled using volume averaging. The ultimate impact of the temperature variation is captured in the Dynamo model by assigning PVT models based on the average gridblock temperature (1 degree Celcius steps). Thermal convection and diffusion is not modeled.

<sup>1</sup> 2857m TVD NAP

### 3.4. Pressure table range

In order to capture the full field life range of reservoir pressures the PVT tables have a pressure range from 1 to 380 barA.

### 3.5. Gas Formation Volume Factor

The wet gas formation volume factor  $B_g$  is given by:

$$B_g = \frac{V_{res}}{V_{sc}} = \frac{Z_{res} T_{res} p_{sc}}{Z_{sc} T_{sc} p_{res}} v_{tot}$$

**Equation 9: Formation volume factor for gas.**

Where:

V = gas volume

Z = gas deviation factor [dimensionless]

p = pressure

T = absolute temperature (either [oK] or [oR])

vtot = volume correction for condensate and water dissolved in the gas [dimensionless]

res = reservoir conditions

sc = Standard conditions

### 3.6. Gas Deviation factor

The gas deviation factor, or Z-factor, is a function of pressure and temperature. De Loos (14) established a polynomial fit on the experimental data (at standard conditions) for the respective PVT regions:

$$Z = c_0 + c_1 p + c_2 T + c_3 p^2 + c_4 p T + c_5 p^3 + c_6 p^2 T + c_7 p T^2 + c_8 p^3 T + c_9 p^2 T^2$$

**Equation 10: Gas deviation factor as a polynomial in pressure and temperature based on a fit through 355 data points**

With:

Z = gas deviation factor [dimensionless],

p = pressure p [barA],

T = temperature [Celsius]

$c_i$  = fitting constant.

The fitting constants presented by De Loos were converted to pressures in bar and temperatures in Celsius, Table 5. The NAM standard reports gas at Normal conditions, see Table 4. Equation 11 gives a correction of the polynomial from Standard Conditions to Normal Conditions.

NAM Normal Conditions		
$p_{sc}$	1.01325	barA
$T_{sc}$	273.16	K

**Table 4: NAM standard conditions**

$$\frac{Z(0, T)}{Z_{sc}} = 1.002914$$

**Equation 11: Correction of the Z factor to NAM standard conditions.**

Gas deviation factors for Harkstede are reported for different 3 temperatures as function of pressure and Equation 10 is fitted to the results (16). Constants for the z factor for Usquert are imported from DREAM and neither temperature dependency nor temperature at which the experiments were performed is reported. The Annerveen Z-factor is reported for three temperatures (17), constants for Equation 10 are fitted to these results. Oude Pekela fitting constants are only available for pressure dependent terms and there is no reported temperature dependency, the measurements were performed at 102 °C (18). Bedum Z-factors are determined for pressures and temperatures (19). The polynomial fit to the data can be found in attachment 1 and the resulting constants Table 5:

Fitting constants $p$ in barA and $T$ in deg C						
	Groningen (14)	Harkstede (16)	Usquert (27)	Annerveen (17)	Oude Pekela (18)	Bedum (19)
$c_0$	1.00011	1.0094	1.003	1.0224	1.002	1.0057
$c_1$	-2.9718e-3	1.3436e-2	-8.020e-4	-3.5248e-3	-1.102e-3	-4.565e-3
$c_2$	-3.56573e-6	-3e-5	0	-1.5e-4	0	-1.68e-4
$c_3$	1.10854e-5	-2.8830e-5	3.777e-6	1.0119e-5	4.453e-6	1.8042e-5
$c_4$	2.84251e-5	-2.7708e-4	0	3.5517e-5	0	5.5167e-5
$c_5$	-8.06064e-9	-9.5613e-11	-2.696e-9	-4.6185e-9	-2.784e-9	-4.1477e-9
$c_6$	-8.99782e-8	6.1776e-7	0	-7.867e-8	0	-2.3115e-7
$c_7$	-7.84459e-8	1.3484e-6	0	-1.094e-7	0	-1.916e-7
$c_8$	4.79532e-11	-9.83e-12	0	1.917e-11	0	2.6215e-11
$c_9$	2.11836e-10	-2.9875e-9	0	1.96e-10	0	8.665e-10

**Table 5: Fitting constants for the polynomial of the deviation factor as function of temperature [°C] and pressure [barA].**

### 3.7. Gas Viscosity

No gas viscosity measurements are available for Groningen, nor any of the peripheral blocks. Similar to GFR2003 and GFR2012, the gas viscosity correlation by Lee and Gonzalez is used (28), which is given by Equation 12;

$$\mu_g = A_1 10^{-4} e^{A_2 \rho_g^{A_3}}$$

$$A_1 = \frac{(9.379 + 0.01607 M_g) \left(\frac{9}{5} T + 491.67\right)^{1.5}}{209.2 + 19.26 M_g + \left(\frac{9}{5} T + 491.67\right)}$$

$$A_2 = 3.448 + \frac{986.4}{\left(\frac{9}{5} T + 491.67\right)} + 0.01009 M_g$$

$$A_3 = 2.447 - 0.2224 A_2$$

**Equation 12: Lee and Gonzalez viscosity correlation for gas**

Where:

$$\mu_g = \text{gas viscosity [cP]},$$

$$M_g = \text{gas molar mass [g/mol]},$$

$$T = \text{temperature [degree Celcius]},$$

$$\rho_g = \text{gas density [g/cm}^3\text{]}.$$

Gas specific gravity ( $\gamma_g = \rho_g / \rho_{air,st}$ ) is calculated using air density at standard conditions (1.293 kg/m<sup>3</sup> (14)). The gas properties for the density and the molar mass are given in Table 6.

	Groningen (14)	Harkstede (16)	Usquert (27)	Annerveen (17)	Oude Pekela (18)	Bedum (19)
$\gamma_g$	0.644	0.640	0.652	0.612	0.610	0.636
$M_g$	18.65	18.53	18.88	17.96	17.649	18.62

**Table 6 Gas properties used in viscosity correlation**

### 3.8. Formation Water properties

There are limited water samples available for Groningen. Five samples were taken, one in BIR-1 (from 1963) and three in BIR-13B (from 1987) but these are incompletely analyzed (29). Based on the BIR-1 sample the formation water is fully salt saturated.

The formation water density is calculated based on the areal trend of the water gradient: 1.17 bar/10m, see GFR2012 (22). In 2015 water was extracted from the core drilled in the ZRP-3A well. Although contamination by drilling mud components may not be excluded this water has a very comparable composition to the BIR-13 samples with exception of the CL- content which is higher in BIR-13 (30). The viscosity of the water and the compressibility of the water are determined according to the Shell Production Handbook vol 4 (31) based on a salinity of 280,000 ppm NaCl equivalent, a tuning factor to compensate for the actual salt composition, and an average reservoir temperature of 100 degree C. The values are given in Table 7.

parameter	Value	Units
$\rho_w$ at $p=346.8$ barA, $T = 100$ deg C.	1172 (8)	kg/m <sup>3</sup>
$\rho_w$ at $p=1.01325$ barA, $T = 0$ deg C.	1225	kg/m <sup>3</sup>
Salinity	280,000	ppm
Water gradient	0.115	bar/m
Water viscosity at res conditions	0.58	cp
Water compressibility	$3 \cdot 10^{-5}$	1/bar

**Table 7 water properties used in the Groningen PVT models (from De Loos (14))**

The water density is calculated according to the Shell Production handbook (31) for Groningen average initial reservoir conditions<sup>2</sup> and surface conditions by Equation 13:

$$\rho_w = 1000.3 - 0.051T - 0.0038T^2 + [0.688 - 0.0021T + 0.0000149T^2]S + [0.0463 - 0.00019T + 0.0000018T^2 - 0.000051S]p$$

**Equation 13: Water density as a function of temperature, salinity and pressure**

Where:

$$\begin{aligned} \rho_w &= \text{water density [kg/m}^3\text{]}, \\ T &= \text{temperature [deg C]}, \\ S &= \text{salinity [kg/m}^3\text{]}, \\ p &= \text{pressure [barA]}. \end{aligned}$$

### 3.9. Volume Correction for Bg

In GFR2012 the condensed water was not modelled. A constant WGR was assumed for the Volume Correction of the Gas Formation Volume Factor. The increasing WGR with declining reservoir pressure was corrected for in the lift-curves.

<sup>2</sup>  $P_{res}=346.8$  barA and  $T = 102$  deg C.

For this model update the water and condensate dissolved in the gas phase are implicitly modeled as functions of respectively temperature and pressure.

Z factors were determined on treated gas samples from the outlet of a separator and contained hardly any condensate and free water according to de Loos (14). The liquid correction accounts the number of moles occupied by gas relative to the number of moles occupied by dissolved condensate and water. In order to correctly model the water production two fractions are defined for the gas phase, a dry fraction and a wet fraction. The dry gas fraction consists of the gas phase and the gas condensate dissolved in the gas. The volume correction of the dry fraction is expressed as:

$$v_{tot\_dry} = v_g + v_c$$

**Equation 14: volume correction for dry surface gas volume with condensate**

The wet gas fraction consists of the gas and condensate fraction and of the water dissolved in the hydrocarbon gas. The volume correction for the wet fraction is expressed as:

$$v_{tot\_wet} = v_g + v_c + v_w$$

**Equation 15: volume correction for the liquid yielding “wet” reservoir gas**

Which are the relative number of moles of gas, condensate and water. By definition,  $v_g = 1$ , and the other two fractions are given by Equation 16 and Equation 17.

$$v_c = \frac{mol_c}{mol_g} = \frac{\rho_{c,sc} V_m}{M_c} CGR$$

**Equation 16: Correction for amount of condensate moles dissolved in gas**

$$v_w = \frac{mol_w}{mol_g} = \frac{\rho_{w,sc} V_m}{M_w} WGR$$

**Equation 17: Correction for amount of water moles dissolved in gas**

Where:

$\rho$  = density (18)

$V_m$  = molar volume for gas,  $22.414 \times 10^{-3}$  m<sup>3</sup>/mol at NAM standard conditions (14)

$M$  = molar mass, all in SI units

CGR = condensate gas ratio [m<sup>3</sup>/m<sup>3</sup>]

WGR = water gas ratio [m<sup>3</sup>/m<sup>3</sup>]

$c$  = condensate

$w$  = water.

$g$  = gas

The values used for the volume correction are given in Table 8.

	Groningen (14)	Harkstede (16)	Usquert <sup>3</sup>	Annerveen (17)	Oude Pekela (18)	Bedum (19)
$\rho_c$	776	793	776	775	778	793
$\rho_w^4$	998	998	998	998	998	998
$M_c$	153	145.6	153	154.2	154.2	140
$M_w^5$	18	18	18	18	18	18
CGR	See Figure 26	2.5	1	40	18.6	9

**Table 8 Properties used for volume correction of different models**

### 3.10. Condensate Gas Ratio

During the Groningen Long Term project (1999-2009) Coriolis meters were installed on all clusters, allowing constant measuring the produced liquid ratio. Before the GLT project liquids were periodically measured by 24h tests in which all liquids were collected for a known maximum gas rate.

The condensate gas ratio (CGR) is modelled based on a linear fit to historical data. Both Vos (15) and Vink (32) show that the condensate gas ratio in the field decreases with pressure. Vos proposes a 4<sup>th</sup> order polynomial fit for the cumulative condensate production as a function of P/Z. However this polynomial will strongly break with the decreasing CGR trend at low pressures. A linear fit seems sufficient when extrapolating the CGR as a function of the P/Z for Groningen results, see Figure 26.

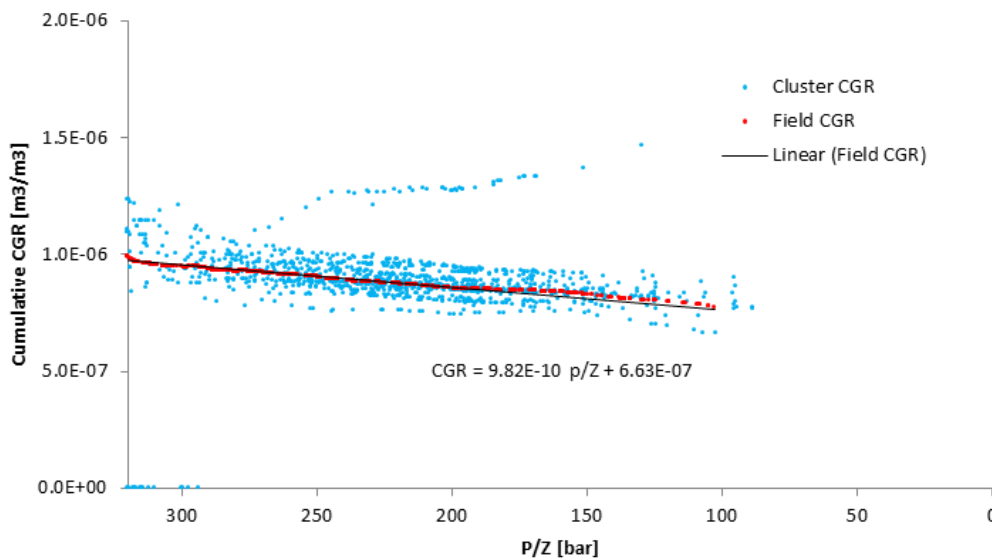


**Figure 26 In blue ratio of cumulative produced condensate over cumulative produced gas (from EC) as function of p/z (from Siesta). In red Groningen field cumulative CGR as function of average field pressure excluding EKL data due to changing gas composition.**

Explaining the decrease in condensate is speculative at this time. Vink investigated the accuracy of the measurements and found that the decline is true and not due to measurement error (33). Since heavier hydrocarbon components are underrepresented in the gas samples taken in the Groningen field, the PVT analysis is not representative for condensate (15).

If the condensate fraction seen at surface is decreasing the missing fraction must stay behind in

<sup>3</sup> Assumed equal to Groningen

<sup>4</sup> Assumed the same for all PVT models

<sup>5</sup> Assumed the same for all PVT models

the reservoir or the well. The liquid fraction will drop out of the gas phase below dew point pressure. However, no phase envelope for the Groningen gas is available. Neither downhole samples nor combined samples have been analysed and the dew point pressure for the Groningen gas is unknown.

No measurements of the dew point are available for the Groningen field. Combined samples are available for Harkstede, Bedem and Annerveen, and dew points were analysed on Harkstede and Annerveen samples. Harkstede gas shows a dew point of 171barA for a CGR of 40 m<sup>3</sup>/mln m<sup>3</sup> and for Annerveen combined samples show a dew point pressures range from 186 barA to 296 barA, for CGR of 10 m<sup>3</sup>/mln m<sup>3</sup> to 33 m<sup>3</sup>/mln m<sup>3</sup>. However these dew point values are not relevant for the Groningen field, due to the significantly different CGR with respect to the Groningen CGR.

Without a subsurface sample it is not possible to define a correct fluid model that would describe the decline seen in the Groningen CGR. Therefore the linear trend observed in historical CGR, Figure 26, is used for CGR forecasts.

### Modelling

The dynamic model calculates the reservoir pressure as a function of cumulative offtake and a polynomial function is available for the Z-factor as a function of pressure, see (34). The cumulative CGR is defined as:

$$CGR_{cum}(t) = \frac{N_p(t)}{G_p(t)}$$

**Equation 18 cumulative condensate gas ratio as function of time, equals the cumulative condensate production over cumulative gas production**

where:

$CGR_{cum}$  is the cumulative condensate gas ratio as function of time

$N_p(t)$  is the cumulative condensate production as function of time

$G_p(t)$  is the cumulative gas production as function of time

A well-established trend is available for the cumulative condensate gas ratio as a function of pressure over gas expansion factor ( $p/Z$ ) from Figure 26:

$$CGR_{cum}(t) = c_1 \frac{p(t)}{z(p)} + c_2$$

**Equation 19 cumulative condensate gas ratio as function of time, equals a linear fit to the decline with decreasing pressure over the gas expansion factor**

where:

$c_1$  is a fitting constant to historical data

$c_2$  is a fitting constant to historical data

$p(t)$  is the field average pressure as a function of time

$z(p,T)$  is the gas expansion factor as function of field average pressure and field average temperature 102.2 °C see (34).

However, the cumulative CGR cannot be directly used for forecasting, this requires the instantaneous CGR:

$$CGR(t) = \frac{q_{cond}(t)}{q_{gas}(t)}$$

**Equation 20 condensate gas ratio as function of time, equals the condensate rate over the gas rate**

where:

- CGR(t) is the condensate gas ratio as function of time
- $q_{cond}(t)$  is the condensate production as function of time
- $q_{gas}(t)$  is the gas production as function of time

The condensate and gas production rates can be obtained from simple newton differentiation of their cumulative productions over time.

$$q_{cond}(t) = \frac{N_p(t) - N_p(t - \Delta t)}{\Delta t} \quad , \quad q_{gas}(t) = \frac{G_p(t) - G_p(t - \Delta t)}{\Delta t}$$

**Equation 21 condensate calculated by deriving cumulative condensate production over discrete timesteps, and ditto gas production.**

where:

$\Delta t$  is a discrete timestep

Hence the condensate gas ratio can be determined:

$$CGR(t) = \frac{N_p(t) - N_p(t - \Delta t)}{G_p(t) - G_p(t - \Delta t)}$$

**Equation 22 cumulative condensate gas ratio as function of time calculated by combination of Equation 21**

The smoothness of the results obtained by this method depends on the length of the time step  $\Delta t$ , where short time steps could cause high amplitudes in the results and long time steps will smooth the results, see Figure 27. For the yearly cycle of business planning a yearly time step is most likely sufficient.

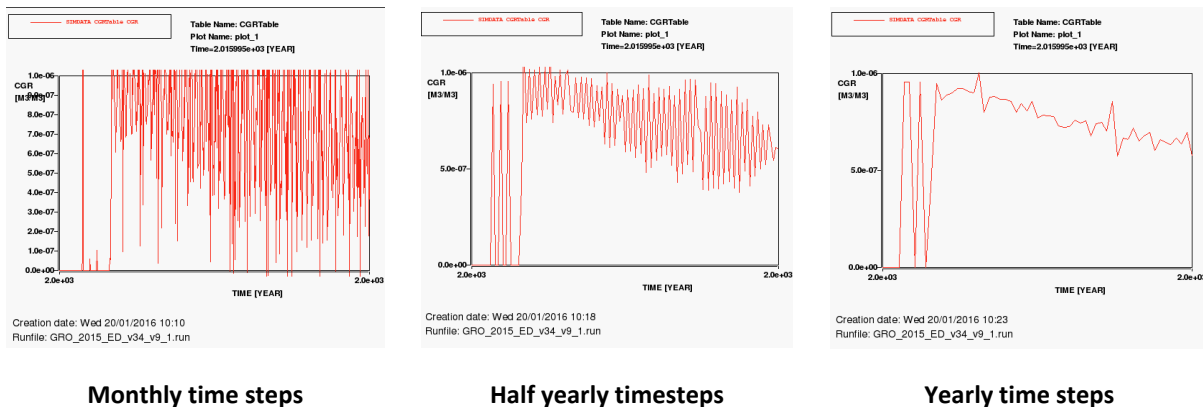


**Figure 27 Effect of time step size in numerical integration on the CGR**

Figure 28 shows the modelled output versus the historical data for the gas condensate rate and the cumulative condensate production. Results based on simulated output on a history matched model of the Groningen field show a satisfactory match to historical data from the NAM-Energy

Components data base. A fit to the data is iteratively achieved by changing the constants in Equation 19. The results below are based on the following constants:

$$c_1 = 7.2^{-10}$$

$$c_2 = 7.34^{-7}$$

The resulting CGR of this model is shown in Figure 29.

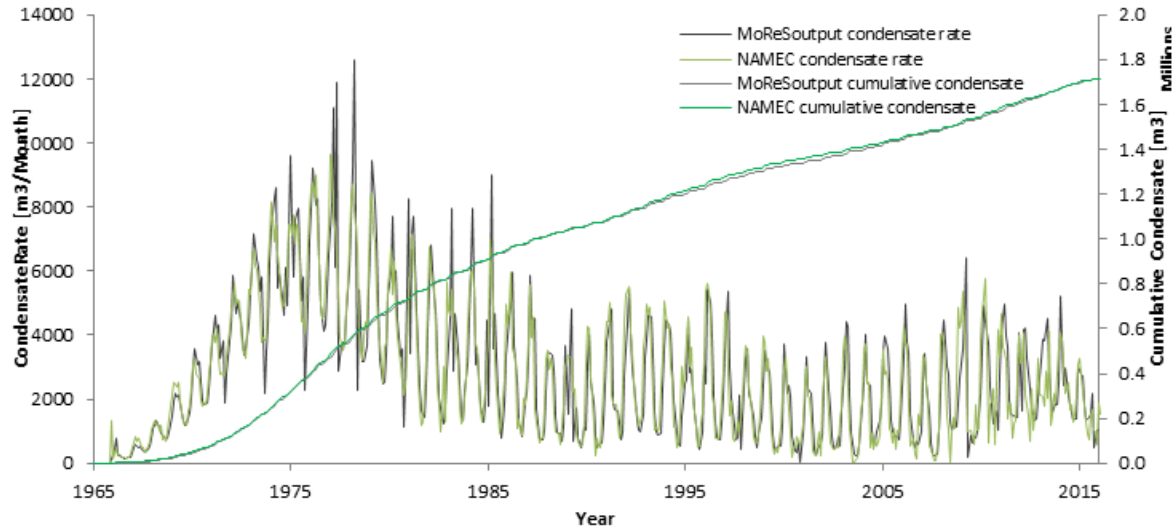


Figure 28 comparison between NAMEC data and MoReS model output for the condensate rate and cumulative condensate production

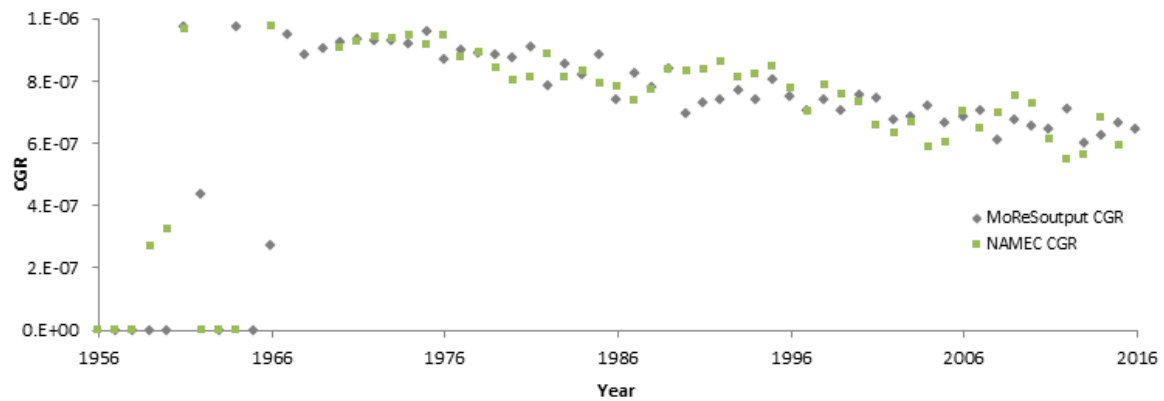


Figure 29 CGR ratio from NAMEC compared to output from the MoReS model for yearly time steps in the calculation

### 3.11. Water Gas Ratio

The water gas ratio (WGR) is modelled according to the Wehe-McKetta Correlation (28):

$$WGR = 135 \frac{Y_w}{1 - Y_w}$$

$$Y_w = A_s A_g p^{\left(\frac{142.3}{T+460} - 1.117\right)} e^{\left(\frac{0.05227p - 9625}{T+460} + 16.44\right)}$$

$$A_s = 1 - 3.92 \cdot 10^{-9} S^{1.44}$$

$$A_g = 1 + \frac{\gamma_g - 0.55}{15500 \gamma_g T^{-1.446} - 18300 T^{-1.288}}$$

**Equation 23: Wehe-McKetta correlation for the water gas ratio**

With:

p = pressure [psi],

T = temperature [degree F],

S = NaCl equivalent salinity of the formation water [ppm],

 $\gamma_g$  = gas specific gravityWGR = Water Gas Ratio [bbl/mln ft<sup>3</sup>].

Implicitly modelling the dissolved water fraction as the wet phase results in the WGR match shown in Figure 30.

Wehe-McKetta determined the solubility of water with an NaCl solution in pure methane. The Groningen water samples show different salt compositions and the Groningen gas is contaminated by other gasses. To correct for this the salinity was adjusted by a fitting constant to achieve a match. The match of the model to historical data is shown in Figure 30.

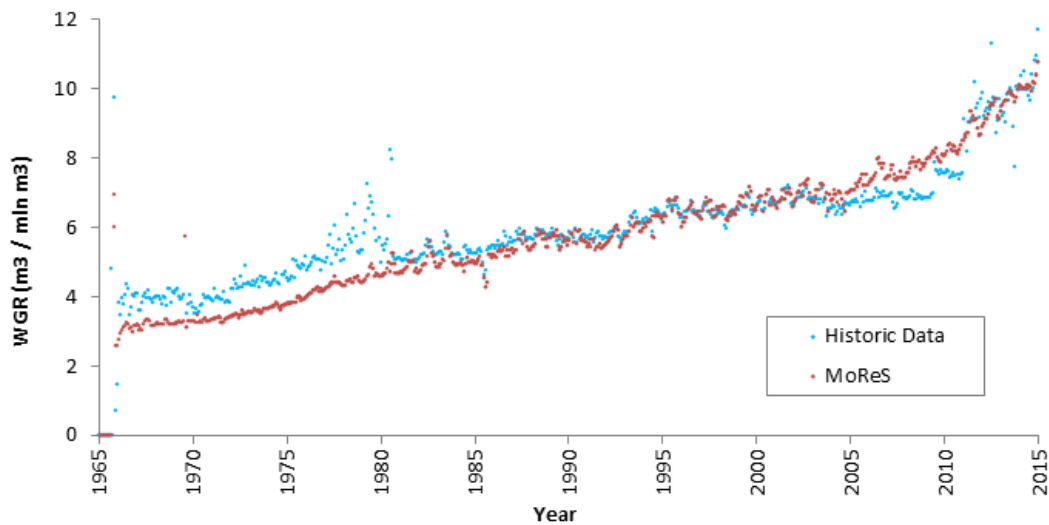


**Figure 30** Achieved model match of the water gas ratio to the measured ratio

## 4. Reservoir Initialisation

### 4.1. Hydrostatic Initialisation

For the 2015 dynamic model update the area of investigation has been significantly enlarged, mostly to the west, in order to improve prediction of pressure depletion and subsidence. The city of Groningen is of particular interest in that respect, located towards the south-west of the model. In Figure 31 the gas saturation in top Slochteren is depicted along with the additional land assets that are now included as a result of enlarging the model area.

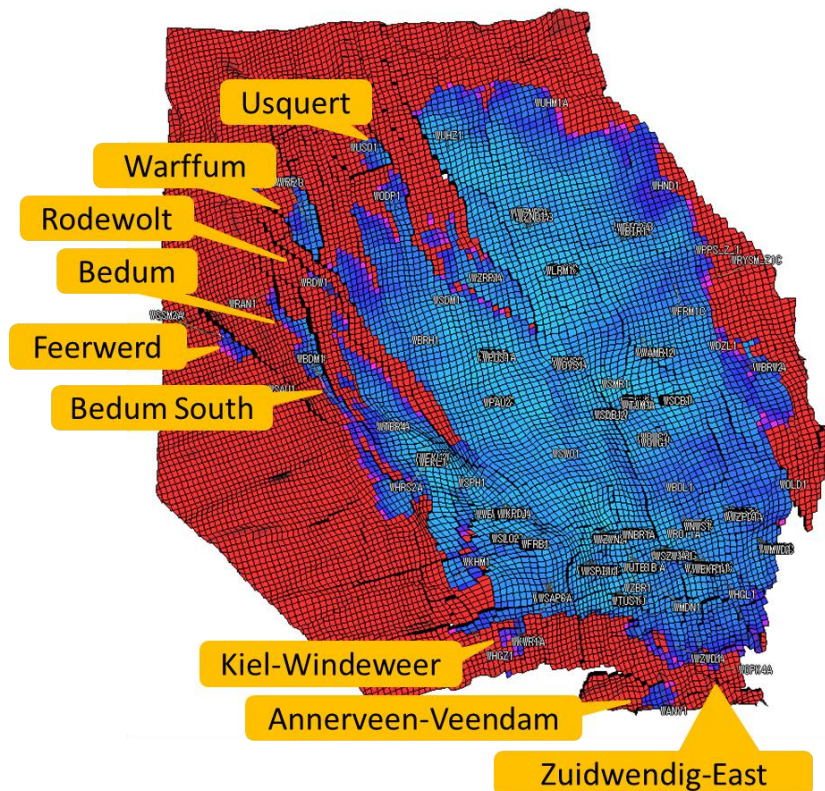


**Figure 31 Model area depicting extent of gas saturation at top Slochteren. In addition to the Groningen field modelled land asset field are also shown.**

The PVT models used for initialization are described in detail in (35), binned to 1° Celcius temperature classes, with a variation from about 80 to 120° C. Correct properties are assigned to all individual fields modelled. Each field is subsequently initialized hydrostatically assuming capillary equilibrium. The capillary pressure models are derived from the Brooks-Corey saturation height model described in (36), binned to 1 percent porosity classes.

The initial pressure in Groningen at the free water level (FWL) is assumed to follow a hydrostatic gradient of 0.117 bar/10 m. This is consistent with the water density model described in (35). However, there is not a single contact level across the Groningen field even though all parts are in pressure communication (37). No significant changes to compartments or FWLs are introduced for this work compared to the 2003 and 2012 dynamic models (38). The set of FWLs are determined from a combination of open-hole logs, RFT and SPTG measurements, see Table 9 and Figure 32. For the additional land fields, contact information is obtained from the corporate database, with a single level for each field, Table 10.

South-West	2995 m
South-East	3006 m
Central	2992 m
East	2972 m
North-East	2978 m
North-West	2984 m
Eemskanaal	2996 m
Harkstede (including Kolham)	3016 m
Hoogezand	3030 m
Oldorp	2967 m
Zuidwending	3017 m

**Table 9 FWL in the Groningen field. All depths are in TVNAP**

Annerveen-Veendam	3035 m
Bedum-South	3002 m
Bedum	3002 m
Rodewolt	3145 m
Usquert	2972 m
Zuidwendig-East	3006 m
Feerwerd	3473 m
Kiel-Windeweer	3303 m
Warffum	3049 m

**Table 10 FWL in modelled land asset fields. All depths are TVNAP.**

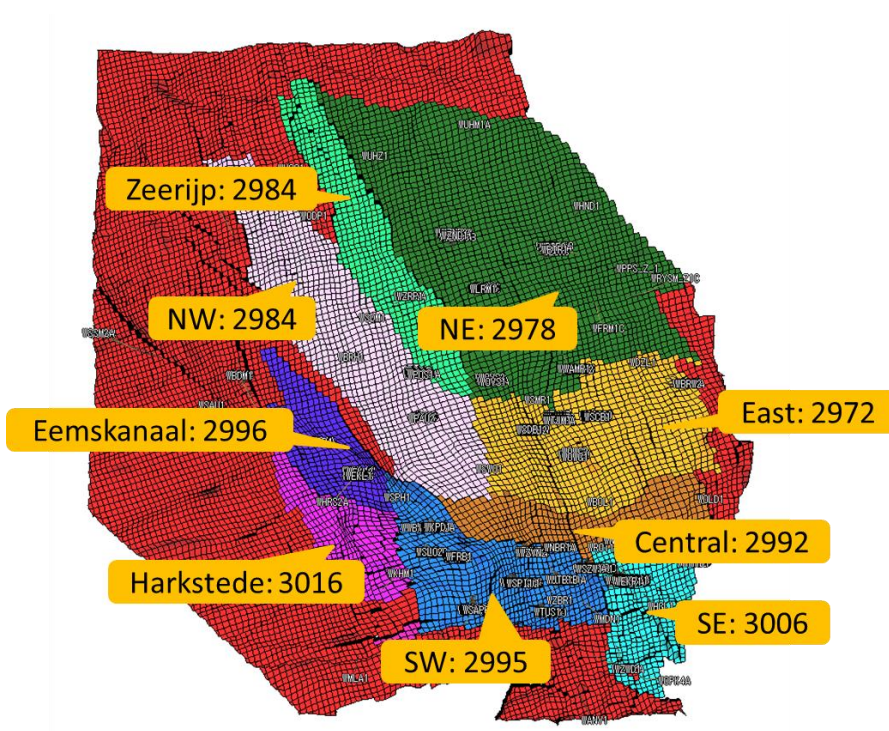


**Figure 32 FWL in Groningen compartments. All depths are meters TVNAP**

Following initialization the pressure at datum, 2875 m TVNAP, is 347 bara across the entire model area. The gas initially in place (GIIP) values are listed in Table 11 and Table 12 for Groningen and land fields. Please note that the values listed for the land fields are not necessarily close to those endorsed by the land asset due to the approximate nature of this modelling.

Groningen Total	2,925 BCM
South-West	355 BCM
South-East	121 BCM
Central	207 BCM
East	465 BCM
North-East	970 BCM
North-West	495 BCM
Zeerijp	91 BCM
Eemskanaal	131 BCM
Harkstede	17 BCM
Kolham	48 BCM
Hoogezand	4 BCM
Oldorp	6 BCM
Zuidwending	16 BCM

**Table 11 Groningen Gas Initially In Place according to dynamic model**

Annerveen-Veendam	1.8 BCM
Bedum-South	2.2 BCM
Bedum	11.3 BCM
Rodewolt	1.8 BCM
Usquert	2.5 BCM
Zuidwendig-East	0.9 BCM
Feerwerd	0.8 BCM
Kiel-Windeweer	0.7 BCM
Warffum	12.3 BCM

**Table 12 Land asset fields Gas Initially In Place according to dynamic model**

#### 4.2. Stability of Initialisation

While the main input to the history matching process is agreement to pressure, PNL and subsidence data, the model should also be checked to ensure that the hydrostatic initialization remains stable in time. It is clear that all parts of the Groningen field are in pressure communication, although many of the faults act as baffles between the different initialization regions (Figure 32). Without a properly defined static model and appropriate fault properties, one could expect that the contact depths defined in Table 9 would eventually equilibrate to a single value. To validate the stability of the initialization, the model has been simulated for 1000 years without any production. In Figure 33 the gas water contact (GWC) at various locations is depicted as a function of time. The actual values might not be exactly the same as listed in Table 9 since they are based on a grid block gas saturation threshold of 35 percent. However, it is the trend over time that is important. The well locations shown are focusing on the periphery and the north of the field. To the south and in the centre, the FWL is located in the Carboniferous which is not part of the model. The regional extent where an initial GWC exists within the model is shown in Figure 34.

From Figure 33 it is clear that the GWC in the different regions do show sufficient stability for the purposes of dynamic modelling. Only in the northern part of the Harkstede block (Eemskanaal-13 well location) is there some movement of the contact due to equilibration with the Eemskanaal region. However, the process is quite slow and the contact remains stable within the timeframe where the field is under production.

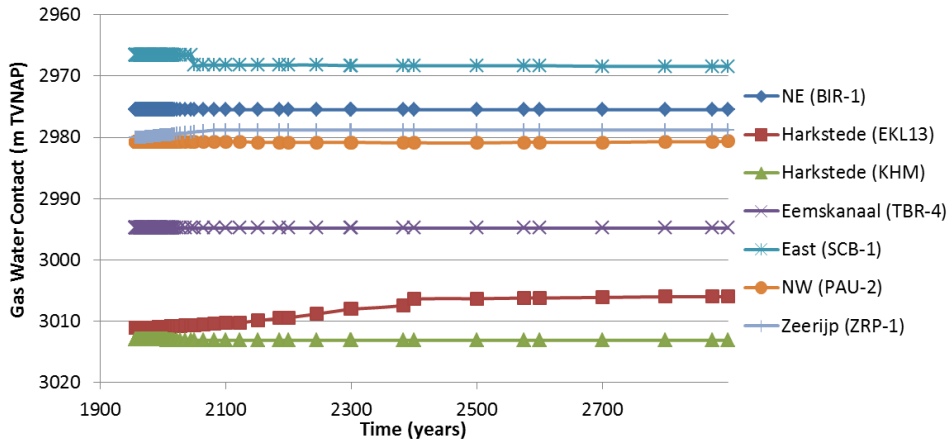


Figure 33 Stability of GWC in selected regions over a simulation period of 1000 years

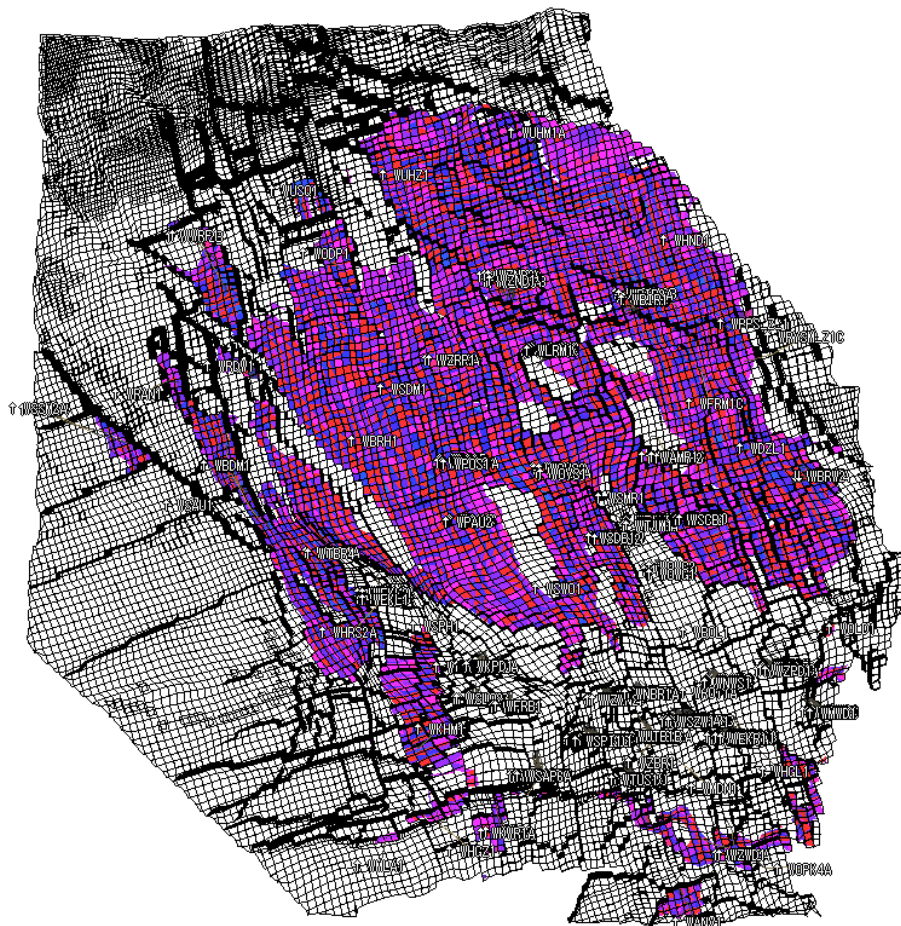
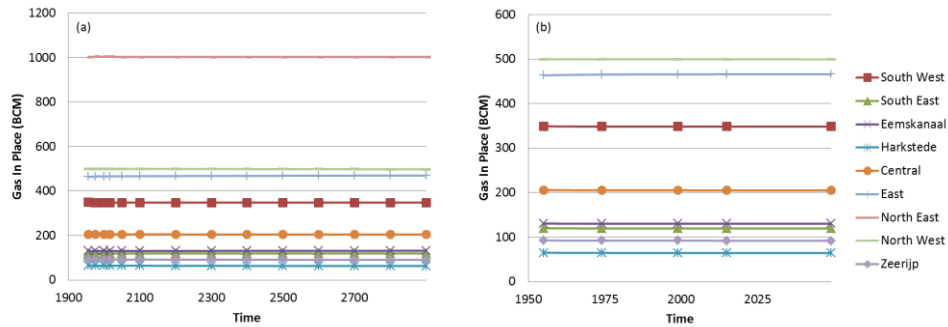


Figure 34 Regional extent where an initial GWC exists within the Slochteren formation

The different FWLs will also cause minor pressure differentials between the regions since the gas gradient is significantly different from that of the water. Movement of gas between the regions should thus also be ensured to be acceptable.



**Figure 35 Gas in place per region as a function of time. Using a single PVT model. (a) shows all regions for the entire 1000 years simulation period whereas (b) is a zoom-in at the production lifetime**

In Figure 35 the gas in place per region is shown using a single PVT model (assuming a 100° C reservoir temperature). Any lateral gas movement is thus only due to different FWL in the regions. No significant movement of gas is apparent on either a long or short time-scale. The biggest change is about a 3 BCM influx of gas to the eastern region (which has the shallowest FWL) during the production life-time of the field. In relative terms, the Harkstede region (which has the deepest FWL) has the biggest change with an outflow of about 1 percent of GIIP (0.7 BCM). For this analysis the Harkstede region includes the Kolham blocks.

Multiple PVT models linked to temperature variation is another possible cause for gas movement since the gas density will vary between the models. The same 1000 year simulation is done for this case, with the results shown in Figure 36. No significant changes compared to the single PVT region case are observed.

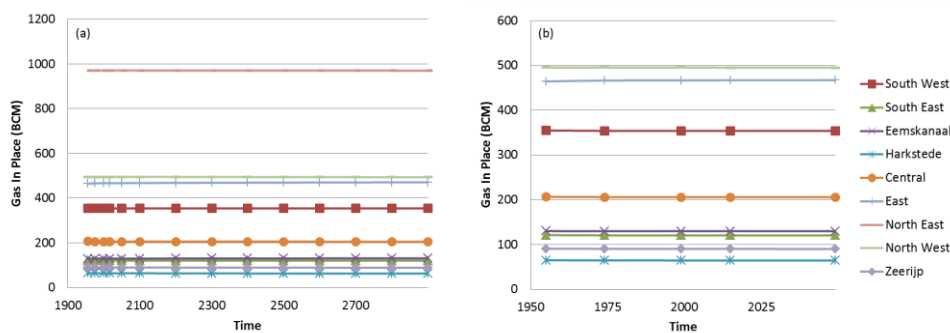


**Figure 36 Gas in place per region as a function of time. Multiple PVT models exist, binned to 1° C variation in reservoir temperature. (a) shows all regions for the entire 1000 years simulation period whereas (b) is a zoom-in at the production lifetime**

### 5. Subsidence proxy

One of the main deliverables of the GFR2015 dynamic model update is to achieve a subsidence match in addition to the more conventional dynamic model history match for the Groningen field, i.e. reservoir pressure data and gas-water contact movements match. To facilitate the subsidence history matching process of the Groningen model a subsidence proxy has been built in MoReS, see Figure 37. The subsidence proxy calculation is approximate, fast and integrated. The proxy will guide history matching and be used in the uncertainty management workflow. Once a limited number of sufficiently different model realisations are history matched the final selection will be made using the subsidence calculations done by the NAM geomechanics team. Matching subsidence data is a direct match to data contrary to matching to for example reservoir compaction. The MoReS subsidence proxy has been agreed and tuned sufficiently to the geomechanics team subsidence results. The subsidence proxy (2D) does not impact the numerical performance of the dynamic model much. Subsidence data is distributed over the field (spatial data) and recorded over time (epochs). Spatial reservoir compaction is subject to interpretation and needs to be calculated (39).

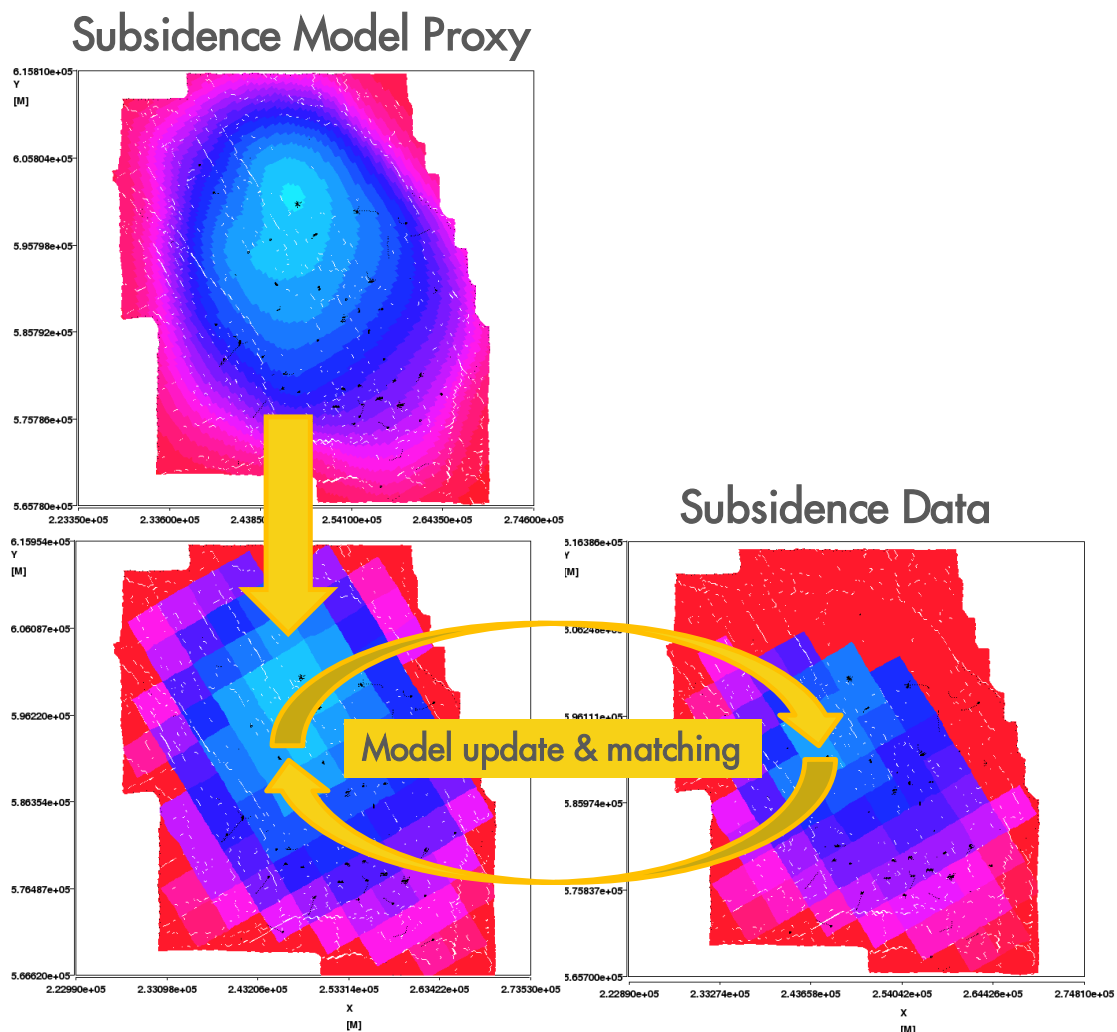


Figure 37 Subsidence Proxy workflow

## 5.1. Theory

A screening calculation to give an estimate of the subsidence for the deepest point of the compaction bowl is given by Equation 24 by J. Geertsma (40). Using a  $c_m$  estimate from data of semi-consolidated sandstone at a depth of burial of 3000m ( $1 \cdot 10^{-5}$ /bar), pressure reduction ( $\sim 300$  bar) and thickness of the compacting interval (150-300m) the estimated maximum reservoir compaction ranges between 50-100 cm, from:

$$\Delta H = \int_0^H c_m(z) \Delta P(z) dz$$

**Equation 24: maximum reservoir compaction as function of uniaxial compressibility and pressure depletion**

Where:

- $\Delta H$  reservoir compaction
- $C_m$  uniaxial compressibility
- $H$  initial thickness of the depleting reservoir
- $\Delta P$  pressure drop in the depleting reservoir

An analytical estimate of the maximum subsidence due to reservoir compaction is given by Equation 25 (41):

$$u_{z0} = 2(1 - \nu) \left( 1 - \frac{Z}{\sqrt{1 + Z^2}} \right) \Delta h \quad (1)$$

- where:  $u_{z0}$  = surface subsidence above the centre of a disc-shaped reservoir surrounded by rock with the same elastic properties
- $\nu$  = Poisson's ratio
- $Z$  = ratio of reservoir depth  $c$  over reservoir radius  $R$
- $\Delta h$  = reservoir compaction, calculated separately<sup>1,3,4</sup>

**Equation 25: analytical estimate of the maximum subsidence due to reservoir compaction**

When using the same reservoir compaction ( $c_m \Delta P H$ ), the subsidence estimate becomes 60-120 cm.

The article "A numerical technique for predicting subsidence above compacting reservoirs, based on the nucleus of strain concept" by J. Geertsma and G. van Opstal from June 1972 (42) gives a description to calculate spatial subsidence distribution pattern above a compacting reservoir of arbitrary shape. This paper estimates that the maximum vertical surface depression above the Groningen field at the end of the productive lifetime of the field will be 75-100 cm.

The model is based on the linear elastic theory of the nuclei of strain in a homogeneous half-space. The model assumes uniform elastic properties for the reservoir and overburden. The reservoir compaction results in a continuous subsidence bowl.

$$u_z(x, y, 0) = - \frac{c_m(1-\nu)}{\pi} \sum_{n=1}^N \Delta p_n \frac{c_n \xi_{xn} \xi_{yn} \xi_{zn}}{[(x-\xi_n)^2 + (y-\eta_n)^2 + c_n^2]^{3/2}} \quad (4)$$

**Equation 26: numerical calculation of subsidence above a compacting reservoir**

The above equation was implemented in MoReS input language. For easier readability some parameters are re-named and the compressibility of each gridblock is included in the summation term:

$$u_z(x, y, 0) = \frac{1 - \nu}{\pi} \sum_{n=1}^N c_{mn} \Delta P_n \frac{L_{zn} l_{xn} l_{yn} l_{zn}}{\left[ (x - L_{xn})^2 + (y - L_{yn})^2 + L_{zn}^2 \right]^{\frac{3}{2}}}$$

**Equation 27: numerical calculation of subsidence above a compacting reservoir rewritten**

where:

- $u_z(x, y, 0)$  vertical displacement at surface, i.e. subsidence (m)
- $x, y$  surface coordinates (m), whereby  $z=0$
- $\nu$  Poisson ratio (ratio of transverse to axial strain. When a material is compressed it usually expands in the two directions perpendicular to the direction of compression)
- $c_{mn}$  uniaxial compressibility of each gridblock (1/bar)
- $\Delta P_n$  pressure change in each subsurface gridblock, for the compacting layer (bar)
- $L_{zn}$  depth of the subsurface gridblock (m)
- $L_{xn}, L_{yn}$  distances in the  $x, y$  direction respectively from the surface location to the subsurface gridblock (m)
- $l_{xn}, l_{yn}, l_{zn}$  dimensions of a subsurface gridblock, hence  $l_{xn} * l_{yn} * l_{zn}$  equals the gridblock volume GBV[<g>] in MoReS

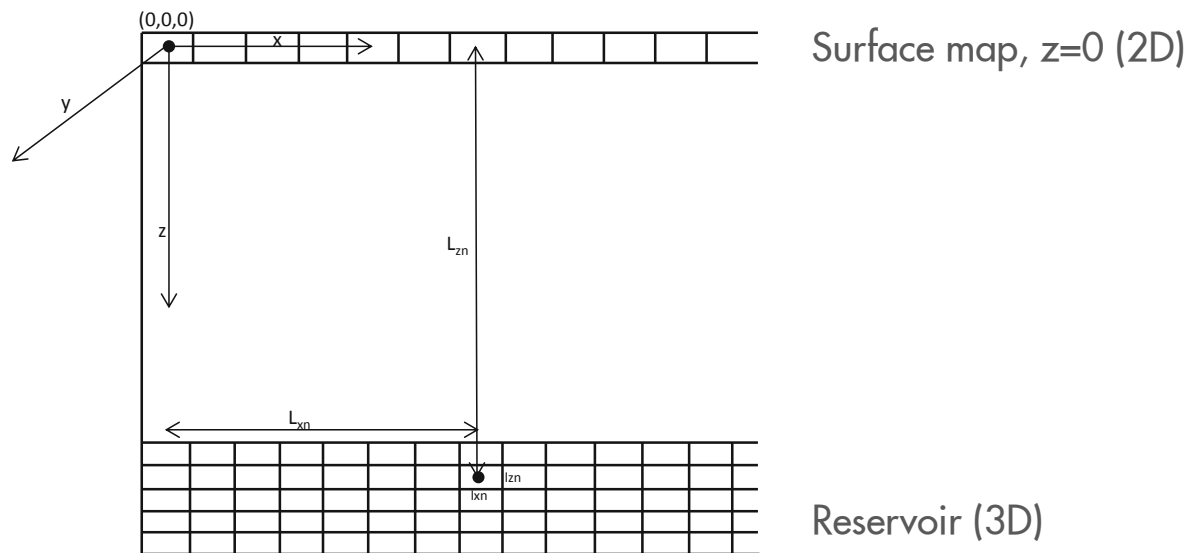


**Figure 38 schematic of subsidence modelling**

This analytical equation for subsidence  $u_z(x, y, 0)$  can be split into three parts:

- The part before the sum, where the Poisson ratio determines how much of the reservoir compaction is contributing to subsidence
- The first terms inside the sum, compressibility and pressure drop. This is partly the linear reservoir compaction equation:  $\Delta h = c_m h_{initial} \Delta P$  but without the reservoir height. The lateral dimensions of a reservoir are large compared to its height and the reservoir will deform predominantly in the vertical direction. Hence the uniaxial compressibility is considered most representative of the reservoir compaction process.
- The last part is geometry, for each gridblock there is a contribution to a single surface location. When the subsurface gridblock is directly below the surface location the

contribution to subsidence is largest and the contribution becomes smaller and smaller the larger the gridblock distance is away from the surface location. The deeper the subsurface gridblock the smaller the contribution to subsidence.

Shell’s SUBCAL tool, used by the NAM geomechanics team, is based on equations described in an article by G. van Opstal “The effect of base-rock rigidity on subsidence due to compaction” from November 1972 (43). The rigid basement model has more complex formulas than the nucleus of strain model as used in the scripts made for the MoReS subsidence proxy.

**5.2. Assumptions and Compressibility**

Using the subsidence proxy in MoReS the procedure described the Production Handbook volume 3 (page 261) can almost be followed to start simple and make it more complex when required.

A Poisson ratio of 0.25 is used.

The relation between the pore volume compressibility and the uniaxial compressibility is (44):

$$CR = \frac{c_m}{\phi}$$

**Equation 28: pore compressibility as function of uniaxial compressibility and porosity**

where:

- CR pore compressibility (MoReS input)
- $c_m$  uniaxial compressibility in  $10^{-5}$  /bar
- Assuming a Biot alpha of 1.0

Estimates of the compressibility of different types of rock are provided in Table 13. For Groningen, a well consolidated sandstone reservoir, the compressibility values range between  $0.3-1.2 \cdot 10^{-5}$ /bar. This is a lower compressibility than given in the paper from J. Geertsma (40).

**Table 13 Range of compressibilities (from Shell Production Handbook 3, Table 9.2-1**

*Table 9.2-1 Range of compressibilities and  $\beta$  for various rock types*

Rock type	Porosity Range (%)	$c_{m,o}$ $10^{-5} \text{ bar}^{-1}$	$c_{m,o}$ $10^{-7} \text{ psi}^{-1}$	$\beta$
Tight Sandstone	0-5	0.1-0.5	0.7-3.5	1.0-0.3
Well Consolidated Sandstone	5-30	0.3-1.2	2-9	0.3-0.1
Friable Sandstone	15-35	1-5	7-35	0.1-0.03
Unconsolidated Sandstone	25-40	4-30	30-200	0.03-0
Carbonate	15-25	0.4-2.5	2.8-17	0.2-0.03 *)

\*) It should be noted that after pore collapse in carbonates (see 9.2.3) the  $c_{m,o}$  value becomes much higher, in which case  $\beta$  becomes insignificant.

It is noted in the Shell Production Handbook volume 3, page 266 (44) that the core derived compressibility values may be higher than those observed in the field. This is thought to be due to the non-native state of the core material and possibly due to core damage not obvious from visual inspection. Care has to be taken therefore in the use of compressibility data derived from

core analysis. The core data derived  $c_m$  may be pessimistic resulting in more reservoir compaction and consequently more subsidence.

The GFR2012 dynamic model used the  $c_m$  from first cycle core data (22). A third order polynomial fit as function of porosity has been used. Instead of a constant of 0.63 as indicated in Figure 39, a base case constant of 0.58 is used in the model:

$$CR = c \left( 31.647327 \phi^2 + 62.719381 \phi - 9.654187 + \frac{0.664682}{\phi} \right) 10^{-5}/bar$$

**Equation 29: A polynomial fit of rock compressibility as a function of porosity**

The GFR2012 uncertainty range used is  $c$  from 0.50 (min) to 0.58 (base case) to 1.0 (max). However this subsurface uncertainty parameter has been screened out in the GFR2012 models (BP12, the winningsplan 2013 models, GFR2013 BP14 model and ARPR) because it only has a small impact on the history match quality (tornado screening on RMS field pressure).

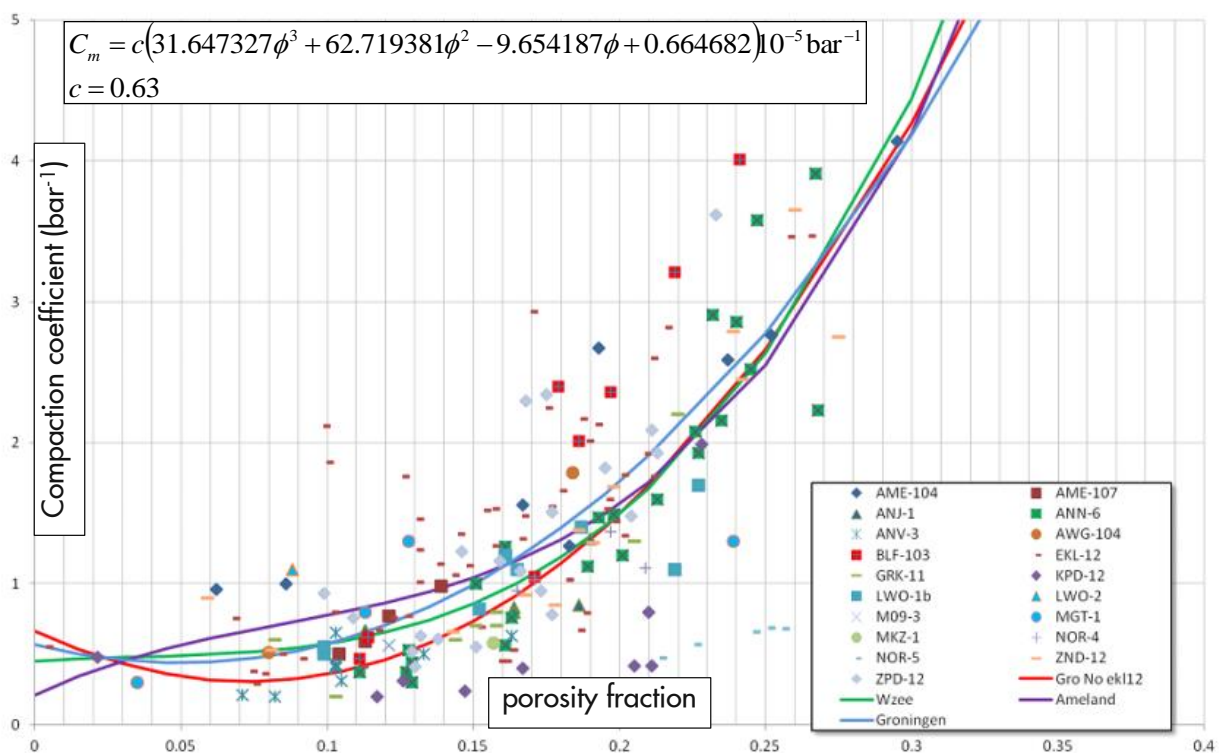
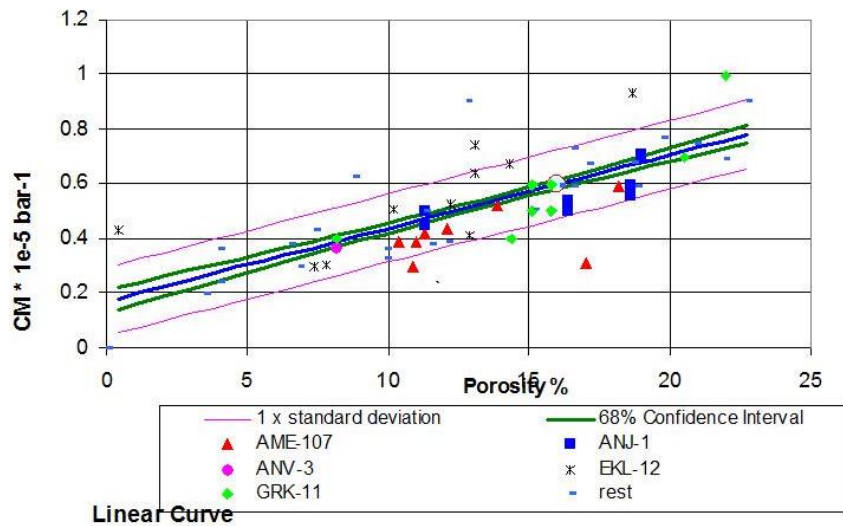


**Figure 39 Uniaxial compressibility coefficient relation versus porosity based on first cycle  $c_m$  core data, from (22) The constant which has been used in the GFR2012 models is  $c=0.58$  instead of the  $c=0.63$  as noted in the plot**

The GFR2003 dynamic model used a compressibility relation from the second cycle  $c_m$  data, see Figure 40. The compressibilities of the second cycle measurements are lower. This data was used for the Winningsplan submission of 2003 with the linear equation:

$$CR = \left( 2.6918 + c \frac{0.16946}{\phi} \right) 10^{-5}/bar$$

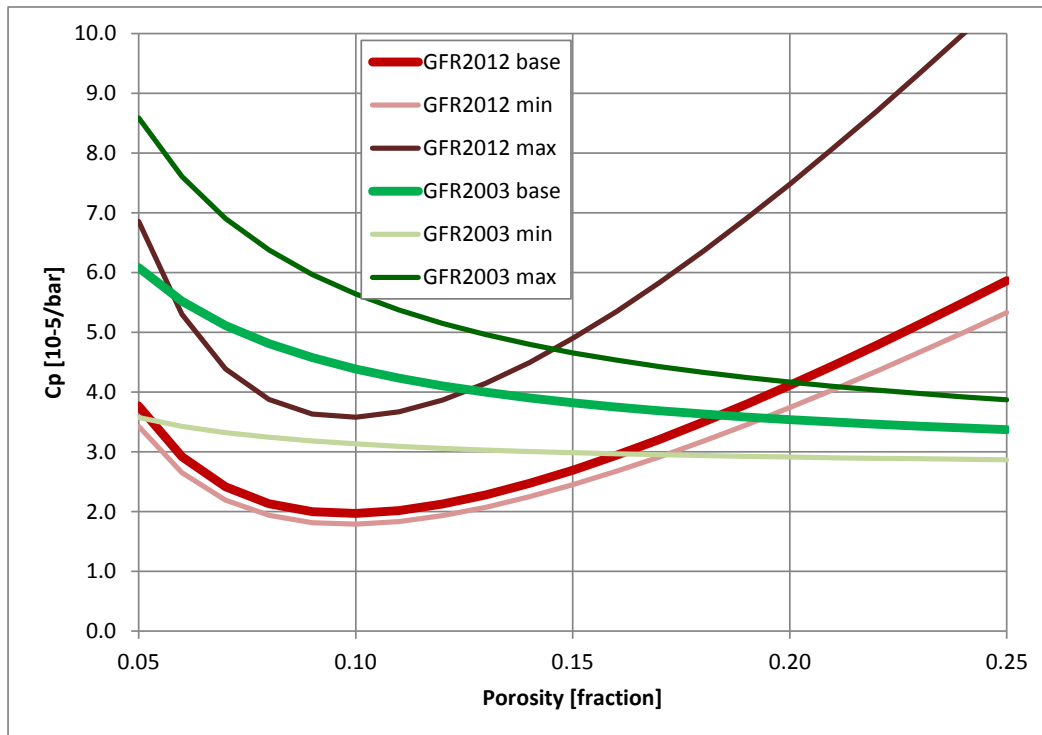
**Equation 30: Rock compressibility as function of porosity**



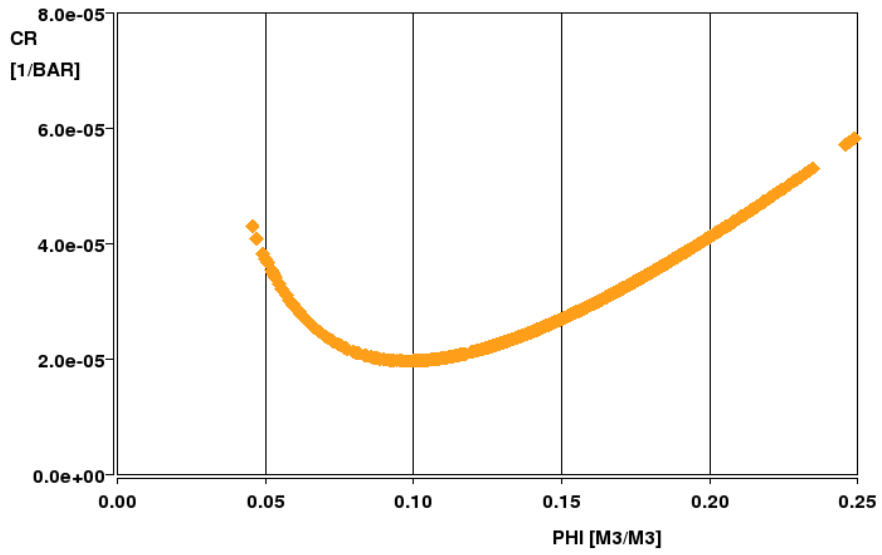
**Figure 40 Compressibility coefficient relation versus porosity based on second cycle cm core data (45)**

Figure 41 gives a comparison of the pore compressibility used as input for the GFR2003 and GFR2012 models. As shown in the cross-plot Figure 42 the red curve is implemented correctly. The pore compressibility of the GFR2003 is decreasing with increasing porosity (because the linear relation with the  $c_m$ ). Below a porosity of 10% the GFR2012 function follows the same trend as the GFR2003. For a higher porosity the GFR2012 trend is reversed.

In the model most porosity values fall between 0.1 and 0.2 see Figure 43. In this porosity range the compressibility of the GFR2003 model is higher than what is used for the GFR2012 model.



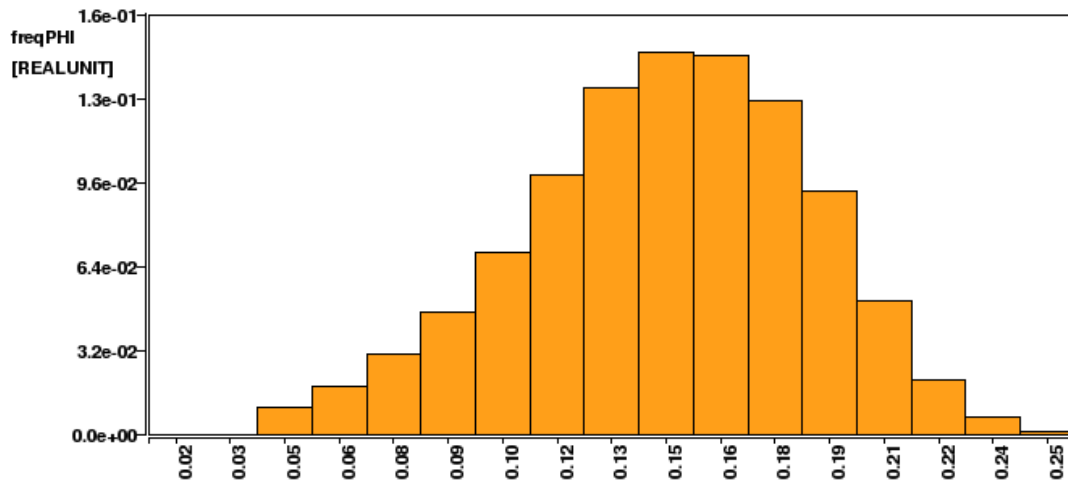
**Figure 41 comparison of pore compressibility (MoReS input) between GFR2003 (green) and GFR2012 (red)**



Creation date: Tue 26/05/2015 15:05

Runfile: Groningen\_2015\_cleanSheet\_v15\_HM\_1.run

Figure 42 Cross-plot of the pore compressibility versus porosity using the CR function of the GFR2012



Creation date: Tue 26/05/2015 15:05

Runfile: Groningen\_2015\_cleanSheet\_v15\_HM\_1.ru

Figure 43 porosity histogram of the GFR2015 first pass dynamic model

## 6. History Matching and Forecast Uncertainty Analysis

### 6.1. Summary

This text explains the history matching and forecast uncertainty analysis done for the Groningen field review of 2015 as input to the Winningsplan 2016. The goal of the applied workflow is to match the Groningen field and the peripheral Land Asset fields in one model to available subsurface and subsidence data in order to use the model for forward predictions of a possible range of field depletion and subsidence.

The model will be used as the basis for the forecasts on recovery, pressure distribution, subsidence and consequently hazard calculations. The objective is to have one consistent integrated view for the full Groningen field and peripheral fields. The modelling suite as produced in this study can be used to support full-field development activities or production scenarios, by giving a range of predictions for production and subsidence. The base model can also be used to support individual well activities, although some additional modelling work will be required to assess the outcome and the uncertainty ranges for each specific activity. The model can also be used for the calculation and booking of reserves.

There are two reasons for the update of the history match. Firstly, the results from the dynamic reservoir model are used by the geomechanicists to predict future subsidence. The previous model update, GFR2013, had not been constrained by subsidence data. Calculated subsidence based on the results of that model resulted in significant mismatches to observed subsidence. Secondly the previous model area did not incorporate the subsurface beneath the city of Groningen. Therefore the model area has been extended. This extension required the inclusion of all Land Asset fields within the model boundaries. The Land fields require a fit-for-purpose history match since their behaviour will impact the calculations of subsidence by the model.

This work started off on the clean sheet model v17 mentioned by Schrama (1). A priori the model shows an overall good match in the central clusters. However, pressure lags in the periphery were not properly captured. There was a clear need for history matching. The history matching method applied is comparable to the method applied in GFR2012-2013. A large ensemble of different models is generated. Based on a quantification of the mismatch to data a few best models are selected. However, this approach varies in two main aspects. Firstly not only pressure data from SP(T)G measurements is matched. Also RFI, PNL and Subsidence data has been taken into account. This means that the history match for all models in the ensemble is quantified by 4 mismatch indicators. Secondly, not only global mismatches are investigated but the match has been improved by investigating local mismatches.

Model parameters are changed to minimise the mismatch to historical data. This model is by no means the first approach to history match Groningen and history matching process was significantly steered by matching parameters that were applied in GFR2012-2013. The previous work has also been reviewed by SGS-Horizon and TNO which led to suggestions to improve the model and the history match. These suggestions have been implemented where possible.

New parameters were introduced to improve the match to data which had not been incorporated before, for instance subsidence data. In total 96 parameters are used in the history matching workflow, see Appendix 2. This number is large but necessary to improve all regions of the field.

Care has been taken not to use unexplainable or unrealistic multipliers. Geologists, geomechanicists and petrophysicists have been continuously in the loop during these updates.

Currently the best matched model has an field average mismatch to static bottom hole pressure measurements (SPG) of 2.17 bar, an average mismatch to observed water contact rise (PNL) of 1.96m and an average mismatch to subsidence of 4 cm. Due to under sampling and the use of effective parameters the history match model is by definition a non-unique solution.

In order to investigate the impact of this non-uniqueness the uncertainty to ultimate recovery has been analysed. Within the variable model range a large ensemble of different models has been used to generate forecasts. Models that have a poor history match are discarded from the ensemble since they do not reflect current data from the field, and therefore are likely poor candidates to predict trustworthy forecasts. The set of good matches predicts a range of possible ultimate recoveries. A second test has been performed to see if outlying models can be improved and still fall within the range, which had a positive result.

### 6.2. Reservoir Behaviour

This section describes the dynamic behaviour of the Groningen reservoir. The Groningen reservoir consists of the Slochteren sandstone and the Ten Boer claystone and is capped by Zechstein salt. In the south the field overlies the tight Carboniferous source rock and in the north the reservoir is bound by the gas water contact. The reservoir has a thickness of 70-240 meters and a net hydrocarbon interval of up to 123 meters. The average porosity of the reservoir is 17%, ranging from 10% to 25% with the highest porosities in the central part of the field. The average permeability is 260mD with high permeability streaks up to 2D. Over 1600 faults have been identified within the Groningen closure. Initially the pressure was 346.8 bara at datum level 2875m TVNAP. The GIIP of the Groningen field is approximately 2913.9 billion Nm3. The reservoir contains a low calorific gas contaminated with 14% nitrogen and 1% CO2. In the south-western periphery and the far south of the field higher calorific values are measured. The field currently has 256 producers (27 mothballed producers), 2 water injectors and 29 observation wells (46).

The Groningen field is produced primarily under a gas expansion drive mechanism, see Figure 44.

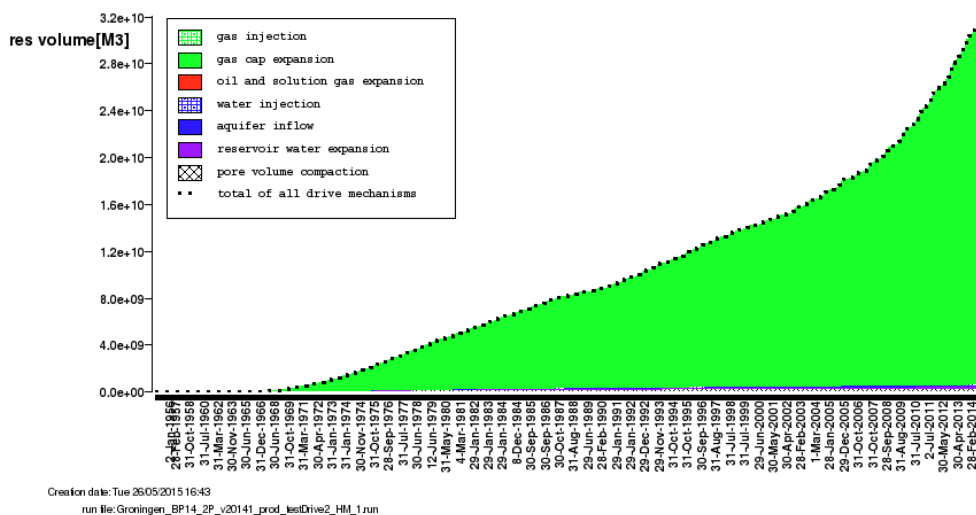


Figure 44 Drive mechanisms in the Groningen field as a function of time

The Groningen field is produced primarily under a gas expansion drive mechanism. The field has been subdivided in a number of compartments based on the interpretation of faults, gas water contact, reservoir pressure and gas composition. The different effects that govern the pressure behaviour of the field are schematically shown in Figure 45 **Error! Not a valid bookmark self-reference.**, courtesy of GFR2003. Pressure differences in the field are caused by the distribution of producing clusters across the field. During the life time of the field the number of clusters and their production policy has changed. This caused field-wide pressure differentials, as is indicated by (5) in Figure 45 **Error! Not a valid bookmark self-reference.**. At a well level pressure difference occur in the model due to the near well pressure losses and pressure losses in the wellbore governed by corresponding lift models(1,2,3) in Figure 45. Interference amongst wells within the same cluster causes pressure disturbances at cluster locations (4) in Figure 45. In some parts of the field pressure lags are observed that are caused by faults (7). Several sizable aquifers are connected to the Groningen reservoir providing pressure support to the field (6). Due to the compressibility of the rocks the pore volume will decrease with production this leads to compaction of the reservoir. This compaction will result in a very small amount of pressure support by volume reduction (8).

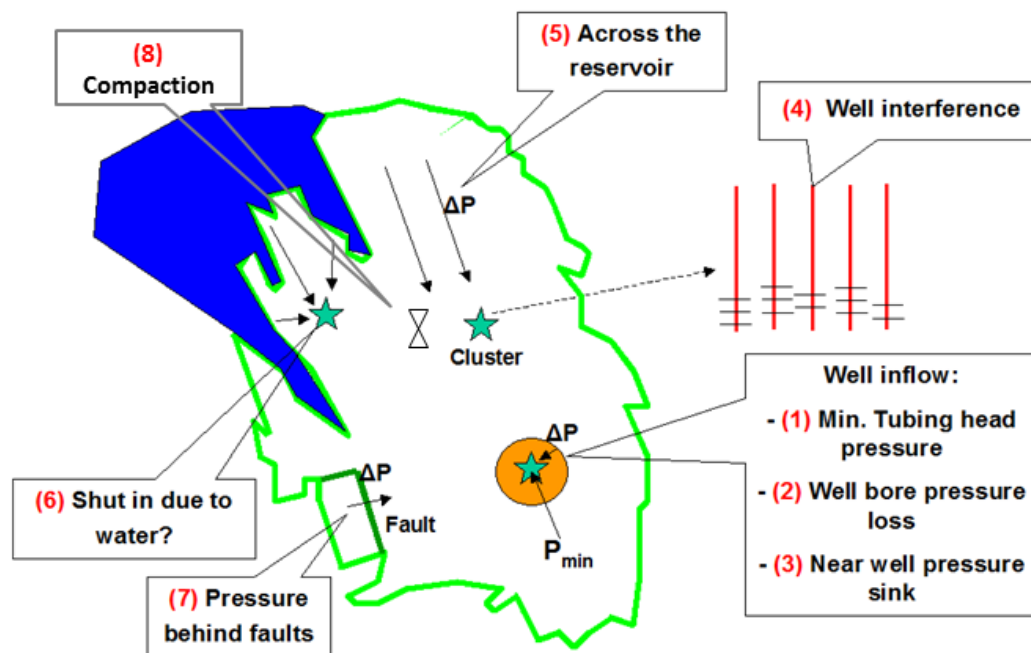
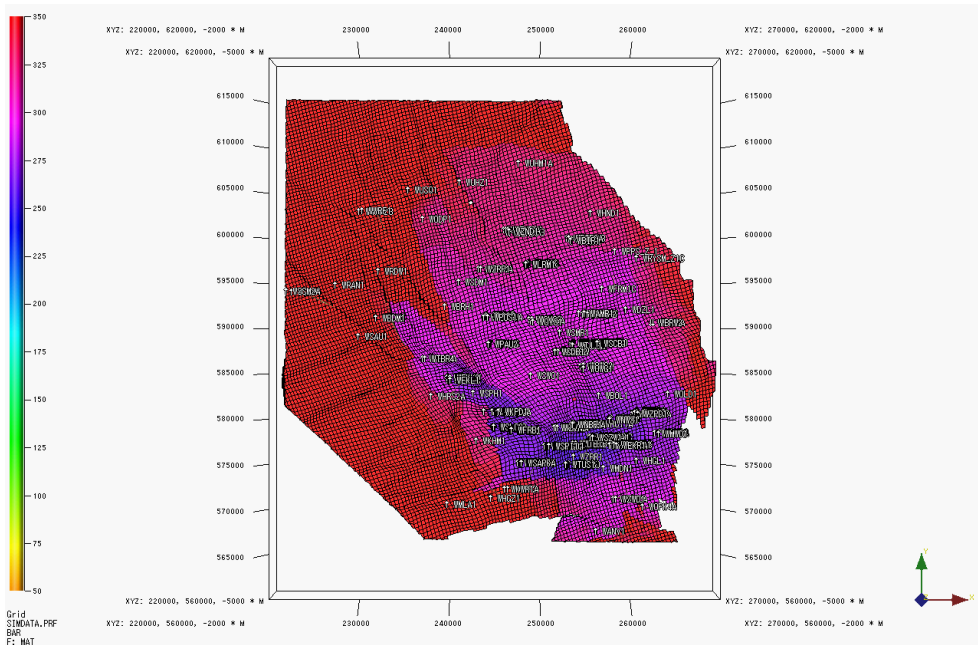


Figure 45 Schematics explaining pressure drops in the field

Groningen field production started in the south causing an imbalance in the pressure over the field which was at its peak in the 70ies, see Figure 46.



**Figure 46 Pressure in the extended Groningen model on 1-1-1975**

This policy changed when the full extent of the field was better understood. From the seventies until 2014 production was balanced in order to avoid large pressure differences within the main area of the field. This means that the clusters in the north of the field, where the cluster density is lower and in-place volumes per cluster are larger, have been produced preferentially, see Figure 47.

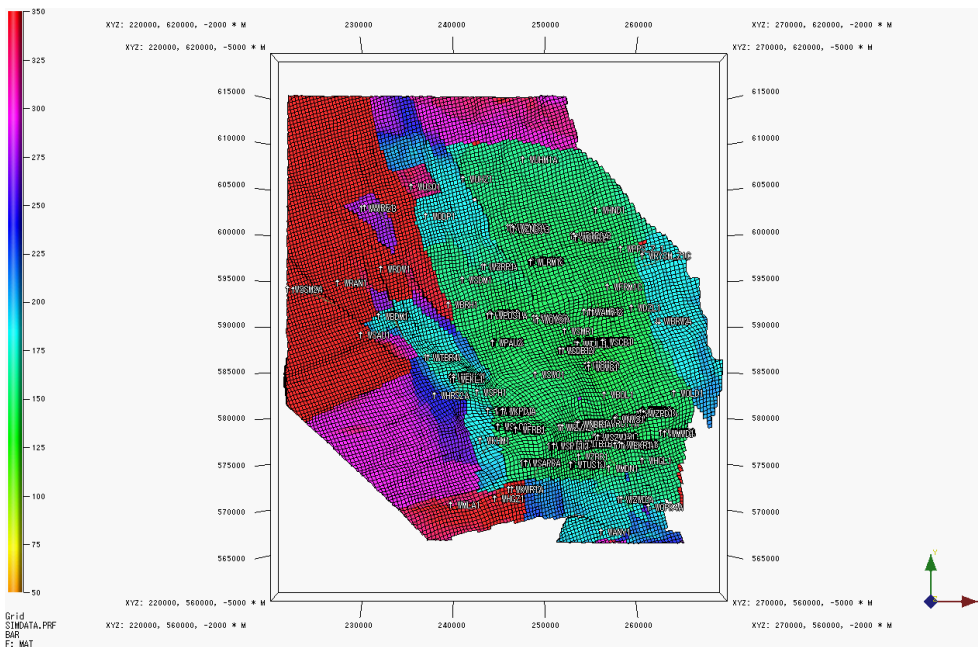


**Figure 47 pressure in the extended Groningen model on 1-1-2000**

Exceptions to this preferential production are the relatively small peripheral blocks at the southern and western edges of the field. These blocks are lagging behind in pressure compared to the main area of the Groningen field. There are 7 land fields in the periphery and the region of the Groningen field. Five of these fields have been or are in production by the Land Asset. These fields are either partly connected to Groningen but have a different gas quality, or the fields are disconnected in pressure from Groningen.

Since January 2014 production caps have been imposed on the field. This measure is in effect to reduce the risk of production-induced earthquakes. First on five clusters in the North of the field, later on the Eemskanaal cluster and currently the whole field is managed by multiple caps. Since November 2015 a gross production limit of 27 billion Nm<sup>3</sup> per gas year is in place. The caps on the northern clusters result in a pressure imbalance in the Groningen field, see Figure 48.

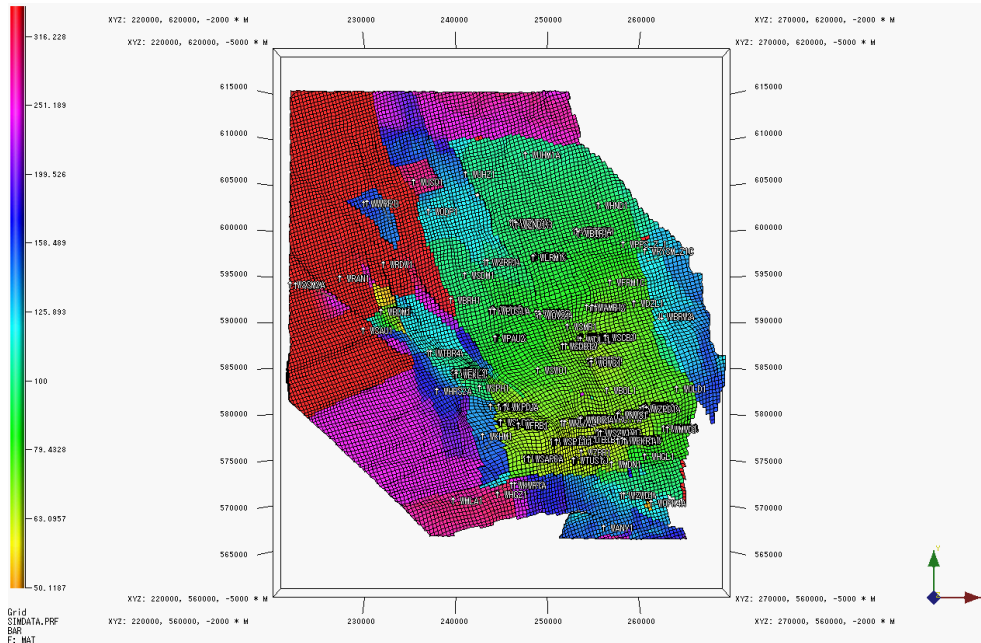


**Figure 48 Pressure in the extended Groningen model on 31-12-2015**

Although most of the gas is currently being produced in the south and the east of the field the northern and western areas of the Groningen field are still being depleted. The caps cause a pressure differential which results in a flow from the north and west to the southern and eastern clusters, see the streamlines of Figure 49.

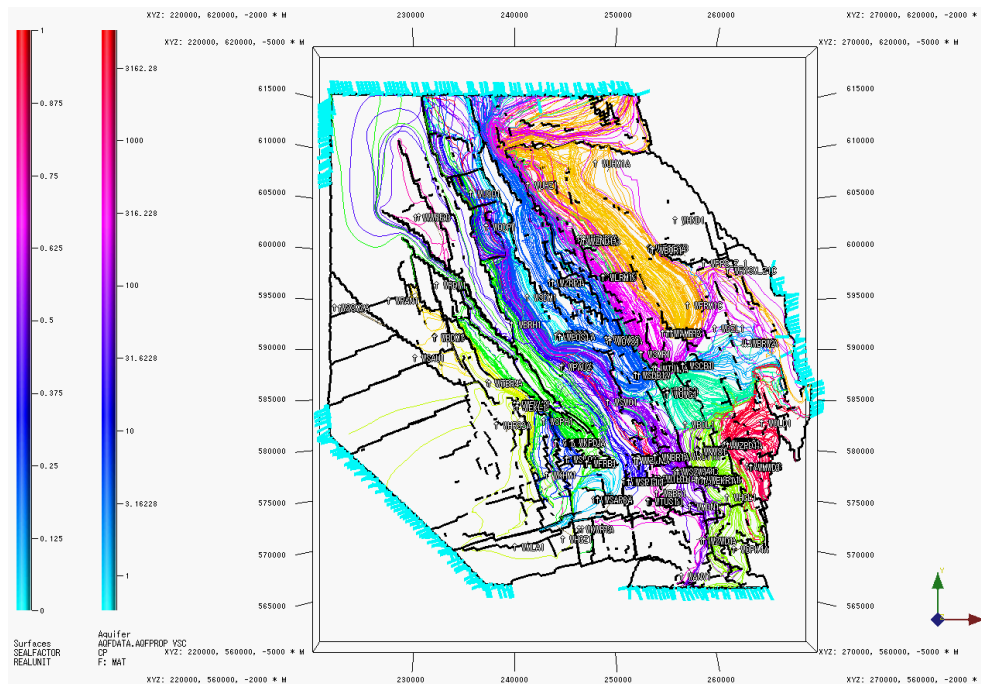


**Figure 49 Streamlines in Groningen at 31-12-2015 coloured by arriving producer, attached analytical aquifers are indicated at the edges of the model**

The gas water contact has been interpreted from logs and ranges from 2971 to 3017 m TVNAP, with a deepening trend from NE to SW Towards the north (Waddenzee/Eems area) and the west the reservoir is connected to several sizable aquifers, see Figure 50.

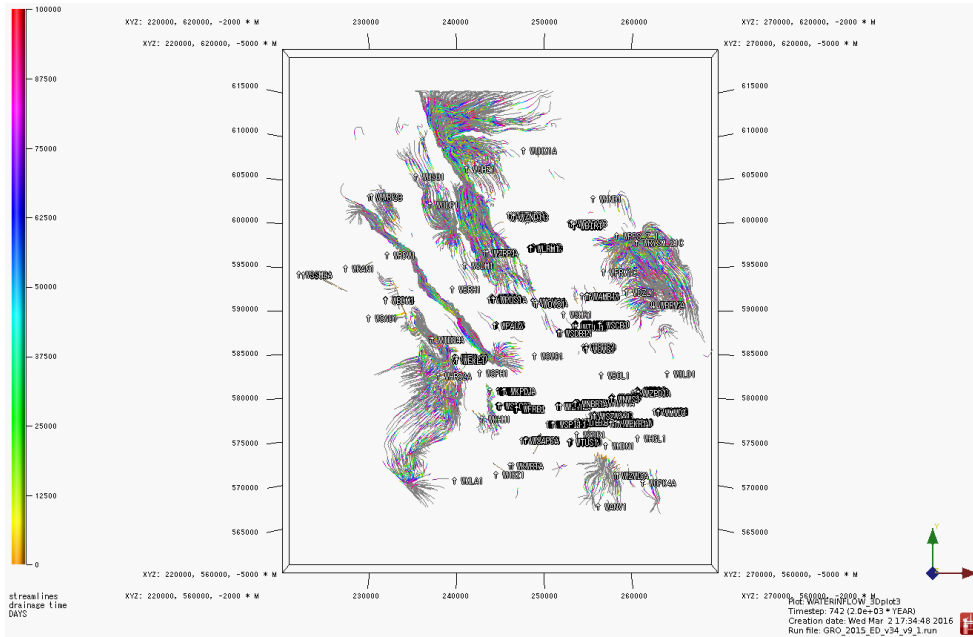


**Figure 50 Water phase streamlines showing the drainage time, indicative for where the water flows in the model**

Water ingress from these aquifers is monitored with regular pulsed neutron logs taken in observation wells. Periodic monitoring of the GWC shows that it remains stable in some areas(HND, BRH, KHML,LRM,SDM,UHM,UHZ, SDB) but has moved upwards in others(OVS, PAU, POS, SCB, ZND, BIR, OLD, HRS, ZWD, DZL, FRM). The impact of water ingress from the aquifers on the depletion of the field is at present very modest and thus constitutes a modest water production risk. Later in the field life larger volumes of formation water may be produced in the wells in the northern and western clusters.

**6.3. Simulator constraints**

The dynamic behaviour in the Groningen field and the peripheral and regional land fields is simulated in a 3D numerical reservoir model. All modelling work has been done and is stored on the shared network drive, see Appendix 1 for full details. In the section below the underlined headers indicate the relevant files. The model is constrained to cumulative gas production which is reported in monthly intervals. MoReS translates the cumulative volumes to a rate constraint per time step. The history matching mode, CONSTR\_TIME, ensures the monthly time steps in the history matching tables are honoured. The solver will run on monthly time steps with exceptions for example for the execution of monitors.

For the Groningen field rate control is set at the production clusters level. Production clusters are modelled as gathering centres with inflow from connected wells. This means the solver distributes the historically required production over all active connected wells. Cumulative water injection at the water injection site Borgsweer is constrained on a cluster level. Borgsweer is modelled as a distribution centre that distributes historical outflow over all active injectors. Production from the Land Asset fields around the Groningen field is constrained at individual wells.

The model is initialized on January 1<sup>st</sup> 1956. Historical cumulative production has been actualized to December 31<sup>st</sup> 2015 and is uploaded from the NAM Energy Components database. The model has 317896 active grid blocks of approximately 450\*450m<sup>2</sup> with varying thicknesses. The model simulates a gas and a water phase. Over the entire history 347 active wells including land wells have been active. The model runs in 86 minutes including the subsidence calculation. All work has been done in Dynamo MoReS v2014.1 in Linux.

[GFR2015/INCLUDE/03\\_HISTORY/UPDATE\\_2015/GRONINGEN\\_SUPERWELL\\_MONTHLY\\_PRD\\_DEC.INC](#)

[GFR2015/INCLUDE/03\\_HISTORY/UPDATE\\_2015/GRONINGEN\\_SUPERWELL\\_MONTHLY\\_INJ\\_DEC.INC](#)

## 6.4. Historical data

In the history match workflow model output will be compared to four data types, SP(T)G, RFT, PNL and Subsidence data. This section describes the data sets. In the two subsequent sections, the model output and the mismatch functions will be described.

### 6.4.1. SPTG

Results from almost 1800 static pressure and temperature gradient (SPTG) surveys are available for all production clusters and observation wells in the Groningen field and the peripheral fields in the model. Measured pressures are converted to datum depth (2875m TVDNAP). Datum corrected pressures are stored in a data file together with recorded shut-in times in days and quality indicators from 1 to 10. Quality indicators are based on a method which weighs each SPG measurement based on the test gauge type, R-square of data points, temperature gradient, number of data points recorded and the shut-in duration prior to testing (47). These quality indicators are used as weights in the history matching workflow which is described later on.

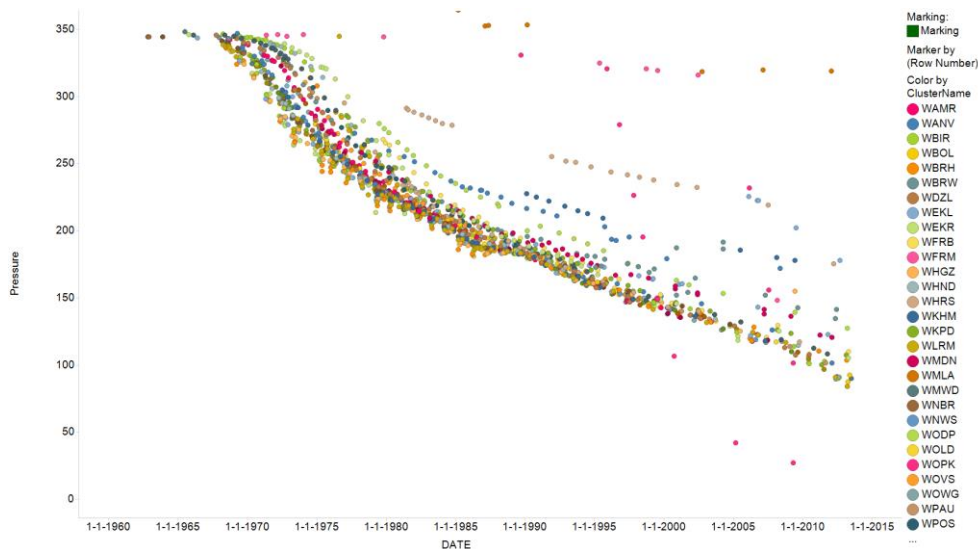


**Figure 51 Static pressures converted to datum depth for the Groningen field and peripheral blocks**

[GFR2015/INCLUDE/03\\_HISTORY/SURVEILLANCEDATA/DEF\\_SPTG\\_v3.INC](#)

### 6.4.2. Subsidence data

Subsidence data has been measured throughout the production life of Groningen. This model compares the subsidence between October 2013 and the first full field measurement in 1972. Before 1972 the full extent of the field was unknown and only partial measurement coverage of the Groningen field is available. Because of the manual method of measuring and because of

local subsidence due to dikes or local mines in the overburden some data points are not stable. The geomechanics department has provided the RE team with a set of stable data points, discarding all unstable measurements, Figure 52. Measured subsidence is averaged over large grid cells as was described in the GFR2015 “clean sheet” report (48).

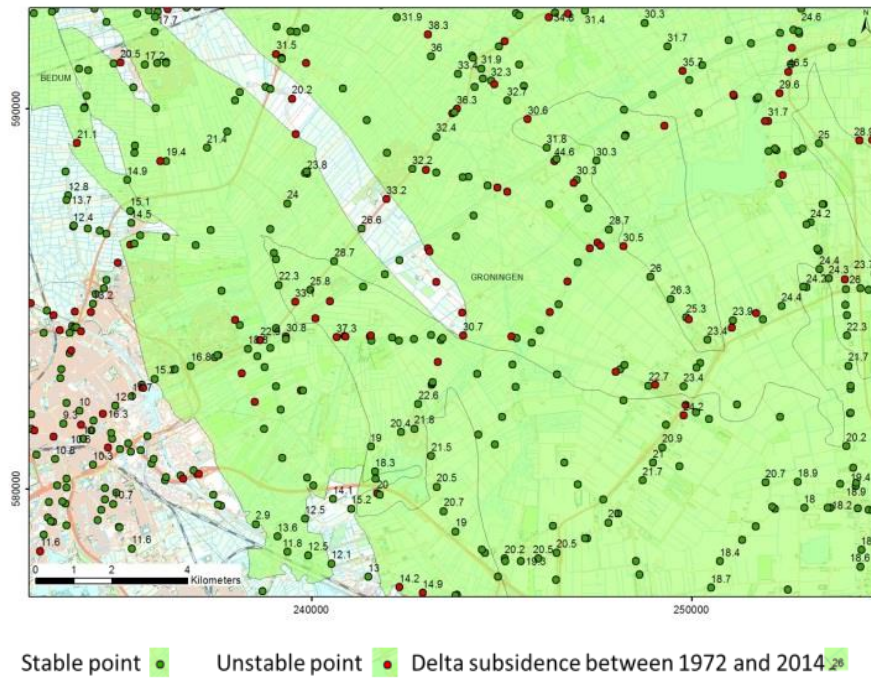


**Figure 52 Example of subsidence data points showing stable and unstable data points and the subsidence between 1972 and October 2013**

GFR2015/INCLUDE/03\_HISTORY/UPDATE\_2015/SUBINC31102013LARGEGRID.INC

#### 6.4.3. RFT

For the Groningen field and adjacent land fields results of 41 repeat formation tests (RFT) are available. All RFT measurements are performed in open hole before the completion is installed. Drawdown tests are performed at different heights to obtain a reservoir pressure profile in depth. Only data points which had sufficient time to stabilize and which are in the net reservoir section are stored in a dataset.

GFR2015/INCLUDE/03\_HISTORY/SURVEILLANCEDATA/DEF\_RFT\_V3.INC

#### 6.4.4. PNL

Pulsed Neutron Log data is available in most of the field to track the gas-water contact rise. Water contact rise in the Groningen field has been measured by 217 pulsed neutron log surveys to date in 30 wells. PNL data is defined as an interpreted height in true vertical depth. The number of data points per well varies from 1 to 17. Quality of the interpretations is assured by the petrophysicist. The weight of each data point is equal. The interpreted contact rise does not reflect a certain change in saturation, e.g. from connate water to 50% water saturation, but an interpreted highest observed water level.

GFR2015/INCLUDE/03\_HISTORY/SURVEILLANCEDATA/DEF\_PNL\_V2.INC

### 6.5. Model output

The goal of the workflow will be to minimise the mismatch between the model output and the four types of historical data. Therefore the model output has to be comparable to the measured values. Where possible MoReS functionality in is used to generate the correct model output. However, subsidence, RFT and SPG require a fit for purpose approach which is not readily available in the given set of tools. Therefore fit for purpose functions have been made.

The workability of the model requires a practical run time. Simulating all measurements at the exact time of measuring will add time steps to the simulation, significantly increasing the run time of the model. The modelled output is therefore interpolated from tables and the interpolated value is then matched to the respective measurement.

#### 6.5.1. SP(T)G

SP(T)G measurements are acquired under static conditions. Prior to a SPTG measurement a cluster is shut-in, typically for a few days. This shut-in will allow the pressure to stabilise and the bottom hole pressure will approach reservoir pressure. Observation wells are by definition static because there is no production to disturbs the bottom hole pressure. In order to compare the model output to static measurements the pressure output of MoReS should reflect these static conditions.

For every producing and injecting well in the Groningen model a pseudo static bottom hole pressure is generated which can be compared to SP(T)G data. Because the simulation has monthly time steps, shut-ins of a few days cannot be modelled explicitly. Therefore the bottom hole pressures in standard TSS1 tables generated by MoReS cannot be directly compared to SPTG measurements.

To obtain comparable pressures model outputs the IPR range functionality is used. A range is determined in the model that corresponds to the transient travel distance due to a three day shut-in, where the size of the range depends mostly on permeability. The average pressure over this range equals the shut-in pressure after three days of shut-in. SP(T)G measurements converted to datum depth are compared to these pressures. This is the same approach as has been applied in GFR2012 (22). An example of the model output compared to the measurements for a production cluster is shown in Figure 53.

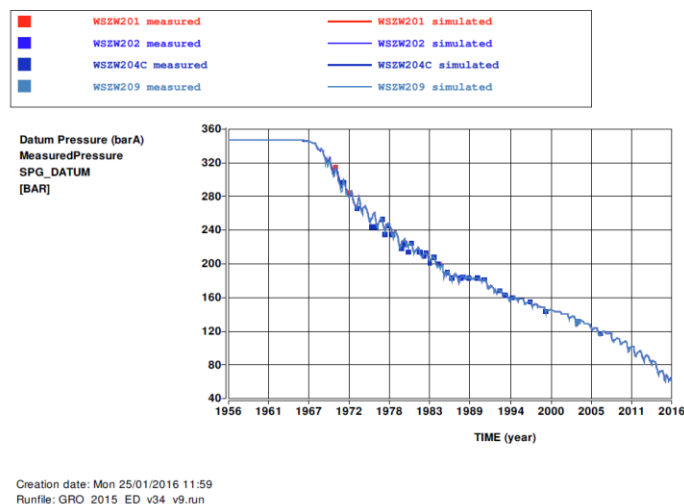


**Figure 53 Static bottom hole pressures at datum level over time for Scheemderszwaag cluster comparing the measured data(squares) to simulator output (line).**

Current functionality will only calculate the IPR range for a single shut-in duration; this value is set at 3 days. An error is made for measurements obtained after longer or shorter shut-ins. Almost all static measurements at a cluster level last shorter or longer than 3 days, see Figure 54.

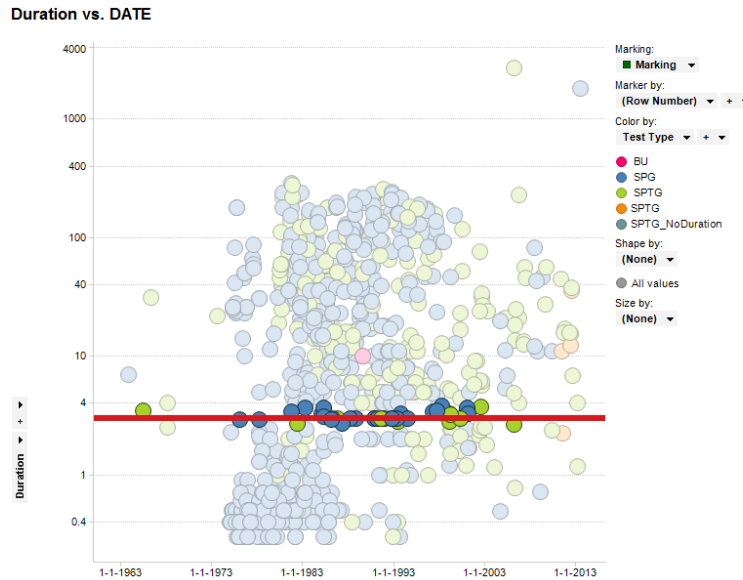


**Figure 54 recorded shut-in prior to SPTG measurements, 38 out of the 1178 data points have a recorded shut-in of 3 days**

In order to investigate the sensitivity of the range a test is made for shut-in times of 1 or 10 days. For example, the maximum difference in the pressure output for PAU3 between 1 day and 10 days of shut-in is 0.27 bar. This difference is shown in Figure 55. Note that Figure 55 only shows 2010-2015 for clarity and that the difference during this time exceeds IPR range dependent pressure difference calculated from 1956-2009. This is well within the maximum gauge accuracy of 0.41 bar (49). The maximum error is acceptable.

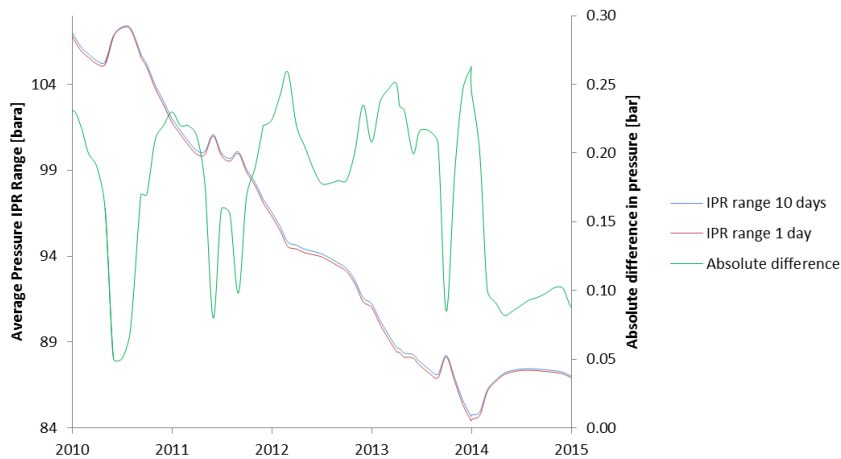


**Figure 55 Average model pressure in the IPR range of PAU3 as function of time for an IPR Range of 10 days (blue) and 1 day (red) and the absolute difference between these pressures (green)**

GFR2015/INCLUDE/03\_HISTORY/DEF\_SPTG\_MONITORS\_V02.INC

6.5.2. Subsidence proxy

Output of the subsidence proxy in MoReS is projected on a large grid of approximately 4by4 km<sup>2</sup> and then exported to an excel file. This excel file is compared to the stable subsidence data in Python script. This python scripted tool has been made by the geomechanicist for the specific

purpose of visually comparing the modelled proxy output with subsidence data during the history matching workflow. An example of our model output, the measurement and the subsidence delta is shown in Figure 56. The assumption in the workflow is that all subsidence is caused by compaction in the Groningen or adjacent reservoirs only. Even though other sources impact subsidence it is beyond this work to model these impacts separately.

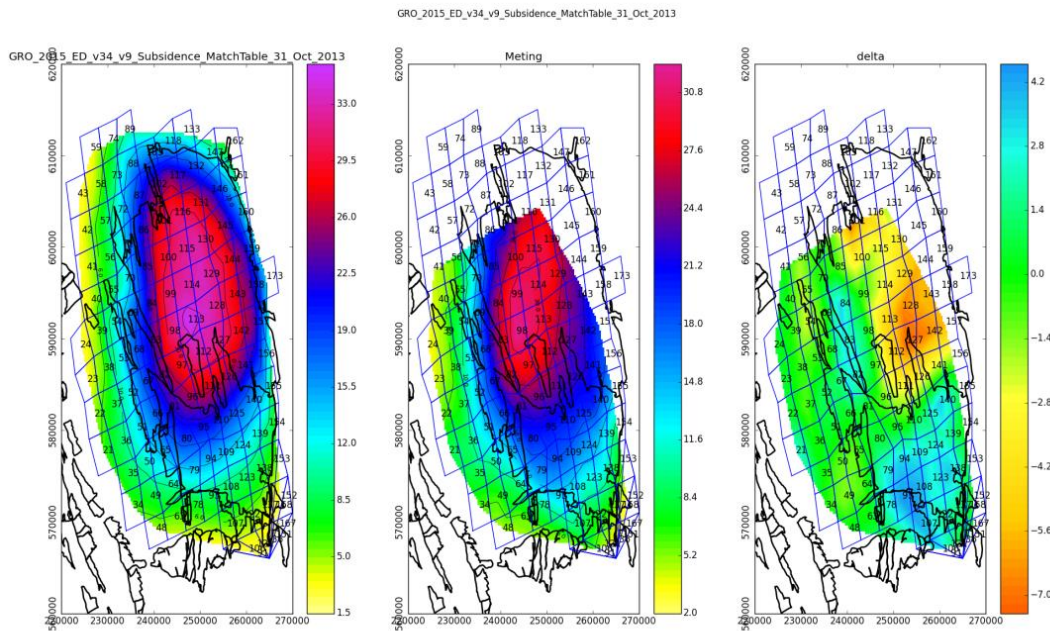


**Figure 56 Subsidence proxy output (left), measurement output (middle), difference between model and measurement (right) all in cm**

### 6.5.3. RFT

Output to compare RFT data to is generated for all wells that have RFT data. A monitor generates a pseudo-RFT at the date of the corresponding measurement. The model output is the reservoir pressure in every grid cell along the trajectory of a well. An example of a comparison between measured RFT data and model output is given in for the recently drilled ZRP-3A seismic monitoring well.

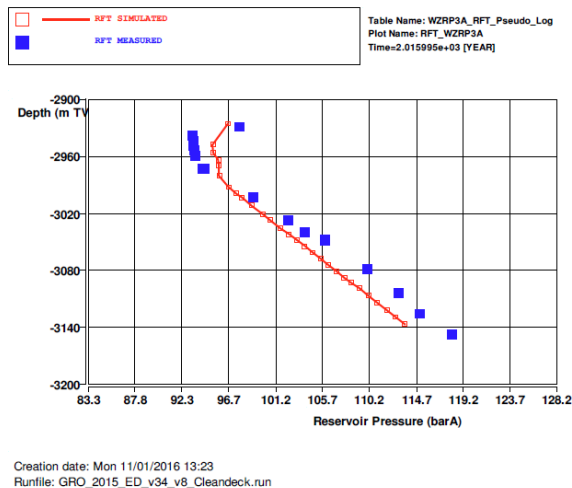


**Figure 57 Example of RFT data (blue) compared to model output (red)**

GFR2015/INCLUDE/03\_HISTORY/RFT\_MATCH\_V1.INC

### 6.5.4. PNL

The interpreted height in m TVDNAP of the gas water contact is reported in a table as a function of time. Water influx is modelled with the MoReS functionality “FluidContactsSetup”. This functionality determines the height of the water within a grid cell and shows the increase along a column. A column is defined along the trajectory of a well. The function checks the water saturation within each grid cell along this column. Every grid cell above a certain saturation threshold is said to contain water. The first cell with a water saturation below this contact is partially filled with water. In this grid cell the water height is calculated as a function of the thickness of the cell and the saturation.

This allows for a gradual increase in the saturation within this cell until the threshold is reached and the water level jumps to the cell above. The disadvantage of this function is the possibility of sudden jumps in the modelled height due to the numerical resolution. The sensitivity of the threshold saturation has been investigated for a range of values ranging from 1% to 85%. Adequate results were obtained with a threshold of 35%. This value has been discussed with the petrophysicist and is reflective of saturation changes in the field. An example of the model output compared to interpreted gas-water contact is given for the Delfzijl-1 observation well in Figure 58.

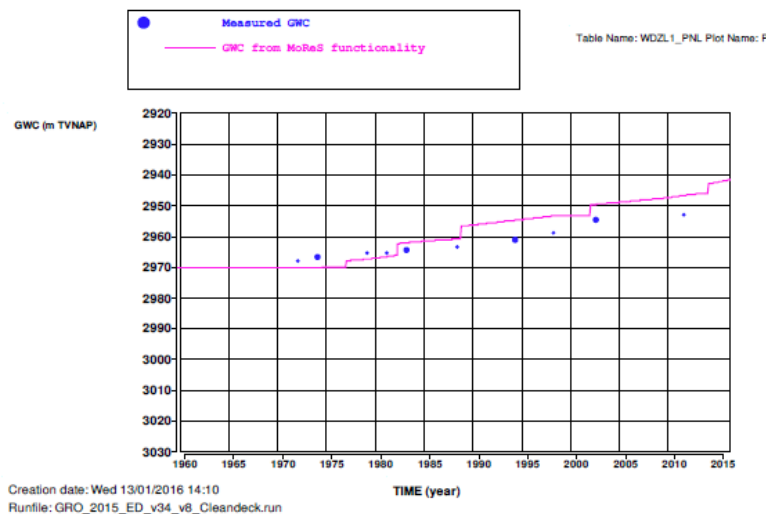


**Figure 58 GWC rise at the location of the DZL-1 well, as measured by PNL and modelled by MoReS, left frame is the well and the grid saturation at 31-12-2014 simulation time.**

The applied function is similar to the approach used in GFR2003 (45), with the difference being the use of standard functionality now instead of the 2003 script. In GFR2012 (22) the water contact was defined to always start at the FWL and it would rise vertically within grid block boundaries until a threshold value was reached, e.g. 10%. The downside of this method is that a very fine vertical grid is required to model a smooth water contact rise and that for one well the FWL is below the reservoir in voided grid blocks (OLD-1).

GFR2015/INCLUDE/03\_HISTORY/PNL\_MATCH\_V1.INC

## 6.6. Mismatch functions

The goal of the history match is to obtain a set of models with a good match to historical data from SPG, RFT, PNL water influx and subsidence measurements. Functions are defined that quantify the mismatch to the four data types. Both global mismatches and local mismatches are quantified..

### 6.6.1. SPG mismatch

In order to quantify the mismatch between the modelled shut in pressure and the SPTG measurements a root mean squared error function is defined. Not all clusters and observation wells have the same number of measurements. In order to equally weigh every location – such as a cluster of producing wells, a single observation well, the water injection at Borgsweer or all wells in a land field – a RMSE value is calculated per location. The average of the RMSE for all locations is the number representing the field wide mismatch. This will prevent wells with a high data density dominating the mismatch number and thus rendering wells with few data points invisible in the global selection of good models. Weights are applied to the data points ranging from 1-10, respectively poor to good.

$$RMSE_{sptg} = \frac{1}{n_l} \sum_{j=1}^{n_l} \sqrt{\frac{\sum_{i=1}^{n_d} ((p_{d,i} - p_{m,i})^2 w_i)}{\sum_i^{n_d} (w_i)}}$$

$$RMSE_{sptg,local} = \sqrt{\frac{\sum_{i=1}^{n_d} ((p_{d,i} - p_{m,i})^2 w_i)}{\sum_i^{n_d} (w_i)}}$$

#### Equation 31(a-b) Root Mean Weighted Squared Error with respect to Static Pressure measurements

Where:

- $n_d$  number of SPG data points per location, with data point identifier  $i$
- $n_l$  number of locations, with location identifier  $j$
- $p$  pressure with subscript  $d$  for measured data and  $m$  for model output.
- $w$  weight value
- $RMSE_{sptg}$  Field average root mean weighted squared error

The difference between Equation 31-a and the functions applied for GFR2012 (22) and GFR2003 (45) is the absence of GIIP weighting in the RMSE calculation. The reason for not applying the GIIP weighting is that some wells in small volume compartments were not noticeable in the global RMSE function despite having a substantial mismatch, such as the Usquert well. A low RMSE value did not necessarily result in a good match for such wells. The resulting model had wells which were matched poorly. To prevent this for this work every location is weighted equally in GFR2015.

FILE: GFR2015/INCLUDE/03\_HISTORY/SPG\_MATCH\_V7.INC

### 6.6.2. Subsidence mismatch

The mismatch function to subsidence data has been described in the GFR 2015 “clean sheet” model report (48). The equation is repeated below for completeness, see Equation 32.

$$RMSE_{subsidence} = \sqrt{\frac{1}{N} \sum_{i=1}^N \left( \frac{X_{obs,i} - X_{model,i}}{\sigma_i} \right)^2}$$

#### Equation 32 Root Mean squared error of the subsidence data point

Where:  $X_{obs}$  observed subsidence data projected on a large grid

- $X_{model}$  model output of subsidence projected on a large grid
- $\sigma$  estimate of the measurement error
- $N$  number of cells in the large grid, with grid cell identifier  $i$
- $RMSE_{subsidence}$  Field average root mean weighted squared error

Subsidence calculations are projected on a large grid. To investigate local mismatches this large grid has been subdivided into 8 regions, see Figure 59. In each of these regions the RMSE is quantified by Equation 32.

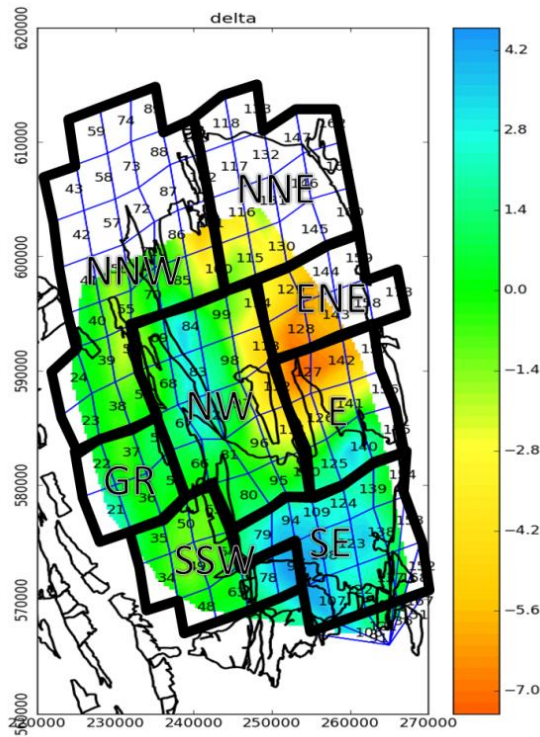


**Figure 59** Eight regions used to quantify the local mismatch for subsidence

6.6.3. RFT

Quantification of the global RFT mismatch is the average mismatch per RFT measurement. The local mismatch is the root mean square of the sum of all pressure mismatches between the measured pressure and a height interpolated pressure from the model output table.

$$RMSE_{rft} = \frac{1}{n_l} \sum_{j=1}^{n_l} \sqrt{\frac{1}{n_d} \sum_{i=1}^{n_d} (p_{d,i} - p_{m,i})^2}$$

$$RMSE_{rft,local} = \sqrt{\frac{1}{n_d} \sum_{i=1}^{n_d} (p_{d,i} - p_{m,i})^2}$$

**Equation 33(a-b)** Root Mean Squared Error with respect to pressure measurements during repeat formation tests

Where:

- $n_d$  number of data points per location, with data point identifier  $i$
- $n_l$  number of locations, with location identifier  $j$
- $p$  rft pressure points with subscript  $d$  for data and  $m$  for model
- $RMSE_{rft}$  root mean squared error of the repeat formation test results

Only for data points that are in the net reservoir a mismatch is determined. Data points in for instance the tight Ten Boer Clay stone clays are not part of the calculation.

FILE: GFR2015/INCLUDE/03\_HISTORY/RFT\_MATCH\_V1.INC

#### 6.6.4. PNL mismatch

In order to quantify a model match to the historical data and compare the quality of the match amongst wells irrespective of the number of data points a root mean square mismatch is defined per well, shown in equation:

$$RMSE_{pnl} = \frac{1}{n_l} \sum_{j=0}^{n_l} \sqrt{\frac{1}{n_d} \sum_{i=1}^{n_d} (h_{d,i} - h_{m,i})^2}$$

$$RMSE_{pnl,local} = \sqrt{\frac{1}{n_d} \sum_{i=1}^{n_d} (h_{d,i} - h_{m,i})^2}$$

**Equation 34(a-b) Root Mean Squared Error with respect to interpreted water height from pulsed neutron log measurements.**

Where:

- $n_d$  number of data points per location, with data point identifier  $i$
- $n_l$  number of PNL measurements, with location identifier  $j$
- $h$  height of the water with subscript  $d$  for data and  $m$  for model
- $RMSE_{pnl}$  root mean squared error for the interpreted pulsed neutron log results mismatch

A possible false mismatch caused by the finite cell thickness in the model is prevented in the script. All initial water levels are initialised at the correct depth in the model, but due to the finite cell thicknesses this depth could shift to the overlying or underlying cell which would cause a mismatch between measured and modelled height. To prevent this type of mismatch the initial value has a 0 m mismatch, and if the modelled value does not change over time with respect to the initial value the mismatch is kept at 0 m. As soon as water ingress in the model results in a deviation from the initial water contact depth the mismatch will be calculated according to Equation 34.

FILE: GFR2015/INCLUDE/03\_HISTORY/PNL\_MATCH\_V1.INC

## 6.7. History matching workflow

The goal of the history matching workflow is to have a fit for purpose model to be used in recovery predictions and subsidence prediction. It is therefore constrained to subsurface measurements and subsidence. Fit for purpose means that non-essential elements which do not

impact decision-making were disregarded. For instance no full field oil phase is modelled; even though this would be required to properly model the small Midlaren oil field in the periphery.

An iterative modelling approach is applied. The first step is to achieve a match at the full field level. This global matching is constrained by the four global mismatch functions and optimised by global matching parameters. A set of models with the best global matches is selected. The second step is to improve the match at a regional level by optimising regional parameter to decrease regional mismatches.

Typically history matching is underdetermined problem with more uncertain parameters than measurements to match to. Therefore it is effective to reduce the number of matching parameters with a similar effect to one multiplier. This effective property modelling is applied in the parameter space. An example is to capture uncertainty in the structure, porosity and net to gross, by one gross bulk volume multiplier. This reduces the number of matching parameters and although the resulting model is not unique this approach makes the process possible and fit for purpose. The applied workflow should result in an improved history match and can also be used to perform uncertainty analysis on the forecast.

Dynamo has a package available for design of experiments called SUM++. In SUM++ a workflow is available that creates a model proxy based on a set of matching parameters and model outcomes. The relation between the model response and matching parameters can be highly non-linear. This means that a high order polynomial is needed to appropriately capture the model response in the form of a proxy. For 10 parameters about 500 runs are needed for one mismatch function (22). Because of the high number of matching parameters due to the scale of Groningen an unachievable amount of runs would be needed to solve for the full set of uncertainties. Therefore an alternative new method is applied which is based on the use of an ensemble of full field model simulations.

#### *6.7.1. Space filling*

Similarly to GFR2012 space filling is applied to scan the solution space of a number of matching parameters. The simulator is used as a black box to generate a large set of models. With the matching parameter set and the model as input and the global and local mismatch functions as output. Out of the many resulting models a few best matched models are selected based on globally satisfying match. Regional improvements are then made by investigating local mismatches.

#### *6.7.2. Adjoint*

Besides space filling there are more methods available for assisted history matching. GFR2012 calculated adjoint-based gradients to look for regions to improve their match on. Adjoint-based optimisation has been attempted for this work. The use of the adjoint a method required the explicit modelling of all shut-ins, which requires many time-steps. This considerably increases the runtime of the model. This did result in a set of gradients but the optimiser did not converge. Although the method is very powerful the adjoint is not set-up to optimise a model to subsidence data. Therefore the method is not suitable for this project.

### 6.7.3. Workflow

In order to constrain the extended Groningen model to 4 available historical data types, within a relatively short timeframe, this work applied a method of assisted history matching based on experimental design.

1. Determine the relevant matching parameters that are likely to impact the mismatch to data. Examples are fault seal factors, gross bulk volume multipliers, aquifer strength and permeability multipliers.
2. Simulate numerous models with matching parameters varying randomly within their uniformly distributed varspace, c.q. space filling.
3. Quantify the mismatch between modelled output to datum pressures interpreted from SPG data, water contacts interpreted from PNL data, stable subsidence measurements and selected RFT data points as described above for all models simulated in step 2.
4. Select the globally best matched models with low mismatches to subsidence pressure and water influx. Because multiple RMSE values are calculated for every model three separate RMS values are plotted in a 3D space with RMSE values increasing away from the origin. The model with closest proximity to the origin is in theory the best, on average, matched model and will be selected for the next step.  
Note that the 3D approach does not allow for the RFT mismatch to be taken into account here. RFT is used in the regional approach which is described later in the text.
5. Interpret the output of the simulation and investigate local mismatches and their correlation to matching parameters.
6. Improve both the varmodel and base case based on optimum matching parameter values from the interpretation.

Repeat steps 2-6 until a sufficient match has been achieved. This workflow is schematically presented in Figure 60.

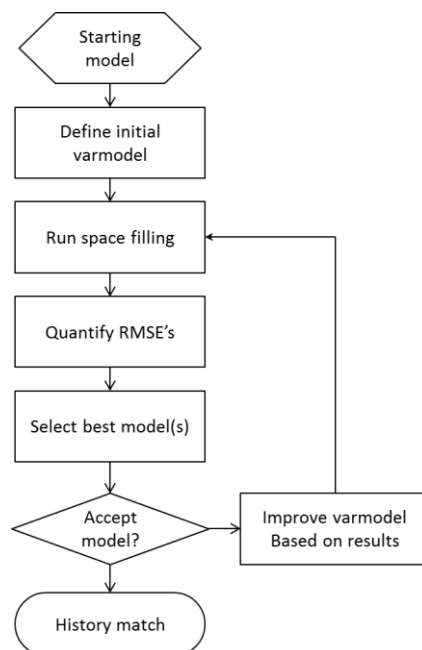


**Figure 60 Workflow history match**

### 6.7.4. Model extension

Initially this workflow was started to match the Groningen field. However, during our attempt of a model match the workflow was interrupted by the decision to increase the scope of the model and include the land fields in the periphery of Groningen and under the city of Groningen. Insights in matching parameters is gained prior to the extension of the model were still taken into account. We did not start with a clean sheet model but continued with the at that time applied set of matching parameters. Obviously some of those parameters changed during the further work.

## 6.8. Globally best matched model selection

In order to elucidate the workflow the following two sections show examples on the model selection and the varmodel improvements.

As is explained in the workflow above the spacefilling generates a set of different models all with their respective mismatches to SPG, PNL and Subsidence quantified. The mismatch to RFT is applied in the regional approach described in the next section. The globally best matched models are defined as those models with the lowest RMS value to all three observables as indicated by Equation 32, Equation 31-a and Equation 34-a. In order to select our top models Spotfire is used to visually show the mismatch functions in 3D space. In Figure 61 a group of optimal models is highlighted in the origin, these models globally have the lowest RMS to all values and could therefore represent an improved model.

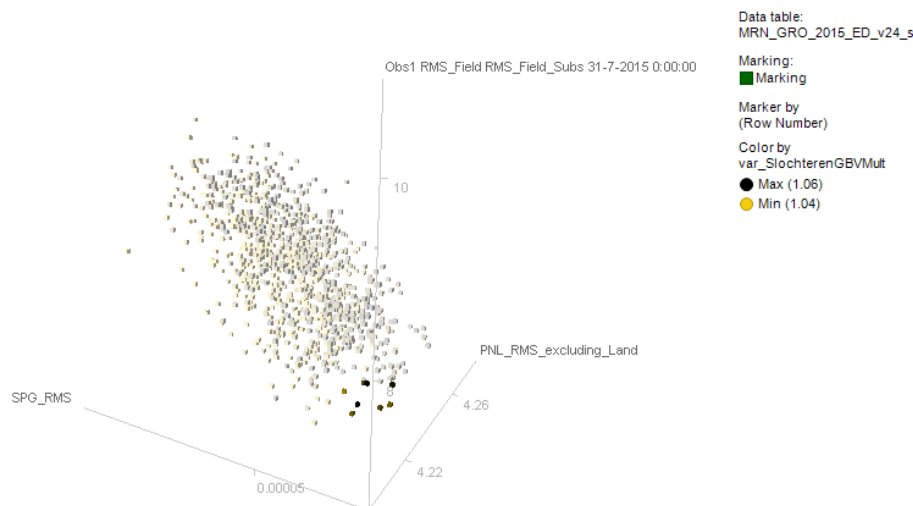


**Figure 61 Example of the global RMSE values for SPG (y), PNL(x) and Subsidence (z)**

## 6.9. Regional model improvements

Multirun also records all local mismatches defined by Equation 31-b, Equation 34-b, Equation 33(a-b) Root Mean Squared Error with respect to pressure measurements during repeat formation tests Equation 33-b, and the regional version of Equation 32. When the best available models are selected as in Figure 61 inspection of these regional mismatches show that although the global match is relatively good, locally some models are very poor. An example of this are the seven model highlighted in Figure 61 and Figure 62. Globally all 7 models are good, yet the local mismatch ranges from poor( 26 bar) to acceptable (2 bar) for a different setting of a fault seal factor. This example shows that the global matches still require local optimisation.

Optimisation is based on a comparison of local matching parameters that impact local mismatches. In the example of Figure 62 the local mismatch to SPG measurements is minimised for a fault seal multiplier ranging from -1 and -1.4. Results like this example are used to improve

local history matches based on the available local mismatch values and matching parameter settings. In the workflow described in Figure 60 the results will lead to the improvement of the variable model. All local mismatches are investigated for a cycle of space filling and where needed the matching parameter ranges are improved.

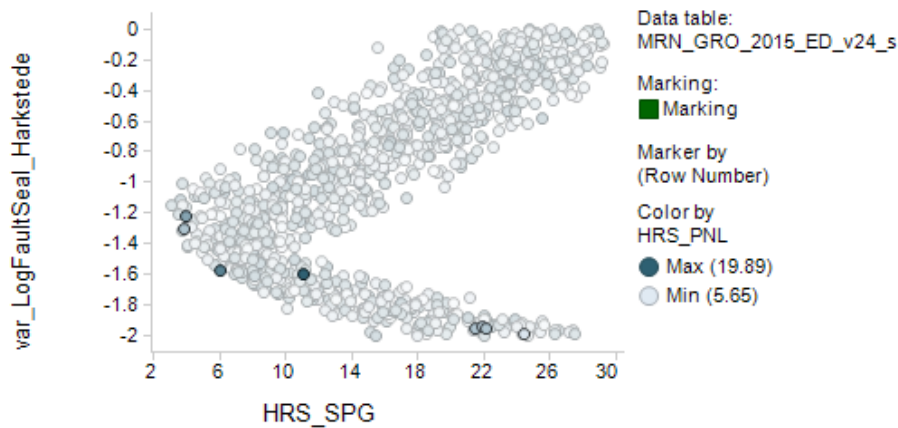


**Figure 62 Example of a local RMSE for the Harkstede mismatch to SPG dependency on a fault sealing factor separating it from the main Groningen field**

Spotfire is used to investigate the large number of combinations between local mismatches and local matching parameters. The goal is to find clear correlations between a local mismatch value and a matching parameter value. This investigation shows three types of result. Firstly, most combinations of matching parameters and local mismatches do not strongly correlate and provide no further insights into optimal matching parameter settings. Secondly, some matching parameters have a strong correlation with a mismatch function and clearly indicate which value results in a good match with Figure 62 as an example. Thirdly, some matching parameters do correlate with a local mismatch function but there is no particular matching parameter value that minimises the local mismatch, see Figure 63. In this figure the mismatch is decreasing with a decreasing parameter multiplier. It is not unlikely that a decrease of the multiplier below the current range could improve the mismatch even further.

In a next space filling experiment such matching parameters are assigned an increased range to investigate the possibility of an improved mismatch. In the example of Figure 63 the fault seal factor is allowed to vary between -3 and -4. If the matching parameter required to achieve a good match becomes unphysical a new set of multipliers is tested.

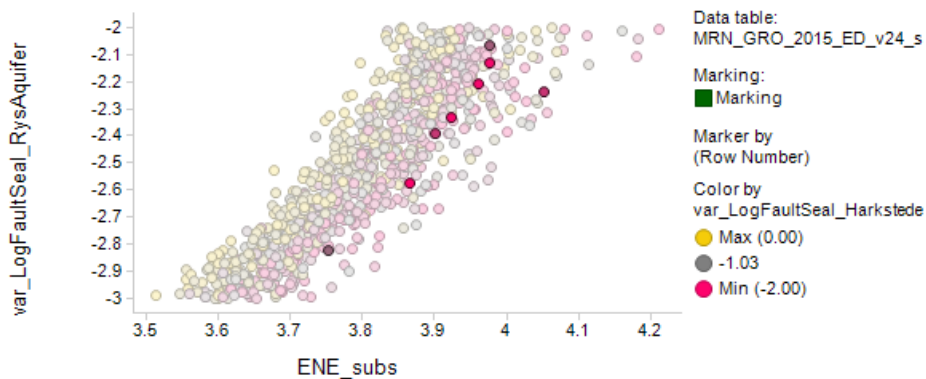


**Figure 63 The impact of the sealingness of a RysumAquifer fault on the local RMSE for the subsidence in the east-north-east region**

Some cases result in insolvable models and they require a new set-up of the matching parameters in order to obtain a good match. An example is given in Figure 64 showing the mismatch to

water influx, pressure and the sealingness of a fault separating the TenBoer-4 observation well from the nearby Eemskanaal cluster. The color scale indicates the sealingness of a fault near the TenBoer-4 observation well. When the fault is more sealing (red) the mismatch to water influx (TBR4\_PNL) is minimised. However, when the fault is less sealing (green) the mismatch with respect to pressure (TBR\_SPG) is minimised. There is no setting to solve this mismatch with the current set-up of matching parameters.

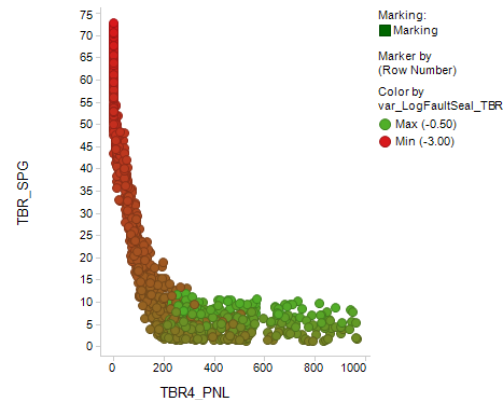


**Figure 64 Mismatch with respect to water influx (TBR4\_PNL) vs. mismatch with respect to pressure measurements (TBR\_SPG) with the colorscale indicating the sealingness of a faultgroup(var\_LogFaultSeal\_TBR).**

The way forward for these cases is to change the parameterisation of the model. For instance, in this particular example a new matching parameter is introduced that controls the fault seal of a different set of faults that impact the separation between TBR-4 and the nearby Eemskanaal cluster. When these faults are made sealing both the water influx match and the pressure match improve, as is shown in Figure 65.

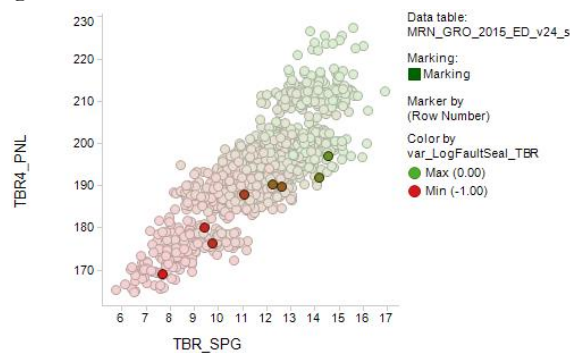


**Figure 65 Mismatch with respect to water influx (TBR4\_PNL) vs. mismatch with respect to pressure measurements (TBR\_SPG) with the colorscale indicating the sealingness of a faultgroup(var\_LogFaultSeal\_TBR).**

## 6.10. Types of Matching Parameters

This section describes the types of parameters varied during the history match. The actual parameters are described after this section. In the next section the actual multipliers and their impacts are described. Variable model parameters are used in the history matching workflow and for the sensitivity analysis on the ultimate recovery of the Groningen field. The matching parameters are uniformly distributed. During the workflow the matching parameter list was added to as the team learned from the workflow.

Unrealistic elements in the history match are avoided by constraining the matching parameter ranges. GFR2013 had permeability multipliers of 75000 or porosity multipliers of 1.43, both

resulting in extreme values. The idea of this work is to use multipliers that can be explained within the physical uncertainty. Some multipliers used early in the project were deemed difficult to explain physically or geologically. For example extreme permeability multipliers in the underwater fraction of the model were deemed unphysical and were therefore removed from the matching parameter table, despite their improvement to the history match.

In the history matching workflow all multipliers ranges are distributed uniformly. Random samples used in the variable models will vary within the given ranges. With the exception of fault transmissibility multipliers and permeability multipliers. These are in effect distributed logarithmically by using them as exponentials. For example a multiplier of -1 will multiply the permeability by  $10^{-1}$ , or by 0.1. This allows for a better scanning of the a large range of multipliers.

#### *6.10.1. Gross bulk volume*

Uncertainties in available energy or volume are partly impacted by structural, net-gross and porosity uncertainty. Because the workflow has to be limited in the number of matching parameters these three uncertainties are captured by one effective gross bulk volume multiplier. The approach to use Gross Bulk Volume multipliers is different to the previous work. GFR2013-GFR2012 applied porosity multipliers to increase energy (22). This work does not apply porosity multipliers for two reasons. Firstly, saturation functions and compressibility are directly dependent on the porosity in the model. Therefore porosity multipliers will have secondary effects on initialisation, flow and subsidence. Secondly, porosity multipliers could result in unphysical values. For example the porosity multiplier needed for a pressure match in the South-West Periphery in GFR2013 was 1.43 in the accepted model. This lead to unrealistically high porosity values and which led to high compressibility and this caused an over prediction of subsidence.

#### *6.10.2. Permeability multipliers*

Permeability in the Groningen field model is based on a porosity-permeability relationship from core plugs. Two relationships have been defined to determine the permeability respectively above and below the gas water contact. For each well the permeability is calculated from the porosity log with these functions. In between the wells the permeability is determined by sampling permeabilities corresponding to the porosity array from the cloud of available porosity-permeability data. This porosity array is based on acoustic impedance from seismic inversion. Because the permeability functions are defined based on Groningen core plugs they are less suitable for the land fields. Therefore the permeabilities in the land fields have to be corrected to agree with available data of these fields, such as well test interpretation results. The multipliers of permeability are exponentials of ten.

#### *6.10.3. Fault seal factors*

The up-scaled model contains 621 faults. Six additional faults are manually entered in MoReS to add connections that were lost during upscaling, all were discussed and approved by the geologist. Flow through all faults is governed by their respective transmissibility. Generally the fault transmissibility is a function of the fault permeability, shale gouge ratio, fault throw and the thickness of the damaged zone around the fault. In the Groningen field cataclasis is the main process that causes a permeability magnitude drop with respect to the host rock. Clay smearing is due to the clean sand of minor importance (22). GFR2012 has shown that the base case for most faults in the Groningen field is to be open (22). However, pressure lags are observed in the edge of the field that cannot be explained with a uniform approach where all faults are open. This

work uses faults multipliers based on the GFR2012 study and new fault groups introduced during the history match of the SW periphery and NW periphery studies in 2013. For the land fields the fault seal settings are based on the models used by the respective subsurface teams. The multipliers of the faults are exponentials of ten.

#### 6.10.4. Aquifers

The aquifers surrounding Groningen are uncertain in their size and permeability. In order to capture this uncertainty the length of the analytical aquifers attached to the Groningen field model is varied within a possible range. The individual aquifers are distributed over a large number of aquifer cells. Each aquifer cell receives its rock properties (porosity, permeability) from the grid blocks to which it is attached. In this way the spatial property trends in the model are reflected in the aquifers. At present it is not possible to apply a permeability multiplier to these aquifer cells (other than the one applied to the grid blocks). However the effect of a permeability multiplier can also be achieved by a multiplier on the water viscosity in the aquifer. Aquifer length uncertainty ranges have been discussed in the GFR2015 “clean sheet” model report (48). The ranges of the lengths in the extended model are similar to the lengths reported by that report with a correction for the fraction that is now numerically modelled. The naming convention of the analytical aquifers has changed, see Figure 66.

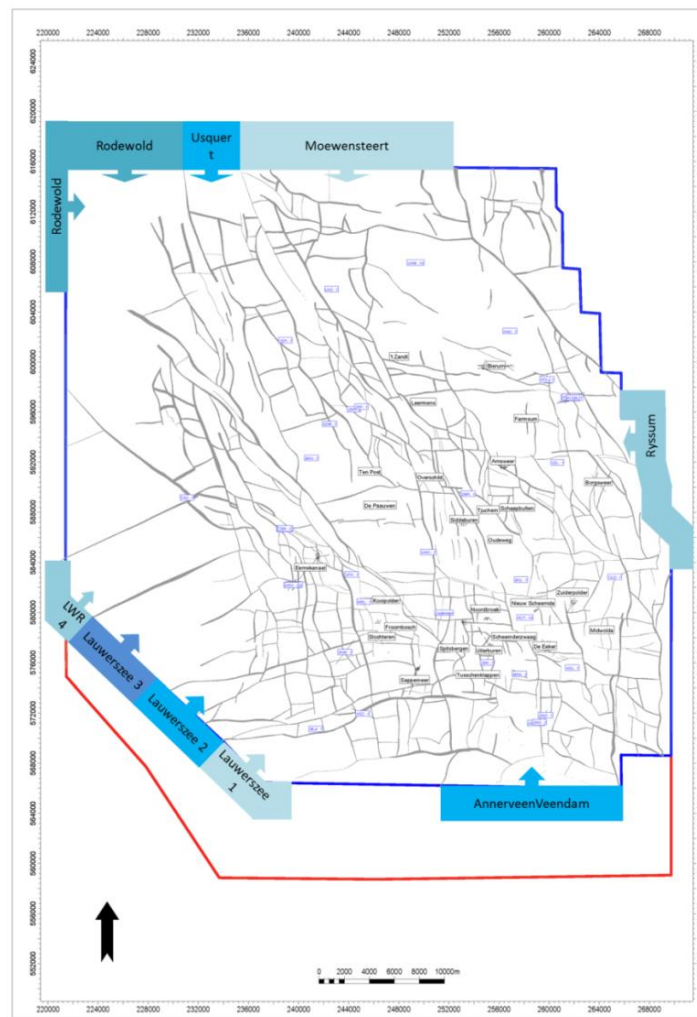


**Figure 66 Analytical aquifers attached to the large grid model indicated by the blue shapes. The blue line indicated the boundary of the extended grid dynamic model and the red line indicates the extent of the static model.**

### 6.10.5. Subsidence

Our subsidence proxy is a function of the pressure depletion averaged on a 2D grid and is calculated with the Geertsma en van Opstal equation, see Equation 35 (48). The uniaxial compressibility and the poisson's ratio are both uncertain parameters that are varied during the history match. Uniaxial compressibility has been measured on core plugs obtained in the Groningen field. A curve fit through the data cloud results in a third order polynomial function of porosity. This function is used in MoReS to set a compressibility for all cells in the model. The fitting constant,  $c$  in Figure 67, through the cloud is varied during the history matching process between 0.5-0.6 (22). Although initial screening of the impact of the fitting constant on the "clean sheet" model resulted in a low sensitivity (48) this work found it will have an impact on the history match to subsidence data and therefore it needs to be included as a matching parameter in the history matching workflow.

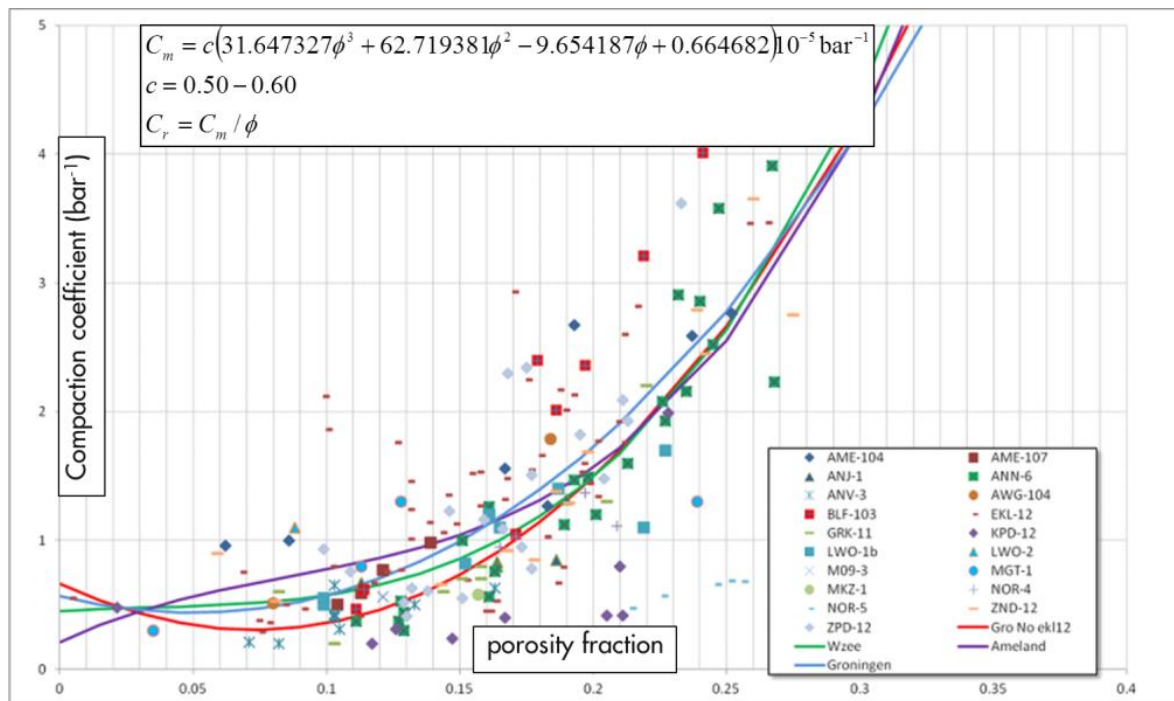


**Figure 67** Compaction coefficient as a function of porosity with a fitting factor between 0.50 and 0.60

Besides the compressibility the Poisson ratio determines the subsidence at surface and the value is set to vary between 0.2 and 0.3 initially. This approximation of Poisson's ratio reflects the entire overburden and is therefore highly uncertain.

$$u_z(x, y, 0) = \frac{1 - \nu}{\pi} \sum_{n=1}^N c_{mn} \Delta P_n \frac{L_{zn} l_{xn} l_{yn} l_{zn}}{\left[ (x - L_{xn})^2 + (y - L_{yn})^2 + L_{zn}^2 \right]^{\frac{3}{2}}}$$

**Equation 35** Subsidence as function of the poisson ratio, subsurface model grid cell location, uniaxial compaction and pressure depletion (48)

$u_z$  is the subsidence (metre)

$x$  and  $y$  are surface locations, hence  $z=0$  (metre)

$\nu$  is the Poisson ratio (ratio of transverse to axial strain. When a material is compressed it usually expands in the two directions perpendicular to the direction of compression)

$c_{mn}$  is the uniaxial compressibility of each gridblock (1/bar)

$\Delta P_n$  is the pressure change in each subsurface gridblocks, for the compacting layer (bar)

$L_{zn}$  is the depth of the subsurface gridblock (metre)

$L_{xn}$  and  $L_{yn}$  are the distances in the x, y direction respectively from the surface location to the subsurface gridblock (metre)

$l_{xn}$ ,  $l_{yn}$  and  $l_{zn}$  give the sizes of a subsurface gridblock (this means  $l_{xn} * l_{yn} * l_{zn} = \text{gridblock volume GBV}[\langle g \rangle]$  in MoReS)

### 6.10.6. Saturation functions

Saturations functions including the relative permeability function and the capillary height function are described in detail in the dedicated Saturation Functions section of the GFR2015 (50). The history match and uncertainty workflow directly copied the ranges and base case values described in that report.

### 6.10.7. Free water levels

Free water levels and their uncertainties are used in the history match and the uncertainty analysis of the forecast. The range of the heights is determined by the petro physicist and is discussed in the GFR2015 “clean sheet” model report (48). The history match and uncertainty workflow applies the ranges described in that report.

## 6.11. Set-up of field-wide parameters

This section will describe all matching parameters that are applied globally. The goal of these parameters it to reduce the mismatch globally prior to regional improvements according to the top down approach of improving the model first globally and then regionally. The subsequent section will discuss regional parameters.

### 6.11.1. Slochteren

The current model does not have enough energy in the gas and the volume is increased with a GBV multiplier. When the static model is up-scaled and initialized as without any volume increase it is not possible to match the historical pressures. Therefore an increase the GBV of the Upper and Lower Slochteren net reservoir is applied. The effect of the multiplier is shown in Figure 68 where two models are compared that are identical with the only difference being that one model does and the other does not have a multiplier on the GBV. Note that the choice to show the Schaapbulten cluster results is arbitrary and that any other cluster is similarly impacted.

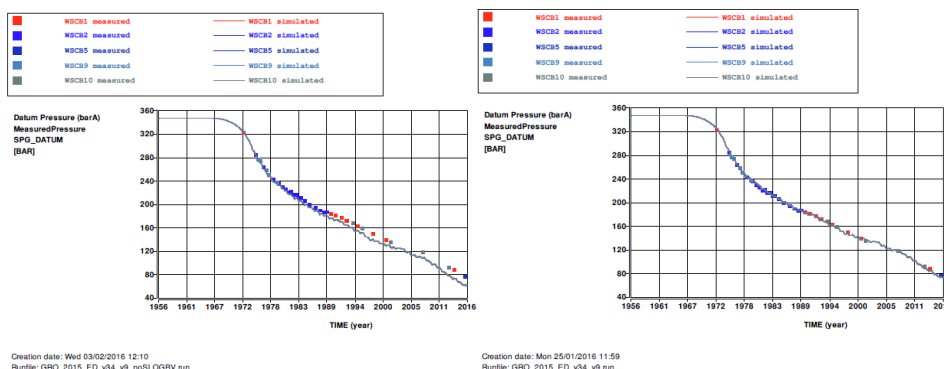


**Figure 68 SPG pressure compared to model output for the Schaapbulten cluster showing the difference between no GBV multiplier on the Slochteren layer (left) and a multiplier of 1.05 on the GBV (right).**

### 6.11.2. Ten Boer Claystone

The permeability in the Ten Boer layer is reduced to match pressures measured by RFT. The Ten Boer layer overlying the Slochteren Sand Stone is a mixture of thin sand layers embedded in shale layers. In the north of the field this layer was deposited in a desert lake environment, aeolian mudflats and rare sheet floods. In the south the Ten Boer is the proximal part of the basin and is a mixture of aeolian mudflats, aeolian sandflats and isolated sheet floods (22). Depletion of pressure in this layer is known from RFT measurements, which found pressure differentials between the Slochteren and the Ten Boer sands ranging from 0 bars to 75 bars. Large pressure differentials are observed in the north of the field. In order to match the reservoir output to these pressure lags a permeability reduction multiplier is introduced for the entire field. Both horizontal and vertical permeability can be reduced (51). Although GFR2012 defined a northern and a southern permeability multiplier the final match has exactly the same multipliers for both the northern and southern Ten Boer layers. Therefore this work does not separate the northern and southern Ten Boer.

### 6.11.3. Ameland Claystone

Based on RFT measurements the Ameland claystone separating Upper Slochteren and the Lower Slochteren is expected to be the cause of a pressure lag. This Ameland effect can have significant effects, especially towards the north of the field where it constitutes a thick shale package. To the South it sands out and the pressure differentials disappear (51). In the history matching workflow a permeability reduction multiplier is applied to enhance this effect. The effect of the Ameland claystone on the model output for a northern production well is shown in Figure 69.

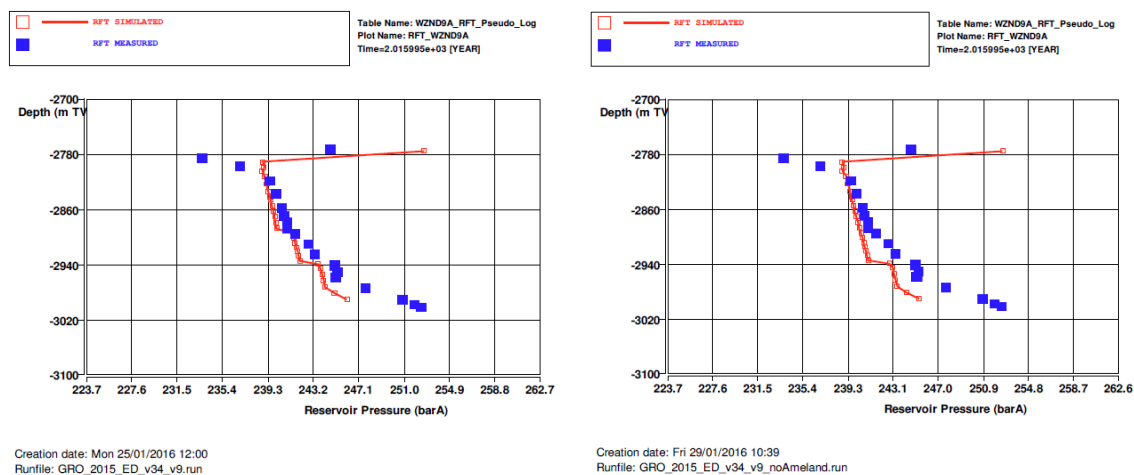


**Figure 69 RFT data compared to model output for the ZND-9A production well, example of pressure lag with(left) and without(right) sealing of the Ameland claystone**

### 6.11.4. Heterolitics lower and upper Slochteren

The sealingness of heterolitics layers in the upper and lower Slochteren is hard to assess. They are local baffles that seem to only have an effect in ZND and ODP according to available RFT data (51). The effect of the heterolitics on the model response for the northern observation well ODP is shown in Figure 70.

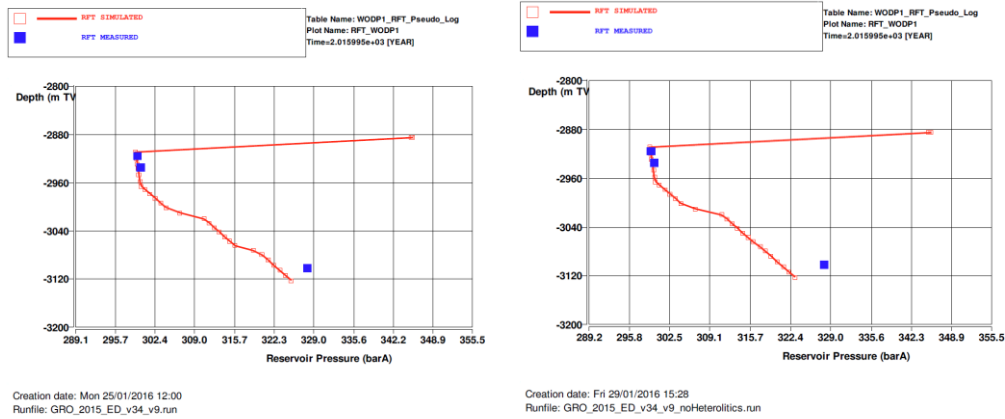


**Figure 70 RFT data compared to model output for the ODP-1 observation well, Impact of the heterolitics multiplier (left) compared to an identical model without the heterolitics multiplier**

### 6.12. Set-up of regional parameters

The description of the local history match uses fault seal factors as local matching parameters. The text will refer to pressures and water contacts observed for the specific wells. These measurements and achieved model results can be found in the attached pdf files.

- [GRO 2015 ED v34 v9 RFT Match.pdf](#)
- [GRO 2015 ED v34 v9 PNL Match.pdf](#)
- [GRO 2015 ED v34 v9 SPTG Match.pdf](#)

Fault groups that impact the reservoir pressure will be mentioned in the text below. There are 36 fault groups defined as matching parameters. Figure 71 shows the faults and the fault groups that were used in the history matching workflow on a map of the extended Groningen field. Note that the colour black in Figure 71 indicates the fault is set to fully sealing and the groups are colour coordinated. The applied sealing factors of the faults can also be found in appendix 2.

**Table 14 Multipliers of the sealing factor of fault group that were used as matching parameters in the history match**

A	USQ_gas, USQ	J	RysAquiferNorth	S	TBR	$\beta$	PosPauTjm
B	ODP	K	RysAquifer	T	BDM5	$\gamma$	SDM
C	RWD	L	BRW5	U	BDM5b	$\delta$	OPK4
D	RWDS	M	PopUps	V	BDM4	$\epsilon$	MLA
E	ZWDNorth	N	SDBtoSZWtoEKR	W	BDM3	$\zeta$	WRF
F	ANV	O	SPHWest	X	BDM	$\eta$	WRF1
G	ANV_N	P	EKLWest	Y	RNM1	$\theta$	LAU
H	NE	Q	KHMTrough	Z	HGZ	$\iota$	HRS_AQF
I	BIRSouth	R	Harkstede	$\alpha$	AMR_LRM	$\kappa$	RWDN





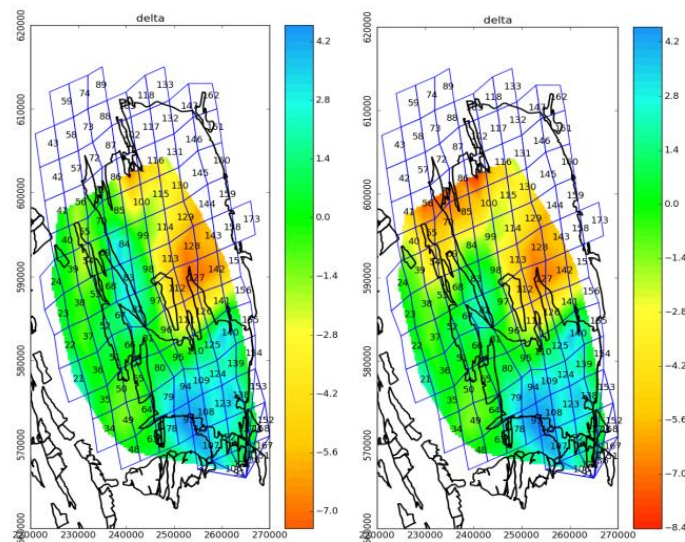


**Figure 74 Effect of a closed aquifer(left) or a connection to the Rodewold aquifer west of BRH-1 (right).**

#### 6.12.2. Zeerijp

The Zeerijp aquifer is a trough separating the North-East and the North-West. Three wells have been drilled in the Zeerijp aquifer: ZRP-1, ZRP-2 and ZRP-3 in between Stedum-1 and 't-Zand cluster. The trough is separated by a large offset fault on both sides and has a connection to the reservoir on the south. To the north they are connected to the Moewensteert aquifer. Pressure in ZRP is matched within 4 bars but the subsidence is still overpredicted.

#### 6.12.3. North East

The North East region is separated by a fault with large juxtaposition from the Zeerijp trough, Figure 71 – Fault H, this is based on the pressure response observed in both Uithuizermeden-1 and Uiterhuizen-1 located in the far north of the field. To the south the region is separated by a group of faults that caused the initial gas water contact to differ, Figure 71 – Fault I. All wells in the North East region are depleting in line with the clusters Bierum and 't-Zand. No water contact rise is observed in the UHM-1 and UHZ-1 observation wells. To ensure there is no water influx from the Moewensteert aquifer a group of faults with large offset north of Groningen is sealed off in the model. Although the pressure match in this region is satisfactory for the SPG the current subsidence in the North East is overestimated in this model, see Figure 56. Further work is necessary to improve this history match, this is described in the recommendations.

#### 6.12.4. Bierum, Borgsweer and the Ryssum Aquifer

Bierum cluster is located in the north-east of the field and east of the cluster are the RYS-Z1, PPS-Z1, HND and DZL observation wells and south-west of the cluster are the Borgsweer injection wells. A fault group is setup in the model in such a way that the water rise observed in the Bierum cluster has the right timing in the model, Figure 71 Fault I and J. In time BIR1, then BIR6, then BIR2A and then BIR13b see water rise. Historically no water influx has been observed in HND north-east of Bierum. It is likely that water does not flow in from the west, since water rise is observed in 't Zand only after 1990, whilst BIR1 see water rise before 1974. To the East of BIR lies the Ryssum aquifer, which could be the main contributor of the water influx. Without any multipliers the order of water rise observed in the PNL measurements will not be



improve the pressure match in the period 1970-1980 when this region is missing energy. Results of an adjoint simulation for GFR2012 suggest an increase in the permeability for this. Log interpretations indicate a lot of heterogeneity in this area. The permeability of different wells lying close together can differ substantially. Large continuous high permeability streaks could explain this behaviour (22). Because these high permeability layers are not captured by the upscaled model a multiplier is applied to improve the match for clusters during this period. In the GFR2013 model a multiplier of 75000 was applied, this model applies a multiplier in the order of 1 to 10. Slight pressure differences within the central region are matched by a large north to south fault group, Figure 71-Fault N. The central region is separated from the South West by a large fault with pop-up structures, Figure 71- Fault M.

#### 6.12.6. *South West*

The south west region is separated from the Eemskanaal region and the Central region. This separation is based on observed pressure differences and initial gas water contact differences. In the south of the South West lies the Hoogezand block which has been drilled by the HGZ-1 observation well. This well found a different gas water contact and a pressure lagging with respect to the pressures in the South west. A fault is separating the Hoogezand block from the South west, Figure 71 – Fault Z. The Slochteren satellite and the Froombosch and Kooipolder clusters are located east of the Eemskanaal cluster. Eemskanaal is separated from these clusters by a fault just west of the SPH-1 observation well, Figure 71 – Fault O.

#### 6.12.7. *Eemskanaal region*

The TBR-1 and -4 observation wells and the Eemskanaal production cluster are located in the western periphery of the Groningen field. In order to achieve a match for the Eemskanaal cluster needs to see slightly larger volumes than those in the static model. Both the Ten Boer -4 well and the EKL cluster well have an improved match in late field life with pressure support from larger volumes. Far north of the Ten Boer 1 and 4 wells lies the Rodewold-1 well, this RDW-1 well was slightly depleted when it was drilled. Depletion is probably through the aquifer. The pressure match in RDW-1 and the subsidence match dependency in the Rodewold aquifer are matched by a partly sealing fault, Figure 71 – Fault D and Fault x. The Bedum field west of the South-Western Periphery is disconnected from the Groningen field. This conclusion is based on virgin pressures when the wells were drilled long after Groningen production had started and a different gas quality.

Ten Boer wells are slightly lagging in pressure with respect to the nearby Eemskanaal cluster. Also there is no water rise observed in the Ten Boer wells. To match both the water and the pressure a fault is applied as matching parameter separating the Ten Boer wells from the Eemskanaal cluster, Figure 71 – Fault S.

#### 6.12.8. *Harkstede*

The Harkstede block is located to the East of the Lauwerszee aquifer and to the west of the Eemskanaal cluster in the south-western periphery of the field. Two wells have been drilled in the structure; observation well HRS2A and production well EKL13. Pressure is lagging with respect to the nearby EKL cluster from which it is separated by a set of faults, Figure 71 – Fault P and Fault R.

This block as an initial in place gas volume of 10.5 billion Nm<sup>3</sup> according to the static model. However, according to p/z-analysis of the EKL13 well an initial in place volume is expected of approximately 17.05 billion Nm<sup>3</sup> (52).

GFR2013 applied a porosity multiplier of 1.43 to achieve the pressure support needed to achieve a match. Alternatively this volume could be explained by the combination of static initial gas in place volumes in blocks: Harkstede North West (3.6 billion Nm<sup>3</sup>) and either Harkstede East (2.8 billion Nm<sup>3</sup>) or Bedum South (2.6 billion Nm<sup>3</sup>). In this model the Harkstede main block is in pressure communication with the Harkstede North West and the Harkstede East block. To achieve sufficient pressure support. The Harkstede main block has a gross bulk volume multiplier of 1.17 as a base case. To match the water influx observed in the Harkstede block a fault separating the block from the Lauwerszee Aquifer is used as a matching parameter, Figure 71 – Fault t.

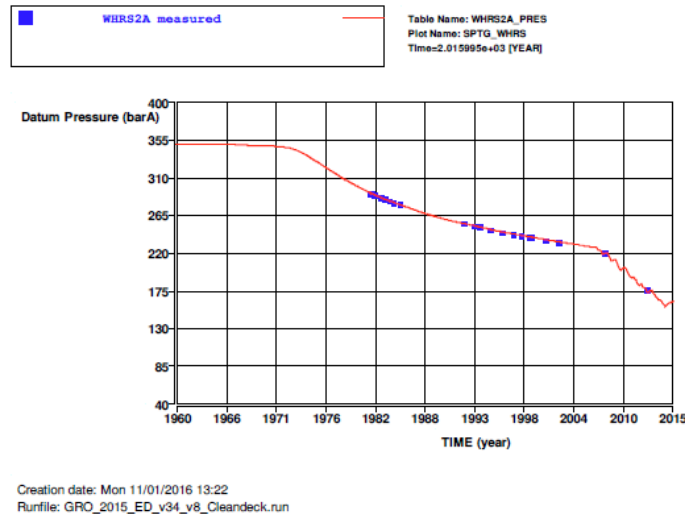


Figure 78 Example of SPG data (blue) compared to model output

6.12.9. Lauwerszee Aquifer

The Lauwerszee aquifer is located west of the Harkstede block and directly below the city of Groningen. Based on subsidence match the pressure should not deplete in the numerical section of the aquifer. A group of faults helps improve the history match to subsidence west of the Groningen field, Figure 71 – Fault 0. Without the multipliers the pressure will drop in the aquifer, which subsequently causes too much subsidence modelled by the proxy, see Figure 79. The aquifer is not completely disconnected from Groningen. This is seen by a water contact rise in the Harkstede block. To ensure both the pressure is matched and the PNL the aquifer lengths of the four Lauwerszee analytical aquifers, shown in Figure 66, are varied to minimise the mismatch.

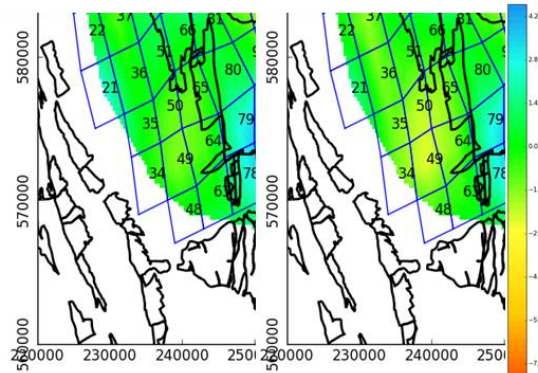


Figure 79 Delta between subsidence data and model proxy in the South West corner of Groningen for two models. Left image GRO\_ED\_v34\_v9 delta subsidence, right image GRO\_ED\_v34\_v9\_noLAU which is an identical model with the exception of a fully transmissible LAU fault group.

### 6.12.10. Kolham

Observation well Kolham-1 is located south of the Eemskanaal cluster in the South Western periphery of the field. Kolham lies in a high and is bounded on the South by fault without juxtaposition. On both the west and east of the high there are bounding faults without juxtaposition. On the north of the high there is a connection to the Eemskanaal cluster. Multiple faults separate Kolham-1 from Eemskanaal. The pressure in Kolham is lagging with respect to Eemskanaal. It is not possible to determine the contribution of individual faults to this observed lag. The model has a partially sealing fault to achieve a reasonable match to the observed pressure, Figure 71 – Fault Q.

### 6.12.11. The Land Asset fields

The following text describes the attempt to match the Land Asset fields within the model closure and the matching parameters used to achieve this match. The locations of the Land Asset fields are shown in Figure 80.

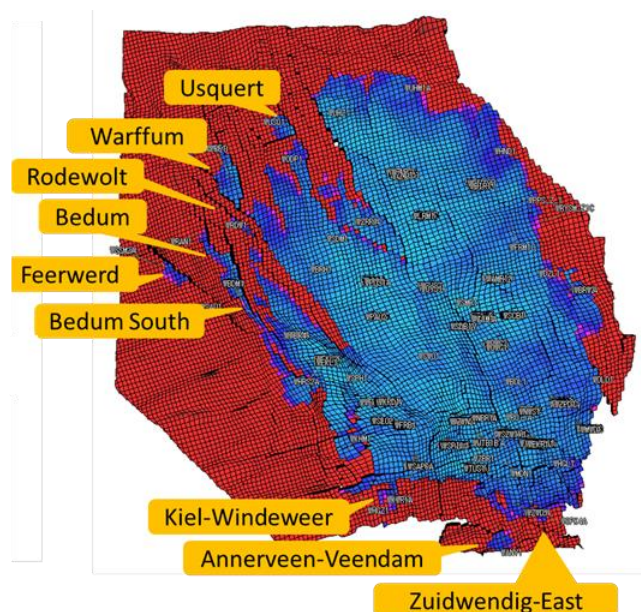


**Figure 80 Location of the Land Asset Fields in the extended periphery of Groningen**

### 6.12.12. Feerwerd

Feerwerd is a tight reservoir with two wells, a horizontal well with an open hole completion - SSM-2A - and a vertical well which has been hydraulically fractured - SSM-4. Due to the coarseness of the model SSM-2A was initially wrongly placed in our model. Therefore the well has been manually shifted. Also the permeability in this field was initially too high. A 2002 well test found permeabilities ranging from 0.35-0.74 mD. A permeability reduction is applied to ensure the permeability is in the order of 0.1-1 mD (53). Pressure measurements indicate SSM2A started production at hydrostatic pressure. The the major fault East of Feerwerd is set to be fully sealing to prevent pressure communication with Bedum and Warffum fields. With the permeability reduction in place the model still has too much pressure support to achieve a match without reducing the volume. A GBV multiplier has been applied to reduce the volume of Feerwerd. The resulting subsidence match in the area is good.

### 6.12.13. Usquert and Oldorp

Usquert is a land field located north of the Groningen field, in the northern part of the North West region. Usquert is in pressure communication with the Groningen field via the aquifer and is significantly lagging in pressure. Due to the reservoir structure, gas in the Usquert field is not in direct communication with gas in the Groningen reservoir, see Figure 81. South of the Usquert structure lies the Oldorp compartment which is substantially depleted with respect to Usquert. Oldorp PNL measurements show a large water influx. This water most likely flow into the reservoir from the North, since the Stedum-1 observation well south of Oldorp-1 see no water rise. To ensure Usquert pressure depletion is in line with the measurements and Oldorp has the observed water influx, this section is modelled as a u-tube by sealing the fault south of Usquert above the water contact, Figure 71 – Fault A. This construction results in the observed model behaviour. Oldorp is slightly lagging in pressure with respect to the Stedum-1 observation well, therefore one of the faults separating Oldorp from Stedum is set to be partially sealing, Figure 71 – Fault B.

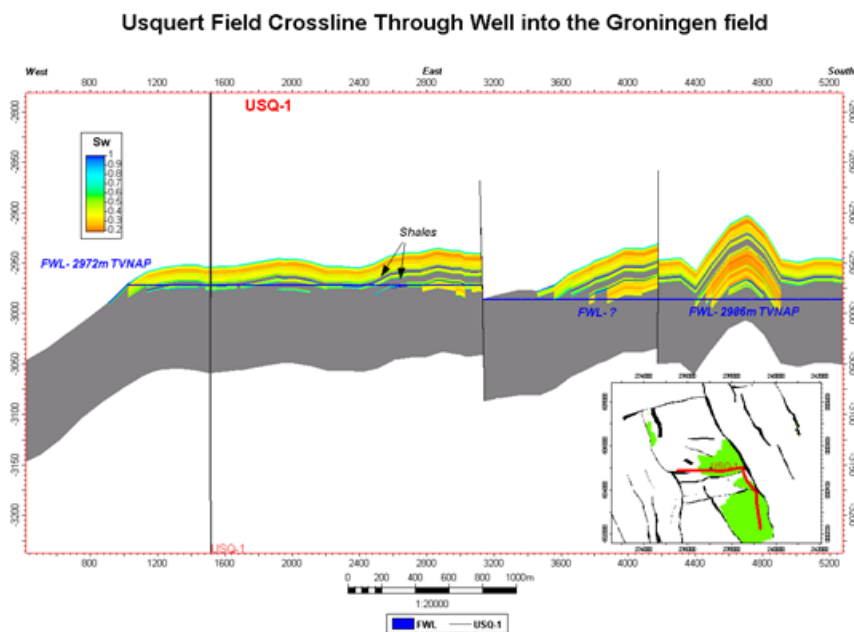


**Figure 81 Usquert field and its connection to the main Groningen field on the South**

### 6.12.14. Kiel-Windeweer

Kiel Windeweer is located south of the Groningen field. Our model is too coarse to properly model Kiel-Windeweer. Because of the coarse scale a fault that separates the field is missing in the model. The KWR wells only see volumes on one side of the fault. To mimic the observed volumes a gross bulk volume multiplier is applied. Permeability in KWR is 1.15 mD according to a 2004 well test interpretation (54). Initially permeability is too high. The permeability is reduced with a multiplier. Prior to production there was no pressure depletion in the KWR field, see Figure 82. To match the initial pressures the surrounding faults are completely sealed to prevent pressure communication with the main reservoir.

Despite these efforts the grid was still too coarse to properly match this field. To investigate the impact of the grid size a very fine scaled model is run and this improved the history match dramatically, see Figure 82. However, this is not a workable solution. The runtime of the fine model with 3.2 million active blocks is almost 3 weeks, compared to 320 thousand blocks which

runs in almost 2 hours. Future work could apply local grid refinement to improve on the history match to pressures.

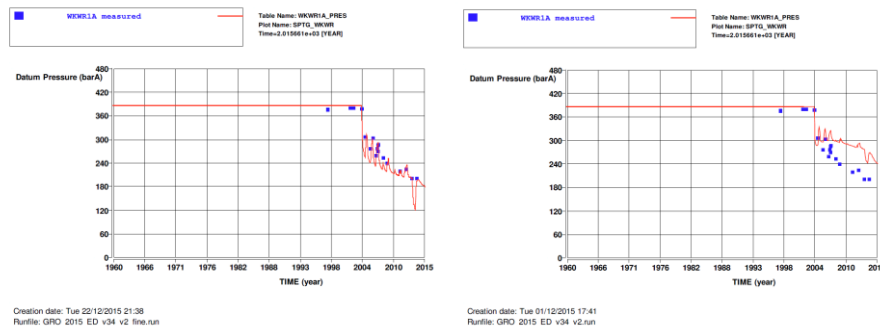


**Figure 82 Pressure match in KWR1A comparing v34\_v2\_fine\_scale to v34\_v2.**

### 6.12.15. Warffum

The Warffum field is located north west of the Groningen field in the Rodewold aquifer. Initial pressures in the Warffum field are matched by applying the reported hydrostatic gradient of 1.16 bar/10 m (55). Warffum was initially undepleted and the field is therefore separated by sealing faults to prevent communication with Groningen or Bedum via the aquifer, Figure 71 – Fault ζ. Observed water rise is different for the two wells in the Warffum field, WRF-1 and WRF-2. In an attempt to match this behaviour the faults separating the wells within the field are used as a matching parameter, Figure 71 – Fault η. To match the energy in the field the bulk volume had to be reduced.

### 6.12.16. Bedum

Bedum is located west of the Groningen field near the TenBoer observation wells. When the Bedum field was in 1970 it was at initial pressure of 349 Bara. The field has been sealed off by faults to prevent pressure depletion via the aquifer or via faults due to Groningen production. The water gradient in Bedum, 1.14 bar/10m to 1.16bar/10m (55), is slightly lower than the one in Groningen instead of 1.17 bar/10m (8). Since Bedum was at initial pressure after Groningen production started the block is not connected to the Groningen reservoir. All the faults between Groningen and Bedum are fully sealing.

Bedum can be divided into four blocks separated by partly sealing faults based on measured pressure differences. From north to south with the well determining the name of the block, RNM1, BDM3, BDM1-2, BDM4 and BDM5. The initial in place gas volume of the Bedum field has been determined dynamically by means of p/z analysis. According to the 2014 RCN the block with BDM1 and BDM2 had a 8.3 billion Nm<sup>3</sup>, the block with BDM3 had 3.7 billion Nm<sup>3</sup>, the block with BDM 4 had 0.56 billion Nm<sup>3</sup>, and the block with BDM5 had 0.5 billion Nm<sup>3</sup> (56). Multipliers are in place to control the degree of separation for all blocks and a gross bulk volume multiplier is used to match these volumes, Figure 71 – Fault T,U,V,W,Y.

The knowledge of separation of the Bedum field from the aquifer is based to a large extent on subsidence data. In the model Bedum is disconnected from the aquifer by a group of faults, Figure 71 – Fault X. If there would be a full connection between Bedum and the aquifer the pressure in the aquifer will drop. This will result in subsidence as a result of compaction due to the lower pressure. However, comparing proxy results for such a depleted aquifer to subsidence data will show that no pressure drop is required for a good match.

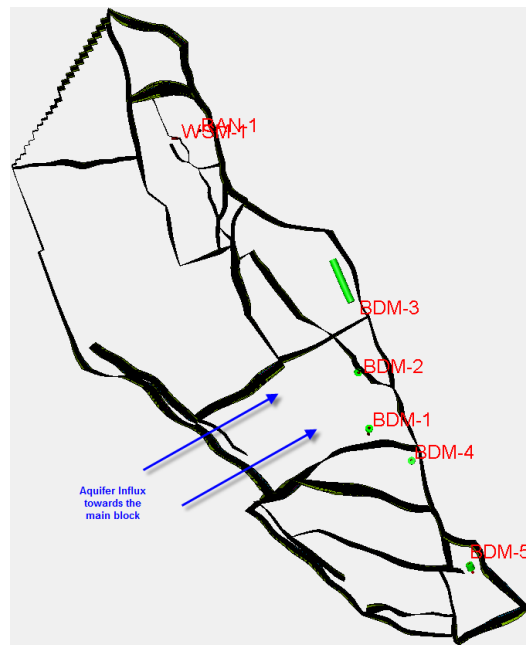


**Figure 83 Bedum field with the Bedum wells indicated, the aquifer direction of flow is indicated by the dedicated field reservoir engineer**

#### 6.12.17. Midlaren

Midlaren is located in the southern periphery of the Groningen field, south of Hoogezand-1. Midlaren is an oil reservoir with a gas cap (57). Given the relatively small volume of the field and the fact it is not being produced, no attempt is made to model the oil phase. A fit for purpose approach is sufficient. Properly matching the reservoir would require the introduction of three phases in the full model. The reservoir is depleted via the aquifer and the measured pressures are matched by controlling the fault seal factors separating Midlaren from the Aquifer, Figure 71 – Fault ε.

#### 6.12.18. Zuidwending and Annerveen

Zuidwending and Annerveen are located south-east of Groningen in the periphery of the field. Wells OPK-4, ANV-1, ZVN-1 and ZVN-2 all see pressure depletion due to pressure depletion of the Groningen field. Observed pressures are slightly lagging with respect to the nearby Groningen clusters, this lag is matched by a fault seal factor Figure 71 – Faults E. Zuidwending-1 and Zuidwending-2 are likely separated by a fault separating these wells this is based on an observed pressure lag. The pressure is matched by a group of faults, Figure 71 – Faults F. The Annerveen-1 well is located in the Annerveen-Veendam field in southern edge of the model closure and measured pressures show a pressure lag with respect to the nearby Zuidwending wells, this behaviour is matched with a fault, Figure 71 – Fault G. Structurally this area is uncertain because of imaging problems due to an overlying salt dome (22).

#### 6.12.19. Zuidwending East (OPK-4)

Zuidwending East is perforated by a single well OPK-4. The reservoir had been depleted before production started by Groningen (58). The gas in place was approximately 890 million Nm<sup>3</sup> based on p/z analysis (59). This initial volume is matched with a GBV multiplier. In order to achieve the correct pressure at the moment production starts faults surrounding the reservoir are set to be partly sealing, Figure 71 – Fault δ. Zuidwending East has higher calorific gas than Groningen (58). The resulting model matches to static bottom hole pressures and the RFT.

### 6.13. History matching results

The RMSE to SPG measurements is 2.17 bar, the RMSE for PNL height is 1.96m, and the RMSE for RFT is 10 bar and a subsidence RMSE is achieved of 4 cm. As is described in the text above a pressure match for some land fields is not necessary or possible with the current grid size. The achieved pressure match for the field and regions within the field is shown in Figure 84. Attached is the file GRO\_2015\_ED\_v34\_v9\_SPTG\_Match.pdf showing the individual well/cluster results as a function of time.

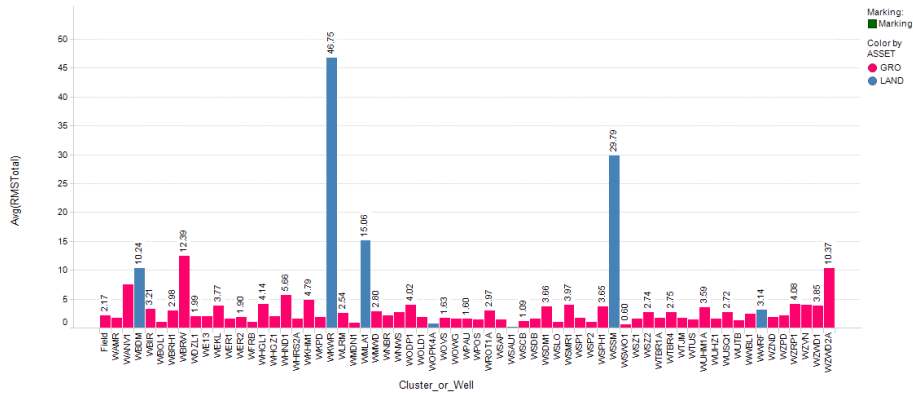


Figure 84 Result of the SPG mismatch RMSE function

The achieved mismatch to water influx is shown in Figure 85. Attached is the file GRO\_2015\_ED\_v34\_v9\_PNL\_Match.pdf showing the individual well results as a function of time.

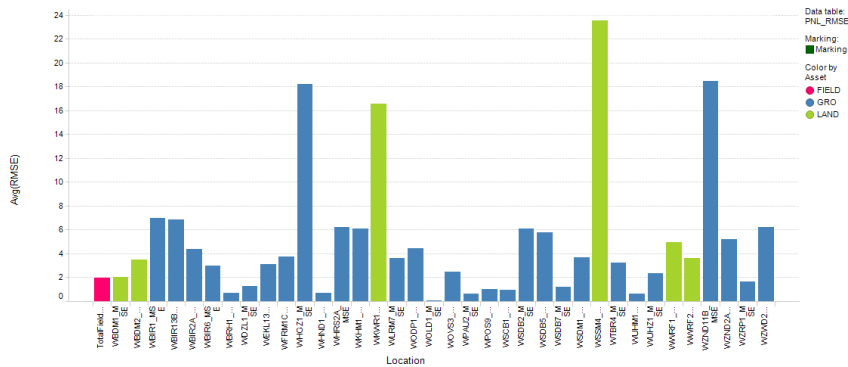


Figure 85 Result of the PNL mismatch RMSE function

The achieved mismatch to RFT measurements is shown in Figure 86. Attached is the file GRO\_2015\_ED\_v34\_v9\_RFT\_Match.pdf showing the individual RFT matches and the model output.

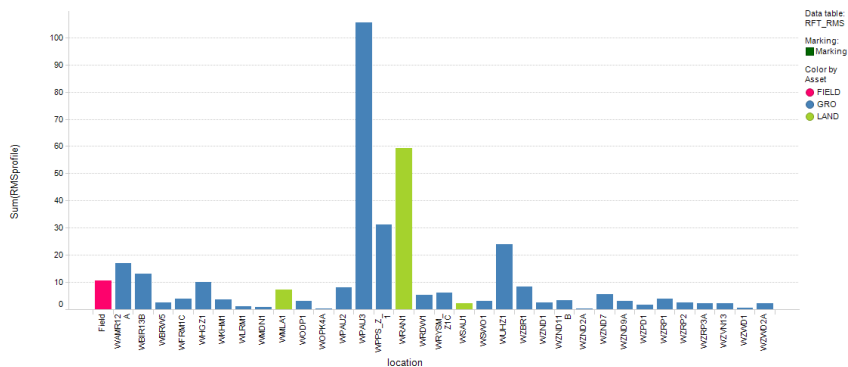
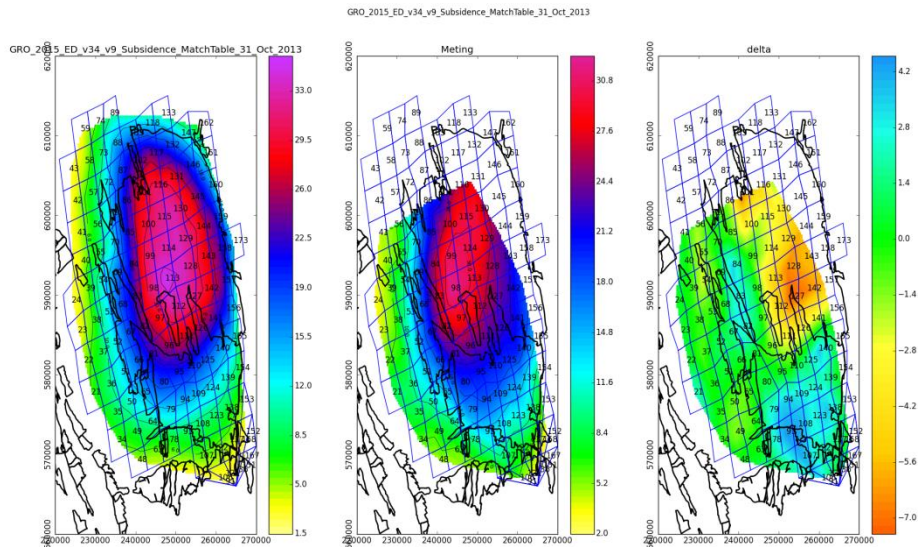


Figure 86 Result of the RFT mismatch RMSE function

The achieved match of the subsidence proxy is shown in Figure 87.



**Figure 87 Results of the subsidence mismatch with the proxy results (left), the subsidence data(middle) and the difference function.**

#### 6.14. Uncertainty analysis workflow

The main purpose of this model is to be the base for generating forecasts for the Winningsplan 2016 with the secondary purpose to use it in business planning and resource volume estimation. Therefore the uncertainty in the ultimate recovery of the field under the current scenario with the assumption of further compression stages is investigated. The history matched model and the resulting matching parameter space will be used in the determination of the range of ultimate recovery for a simplified production scenario. According to the GFR2015 “clean sheet” model report it is very important to use UR instead of GIIP because late field life uncertainty parameters are screened out in the uncertainty analysis based on GIIP, e.g. aquifers or relative permeability parameters. For resource volume estimation purposes the uncertainty in field UR at the end of economic field production life is important. For infill projects the uncertainty in project UR or project value is looked for and for hazard and risk assessment of earthquakes the uncertainty in maximum subsidence may be the parameter. This uncertainty analysis will provide p90/p50/p10 models reflecting the ultimate recovery (48). For other business decisions a similar approach with different objectives will result in a different set of models. The resulting set of models from this work can be used as a starting point but an uncertainty analysis for each specific business decision, such as an infill well, needs to be performed.

The goal is to have a set of models with a sufficient history match that capture the potential spread in the forecast, this is schematically shown in Figure 88.

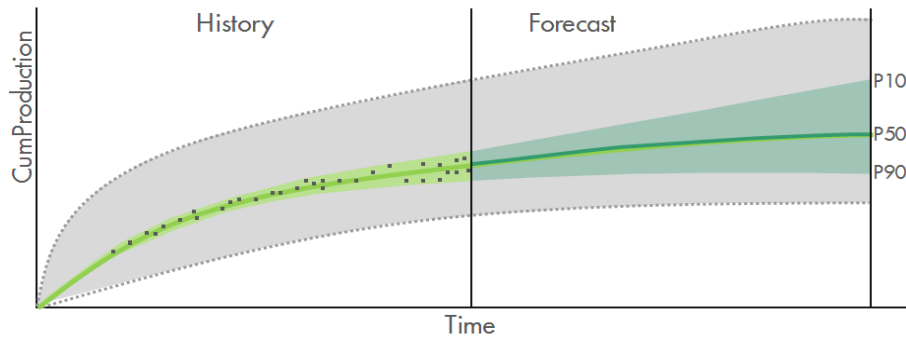


**Figure 88 schematic representation of the uncertainty for ultimate recovery (UR).**

The workflow for the analysis of the uncertainty of the ultimate recovery that is applied is as follows:

1. Generate a set of variable parameters with sufficiently wide ranges to capture enough uncertainty.
2. Assess which variable model parameters affect the uncertainty in ultimate recovery without affecting the history match.
3. Simulate the history match and the forecast for a large number of models all with a varying set of the set of variable parameters.
4. Quantify the sensitivity of the mismatch functions to independent variable parameters.
5. Discard variability of parameters that could reduce the history match.
6. Simulate the forecast with an ensemble of models by varying parameters that do not impact the history match.
7. Determine P10, P50 and P90 members of the range based on ultimate recovery.
8. Test the range of ultimate recovery by investigating a larger set of variable parameters.

### 6.15. Simple forecast

In order to assess the uncertainty in the ultimate recovery, a forecast period needs to be simulated. Two options are available, apply the complex HFPT deck (dynamic optimization) or apply a simple set of forecast constraints which are identical for all runs. The advantage of the HFPT approach is that the model is relatively realistic and that it optimizes the forecast. The disadvantage is that the HFPT deck will result in non-linear effects that could impact the ultimate recovery on top of the impact of the parameters and the runtime is long.

In order to prevent secondary effects and to make all runs comparable a simple forecast is used. The simple forecast run has annual production constraints set for four regions. The respective regional constraints are:

- East:  $(30/39.4) \times 24.5$  billion  $\text{Nm}^3$ ,
- Southwest:  $(30/39.4) \times 9.9$  billion  $\text{Nm}^3$ ,
- LOPPZ:  $(30/39.4) \times 3$  billion  $\text{Nm}^3$
- EKL:  $(30/39.4) \times 2$  billion  $\text{Nm}^3$ .

### 6.16. Assess parameters effecting the HM and not the FC

Before the uncertainty on ultimate recovery is analysed a set of variable parameters is needed which result in an ensemble of models with a sufficiently good history match and that could

cover the full uncertainty range in ultimate recovery, this is the green zone schematically represented in Figure 88. The historical data must be adhered to by all of the models. The starting point of the workflow is the history matched model. Models with a complete mismatch to historical data are not likely to have the predictive capabilities to generate a reliable forecast. These unfit models are the grey envelope in Figure 88.

The set of variable parameters used for the ultimate recovery uncertainty analysis is the same as the set used for the assisted history matching workflow. However, some variable parameters have extended ranges in order to investigate a larger solution space. The extension will ensure a larger possibility of having endmembers with a sufficient spread of possible history matching scenarios. For instance all faults have the possibility to be fully open during the forecast uncertainty analysis.

To ensure a history match the parameters are screened by their independent impact on the mismatch function shown in Equation 32, Equation 31 and Equation 34. This sensitivity is determined with a Tornado Experimental design. If parameters have a large impact on the history match, they will not be varied during the forecast. Since a variation from the history matched base case could reduce the match. Sensitive parameters will be frozen in the space filling exercise. A rough 80/20 approach is applied here, 80% of the effect is controlled by 20% of the matching parameters. The 80% interval for SPG data is shown in Figure 89. Some parameters have a large impact on the history match such as the GBV multiplier on the Slochteren, others do not have an impact on the history match, such as the initial gas water contact in the South East. Similarly to the SPG, the subsidence and the PNL RMSE values are screened, resulting in partly overlapping but partly different matching parameters that screen to be sensitive in the history match.

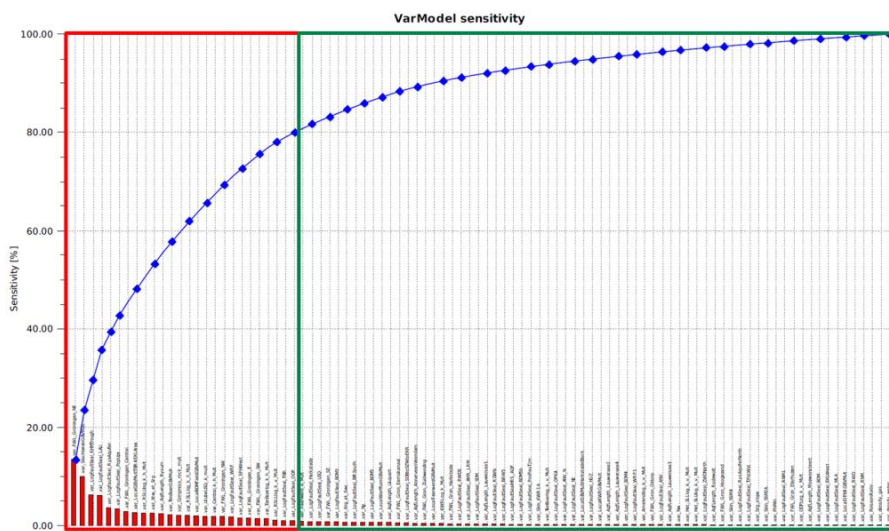


**Figure 89 Screening parameters sensitive to the history match to example for the SPG applying 80/20 selection of parameters**

The sensitivity of the ultimate recovery to parameter variations is analysed too. The idea is that some parameters that do not impact the history match could impact the forecast. The 80% interval of parameter impact on the ultimate recovery is shown in Figure 90. There are 25 parameters in this interval of which 13 do not significantly change the historical mismatch to subsidence, pnl or spg, these are indicated by red stars in Figure 90. These parameters are varied randomly within their assigned range during the forecast uncertainty analysis to generate an ensemble of models that adheres to historical data yet significantly impacts the ultimate recovery.

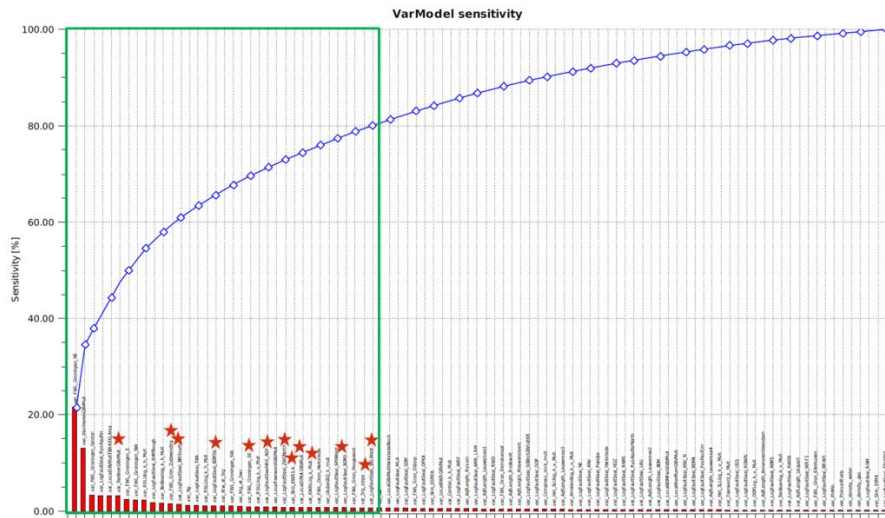


**Figure 90 Sensitivity of the ultimate recovery to independent matching parameters, with 13 matching parameters indicated by a star that do not screen to be sensitive during the history match but fall within the ~80/20 interval**

**6.17. Results of the uncertainty analysis**

A set of matching parameters is set-up with these 13 parameters varying to generate an ensemble of 1000 models. The spread in ultimate recovery ranges from 2785 billion Nm<sup>3</sup> to 2938 billion Nm<sup>3</sup> with the base case history matched model at 2869 billion Nm<sup>3</sup>, these results are shown in Figure 91.

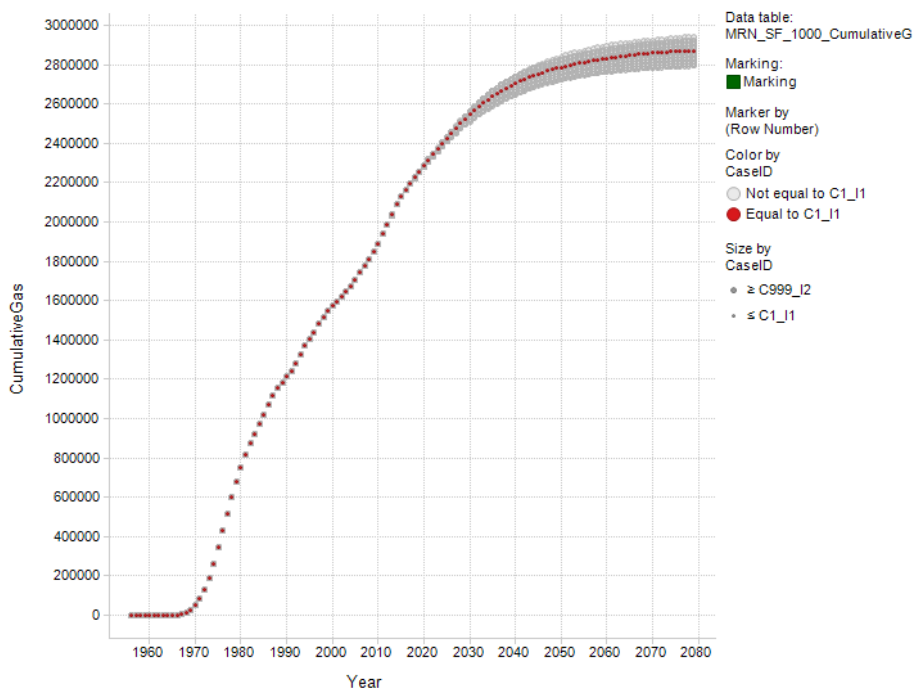


**Figure 91 Results on cumulative gas production and inevitably ultimate recovery for 1000 models**

The required p90/p50/p10 ultimate recovery is based on the cumulative distribution function of the ultimate recovery. Our simple forecast and ensemble of 1000 models results in a p90 of 2801501 million Nm<sup>3</sup>, a p50 of 2838077 million Nm<sup>3</sup>, and a p10 of 2874327 million Nm<sup>3</sup> in ultimate recovery of the Groningen field excluding the peripheral land fields.

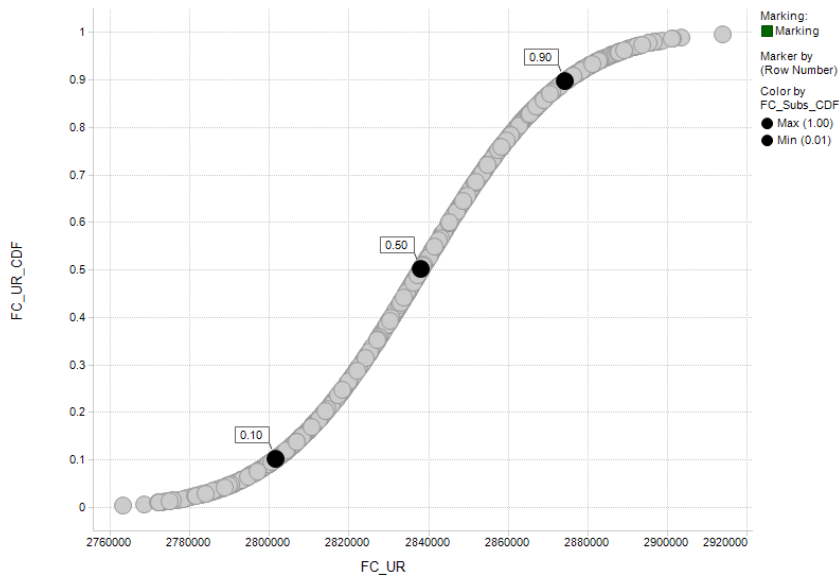


**Figure 92 Cumulative distribution function of 1000 runs for ultimate recovery, p90 2801501 million Nm3, p50 2838077 million Nm3, p10 2874327 million Nm3.**

The applied approach could potentially miss possible scenarios due to the reduced set of variable parameters. This set of variable parameters has been reduced based on the independent sensitivity of parameters with respect to the history match. Different variable parameters could potentially result in an equally acceptable match. In order to investigate these different scenarios the full set of variable parameters has been run in a space filling exercise. Out of this space filling exercise five models are selected that have a good history match. These models are compared to the same distribution described above. All fall within the range of ultimate recovery found before, see Figure 93.

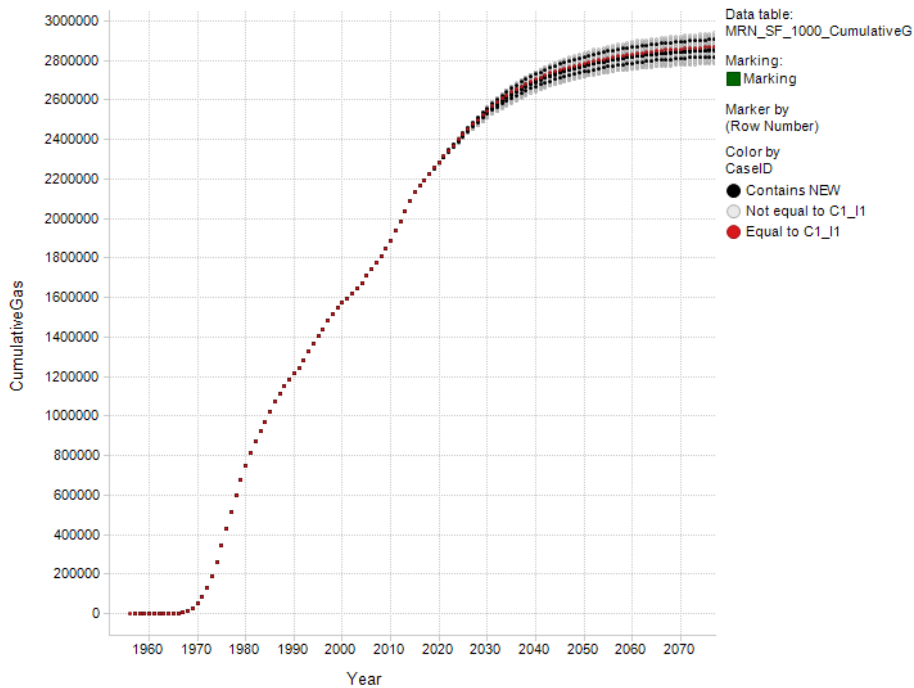


**Figure 93 Spread in ultimate recovery for a sampling of 1000 runs, also 5 tested wide range runs of a full varmodel space filling**

The spread in GIIP has been investigated for completeness and to compare these results to the outcome of GFR2013 and GFR2012 work. The full varmodel space filling exercise used to select the 5 endmembers is also used to generate a distribution of the mismatch function of the SPG compared to the GIIP in the model. The lowest RMSE to SPG is achieved for a model with a GIIP of 2913 billion Nm<sup>3</sup>. This is in-line with the dynamic GIIP found in GFR2013, see Figure 94.

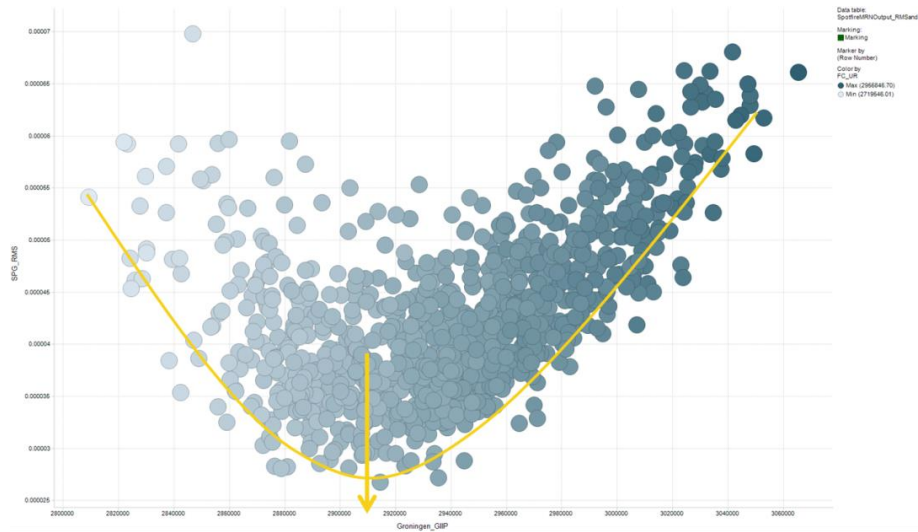


**Figure 94 SPG RMSE as function of GIIP in the Groningen model with the lowest RMSE at ~2913 Bcm**

## 7. Surface Pressure and Flowrate Matching

### 7.1. Capacity matching

One important use case for the Mores model is the ability to forecast individual well capacity, i.e. flowrate as a function of tubing head pressure (THP). While historically the history matching process has focused on the use of subsurface pressure measurements (mainly SPTG), a new feature of this model is extensive use of surface pressure measurements. This is done with the aim to history match individual well surface responses – flowrate and corresponding THP values, known as PQ matching.

What enables this new history matching step is the sophisticated data acquisition strategy in Groningen where all production wells have been equipped with flow and pressure sensors, with continues recording via Exaquantum and PI. Using this data (available since 2011) a filtered dataset has been created using SAS/Wikker. This dataset contains daily average production rates, with corresponding up-times and THP values for all production wells. The up-times allow for wells that are only partially producing during the day to still report a valid THP for the flowing period. In Figure 95 the example of Spitsbergen-6 for 27<sup>th</sup> June 2014 is shown. It was only partly producing during the day, with an instantaneous rate of about 424k Nm<sup>3</sup>/day, corresponding to a THP of 53 bars. The average day production was 239k Nm<sup>3</sup>/day, resulting in an up-time of 0.56. During history matching MoReS will utilise both the day average rate, to ensure correct offtake, and up-times for correct prediction of THP.

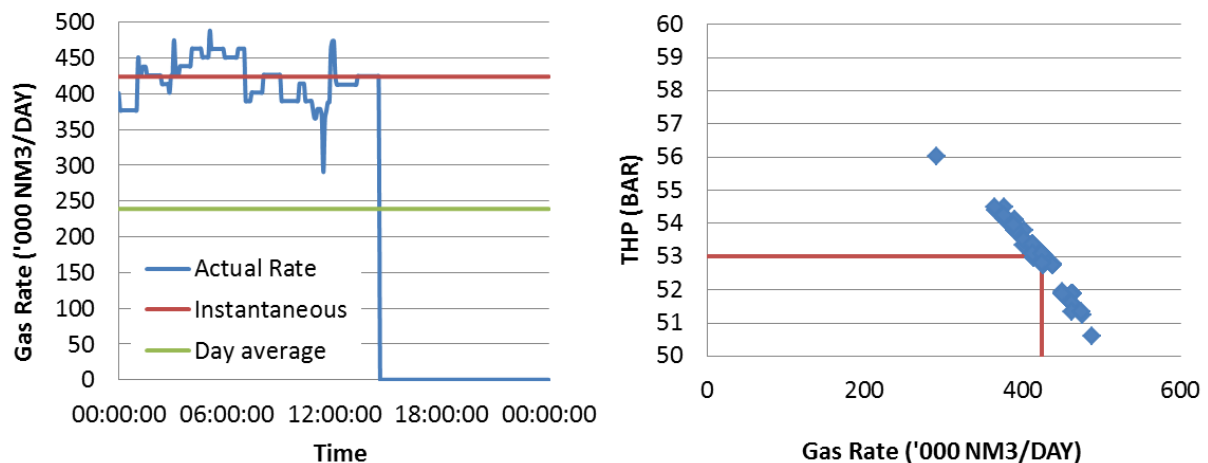


**Figure 95 Procedure for converting continuous data monitoring into MoReS calibration data. Example of SPI-6 on 27<sup>th</sup> June 2014.**

Not all days have a reported THP value – the result of various filters implemented in the SAS/Wikker case. To simplify the matching process we want to exclude data that are dominated by transient pressure effects, hence the case has logical rules that must be met before a THP value is considered to be valid for a production day. This includes minimum continuous flowing time, maximum variation in rate etc. (60).

In Figure 96 and Figure 97 the modelled and actual PQ behaviours of Leermens and De-Eeker clusters are shown for a six months period in 2012 using these daily time-steps. The subsurface model has been history matched but without addressing the performance of individual wells.

Several aspects are worth noting:

- Several of the curves show the same curvature but with a parallel offset. A fixed pressure offset, shifting the curves up and down, would allow for several of the wells to be

matched. The size of the error is not unreasonably large given that the field-wide RMS error to SPG measurements is about 2 bars.

- In some cases the curvature is different, most notably for Leermens 4. This would indicate differences in well productivity. It is unrealistic to capture near wellbore heterogeneity in all cases given upscaling to a relatively coarse simulation grid (resulting in multiple wells on a cluster typically producing from the same gridblocks). Stimulation and damage to the perforation area are also not captured in the model – wellbore skin values were set to a default value of 0.0 for all production wells.
- The central and northern clusters of the field show very little noise in the PQ behaviour, e.g. Leermens. In 2012 they were high on the start-up list (production caps were only introduced in 2014). The combination of fairly constant flowrates with high reservoir quality results in little influence of transient effects. However, in the south (e.g. De-Eeker) there is much more noise in the data. Being low on the start-up list, the cluster is producing more infrequently and with higher variation, resulting in more transient effects and less accepted THP values due to the applied filters. Additionally there is much more influence of seasonal reservoir pressure variation over the six months period. While there is only a gradual decline of about 2 bars around Leermens, in De-Eeker there is maximum local declines of about 13 bars at the end of winter, followed by an almost equal rebound during summer, see Figure 98.

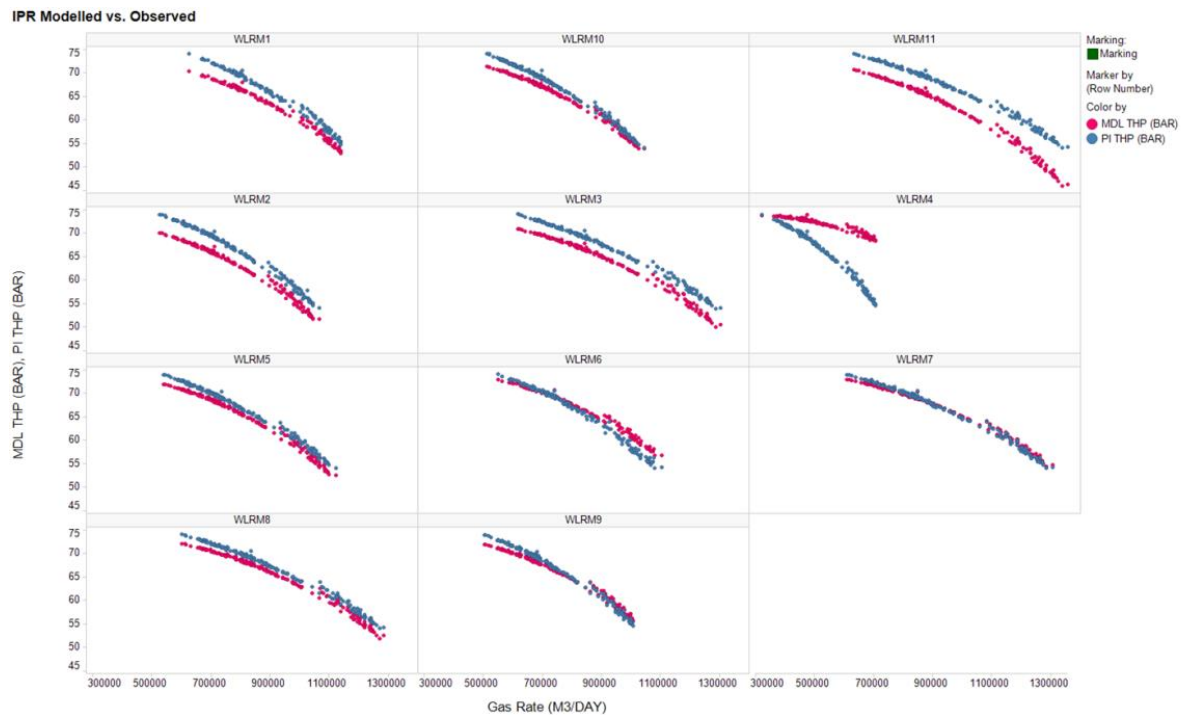


**Figure 96 Comparison of PQ behaviour for Leermens cluster in 2012 prior to matching individual well performance. Model behaviour is shown in red and compared to actual data from PI in blue.**

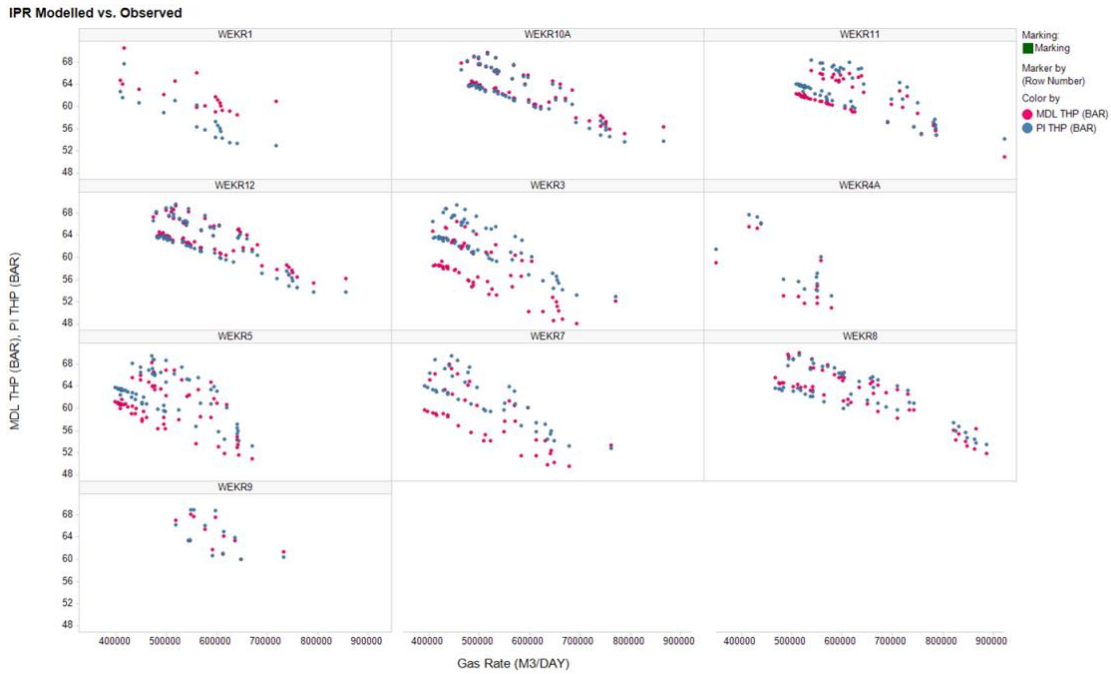


**Figure 97 Comparison of PQ behaviour for De-Eeker cluster in 2012 prior to matching individual well performance. Model behaviour is shown in red and compared to actual data from PI in blue.**

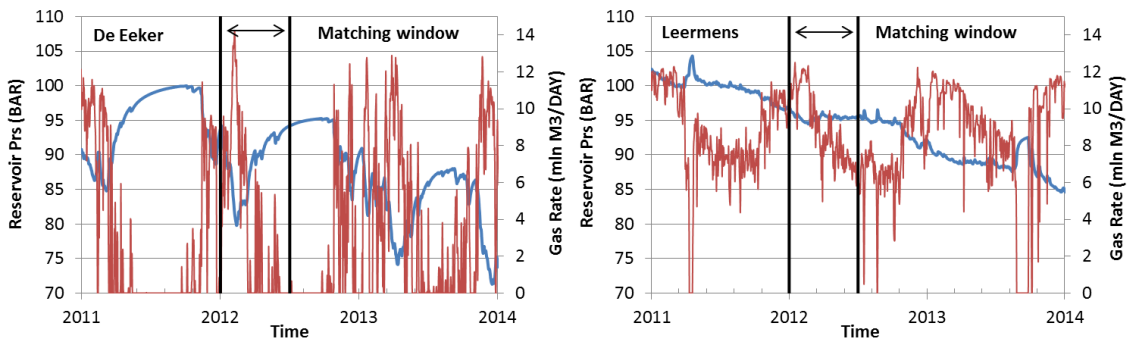


**Figure 98 Production and reservoir pressure for De Eeker and Leermens clusters**

## 7.2. Matching Methodology

Generally the mismatch between actual and modelled PQ response can be improved by (a combination of) three corrections:

1. A vertical shift ( $\Delta p$ )
2. A change in slope
3. A change in curvature

The matching process is (for now) implemented in MoReS, and hence it was assumed that there is a basic set of well inflow parameters that combined with the history matched reservoir behaviour can result in a prediction of surface well capacity that is of sufficient quality to perform forecasting of capacity and offtake. For each well the following parameters are modified:

1. **Pressure offset:** While an overall field-wide reservoir pressure RMS error of about 2 bars is considered very acceptable, for the purposes of capacity prediction it is often too high. For example, for Leermens-3 it corresponds to more than 50k m<sup>3</sup>/day. In the model this correction is implemented in terms of a change to the well pump height. The pump height is the depth from where the lift table is applied. Between the top of

perforation and pump height MoReS applies a gravity head term, i.e. a pressure offset. We further assume that the local pressure error is relatively stable in time. By using pump height the pressure correction will slowly reduce as a function of reducing reservoir pressure, in line with reduction in density, see Figure 99.

- Permeability height multiplier:** The observed well outflow behaviour, as a function of tubing-head pressure, is a function of inflow and lift performance. Both of these are a function of a wide range of parameters like tubing friction factor, near wellbore permeability, interference and damage skin etc. While we attempt to represent these physical attributes as accurately as possible, differences between observed and modelled well productivity will be observed. An extreme example is Leermens-4, as shown in Figure 96. We assume that the amalgamated mismatches originating from all the mentioned sources can be, in part, captured by modifying the permeability height (Kh) multiplier of each well. It's important to note that the applied multiplier is used as an amalgamated tuning factor, and might thus be outside a realistic range if considered solely as a Kh multiplier.
- Non-Darcy Skin:** In addition to a static Kh multiplier, each well can have a modification to the non-Darcy skin. This will result in additional pressure loss at higher flow rates, affecting the amount of curvature in the PQ curves.

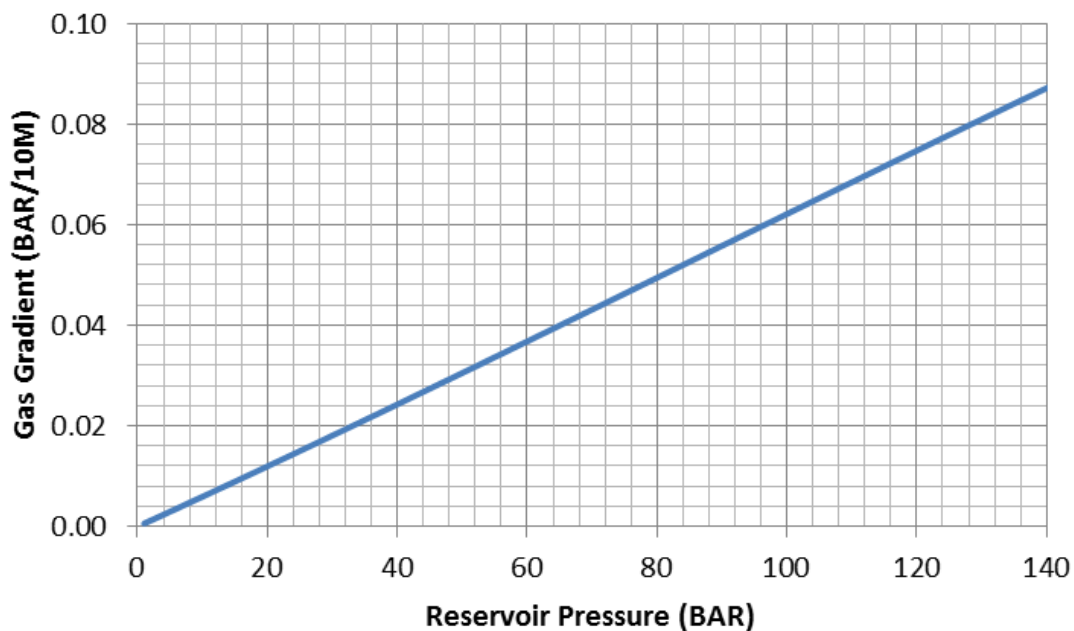
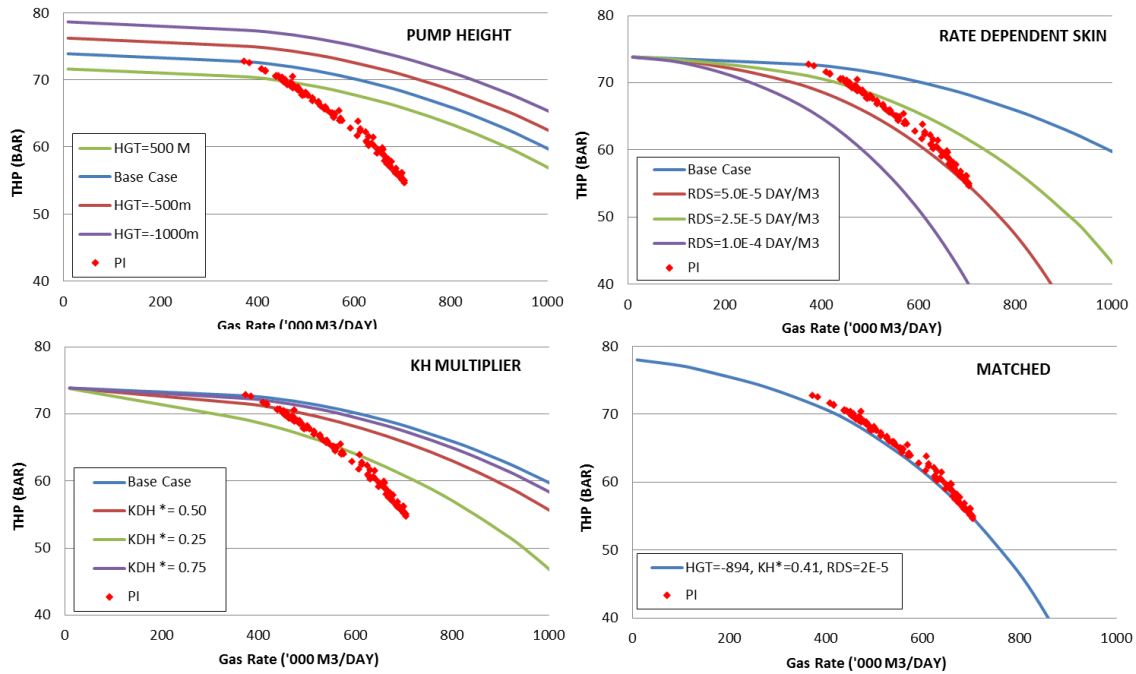


Figure 99 Gas gradient as a function of reservoir pressure assuming 100° C reservoir temperature.



**Figure 100 Matching process example for Leermens-4, with PI data from six months period in 2012**

In Figure 100 the matching process is depicted for Leermens-4. By independently varying the three free variables a good match to the experimental data is obtained. The optimal match is the one that minimizes RMS error in THP to experimental PI data. Matching is done at a certain point in time, in this case July-1 2012. Experimental data is selected from a pre-set window prior to this date. The size of the window is a compromise between minimizing influence from reservoir pressure decline while at the same time having enough data to fully represent the PQ curve. For practical purposes a 6 months window has shown to be a good choice.

The tubing head pressure is essentially affected by three components – reservoir pressure, drawdown and lifting pressure drop. When performing the PQ matching one would like to minimize the effect of declining reservoir pressure over the matching window. In the northern high permeable clusters this is not a significant problem. For example, in the Leermens example the near wellbore reservoir pressure was only varying by about 2 bars. However, in the south the reservoir pressure is typically much more varying. Around De Eeker the reservoir pressure was changing by as much as 13 bars for the same period, as seen in Figure 98.

While much of this is a seasonal swing, it will still strongly affect the PQ curve when plotted as THP vs Q, as seen in Figure 101. For matching purposes a delta pressure is used:

$$\Delta p = p_{res} - THP$$

thus minimising the effects of varying reservoir pressure across the matching window.  $P_{res}$  is in this case the near wellbore reservoir pressure controlling the inflow to the well, implemented using the penetrated block pressures in MoReS. From Figure 101 it is clear that the noise in the experimental PI data is considerably less when plotted with this correction.

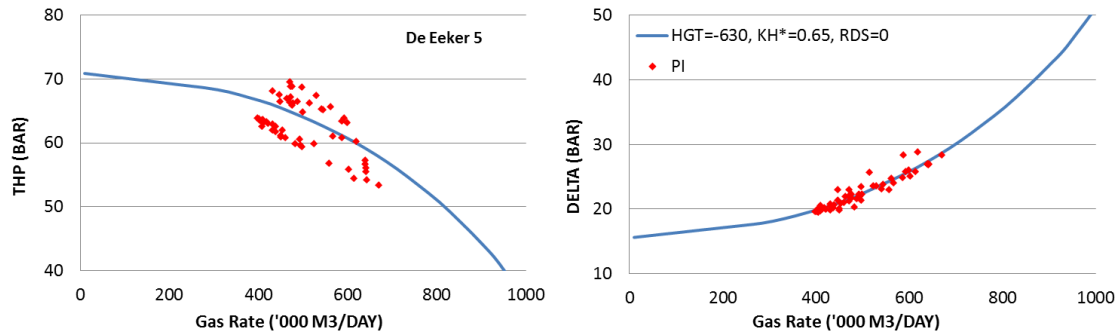


Figure 101 PQ match for De Eeker 5, comparing match on THP vs. DELTA.

### 7.3. Historic Capacity Matching Results

A MoReS script has been developed that automatically matches all Groningen wells using the same methodology. The first quality control of the matching process is to apply the matched tuning parameters to the wells and simulate for the same period that was used in the matching process – in this case the first six months of 2012. In Figure 102 the results for the Leermens cluster is shown. The results, in terms of THP error, for all Groningen wells are shown in Figure 104. The results for both an unmatched, i.e. no tuning parameters applied, and a PQ matched model is shown. The required tuning parameters are shown in Figure 105.

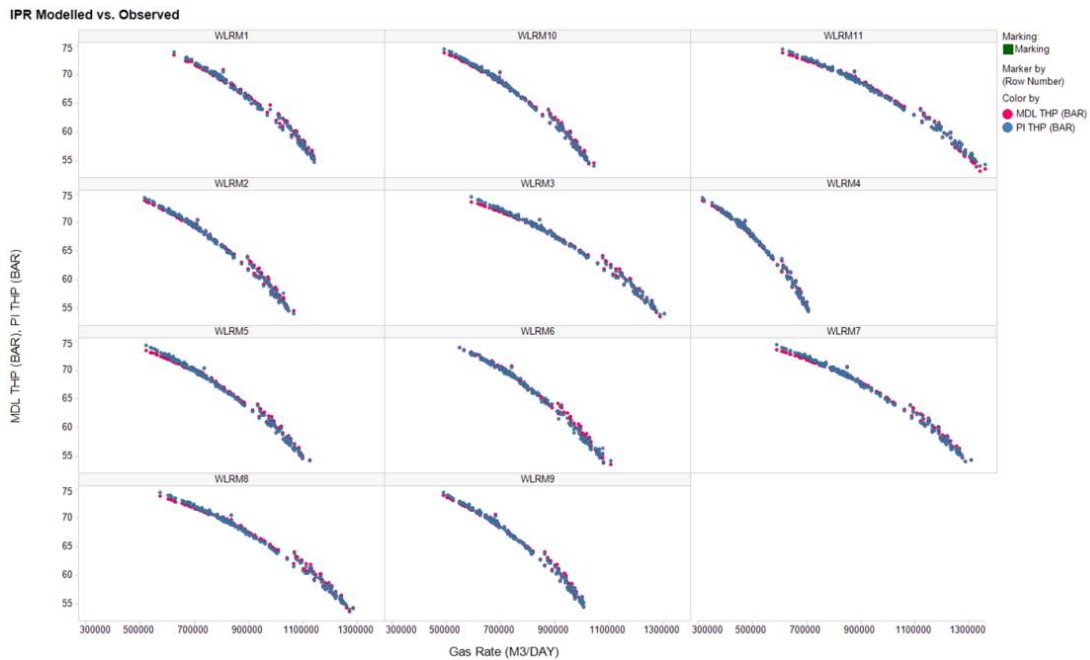
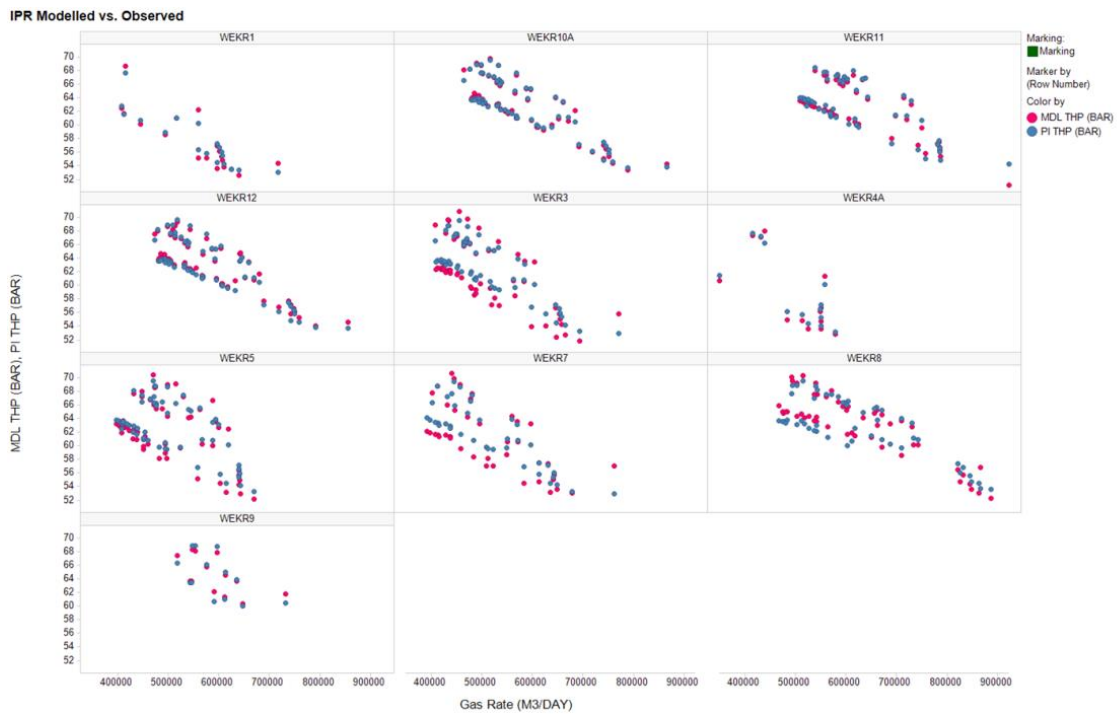
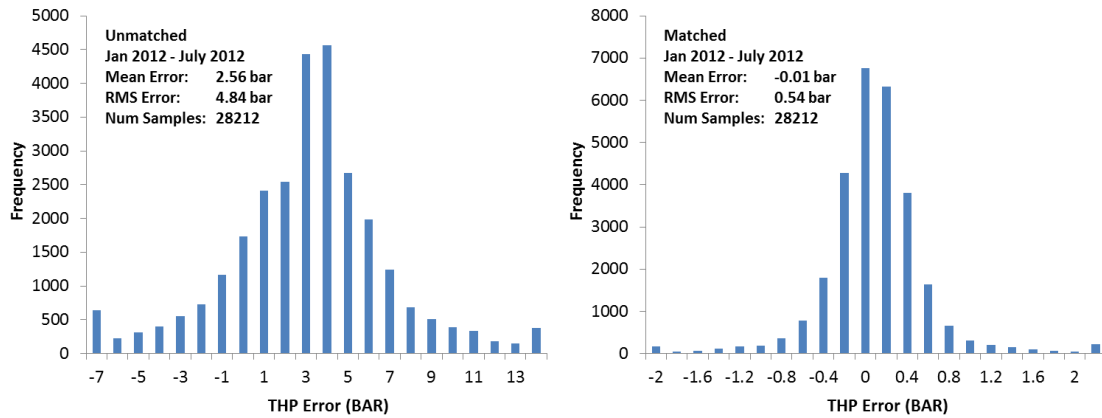


Figure 102 Comparison of PQ behaviour for Leermens cluster in 2012 after matching individual well performance. Model behaviour is shown in red and compared to actual data from PI in blue.



**Figure 103 Comparison of PQ behaviour for De-Eeker cluster in 2012 after matching individual well performance. Model behaviour is shown in red and compared to actual data from PI in blue.**



**Figure 104 Error between modelled and observed THP across 2012 matching window for both unmatched and PQ matched model**

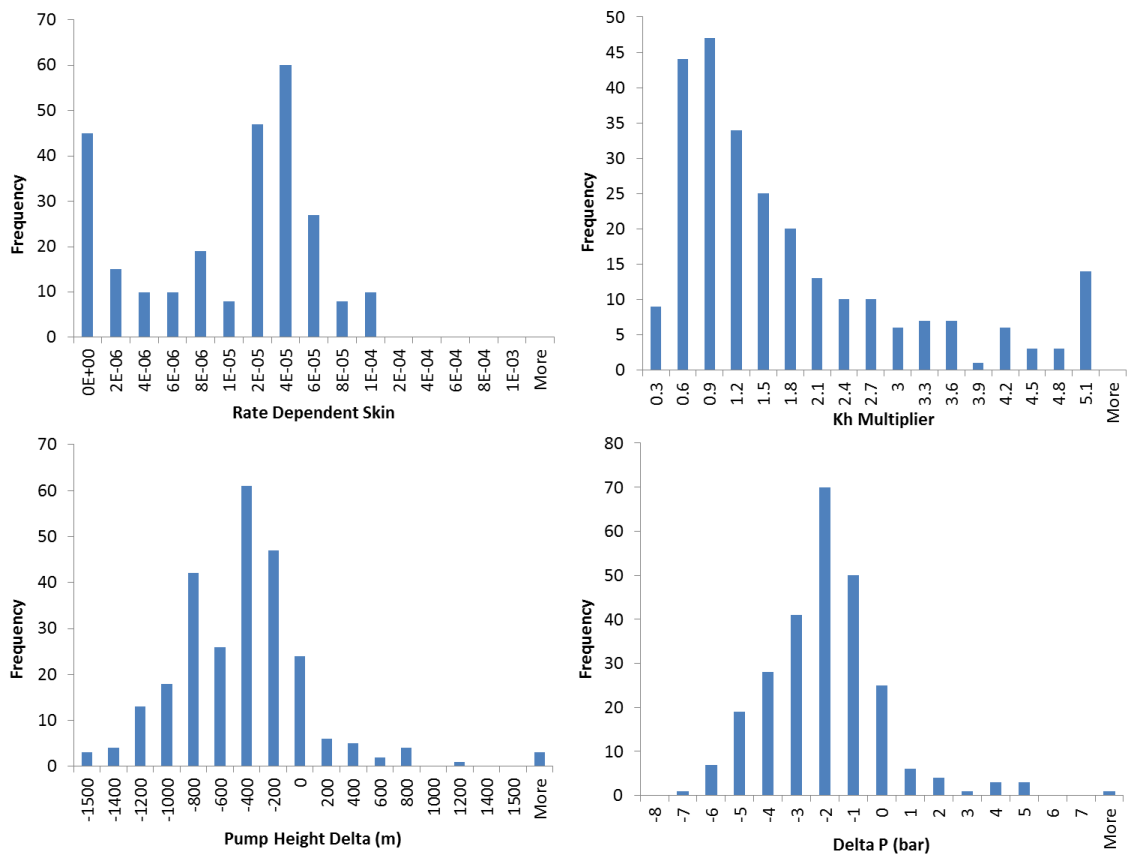


**Figure 105 Applied tuning factors for capacity match done on 2012 data. The pressure delta is represented in the model using a delta on pump height.**

It is also interesting to investigate what the effect is on maximum predicted capacity, defined as the flowrate at a THP value of 20 bars (THP<sub>20</sub>)<sup>6</sup>. We choose to do the comparison at the start of the matching window, i.e. January 2012.

The resulting predicted capacity at field level is 402 mln Nm<sup>3</sup>/day for both the unmatched and matched cases. Even on cluster level the predicted capacities are reasonably close. Only when starting to compare capacity at the well level, do the differences become significant, as shown in **Error! Reference source not found.** and Figure 107. However, for the IPSM (the integrated subsurface and surface model) being able to accurately model individual wells is important since an actual production target for a cluster is achieved by sequentially ramping up individual wells

<sup>6</sup> THP<sub>20</sub> capacity is defined as well flowrate at a THP of 20 bars, and do not account for any surface constraints that might exist.

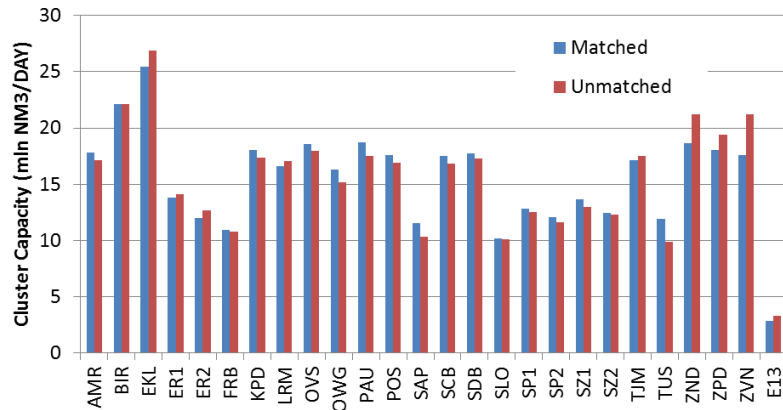


**Figure 106 Differences between unmatched and matched capacity for clusters at January 2012 assuming a THP of 20 bars**

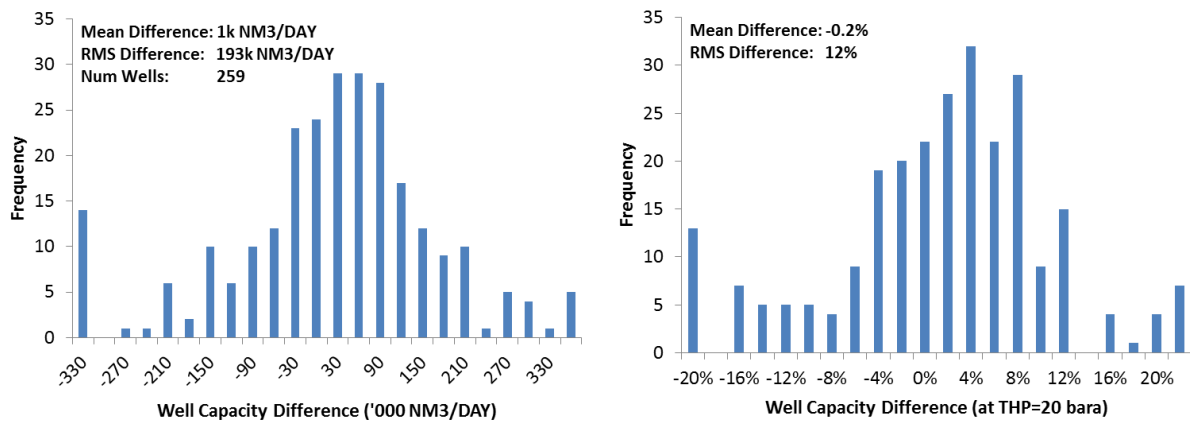


**Figure 107 Differences between unmatched and matched capacity for individual wells at January 2012 assuming a THP of 20 bars**

### 7.4. Capacity Match Forecasting

The purpose of capacity matching is to provide a well calibrated model for high quality forecasting with the IPSM. In Figure 108 the error in THP is shown 1 and 2 years after performing the capacity match. After 2 years the mean and RMS errors have increased to 0.31 and 1.19 bars respectively (from 0.01 and 0.54 bars as shown in Figure 104). In Figure 109 a few examples of PQ matches using 2014 data are shown:

- The vast majority of capacity matches remain good, e.g. Amsweer-10 or Siddeburen-6.
- Some clusters show minor drifts in the pressure history match, e.g. Bierum where the pressure decline seems to be slightly over-predicted. This is not particularly surprising considering the change in production strategy following the restrictions on the LOPPZ clusters from 2014. Further improvements to the history match are being done as calibration data become available.
- In some cases wells are being worked over, e.g. Amsweer-4 had tubing changed out while Oudeweg-6 was re-perforated. Changes to lift or inflow behaviour will require the capacity match to be redone.

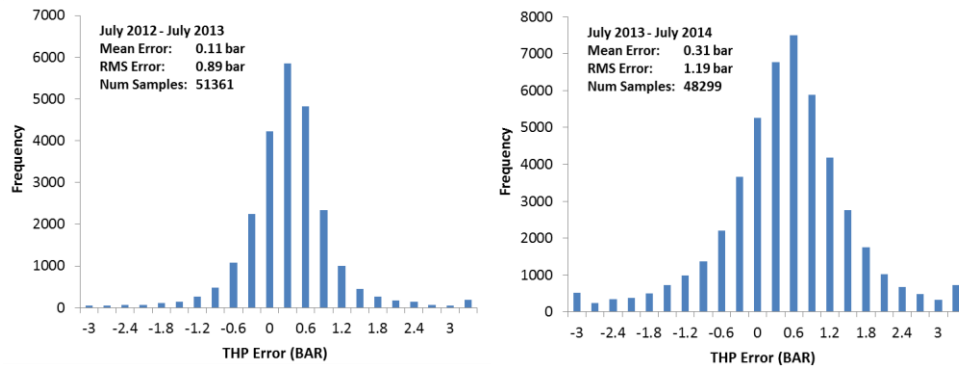


Figure 108 Quality of 2012 capacity match when forecasting 1 and 2 years

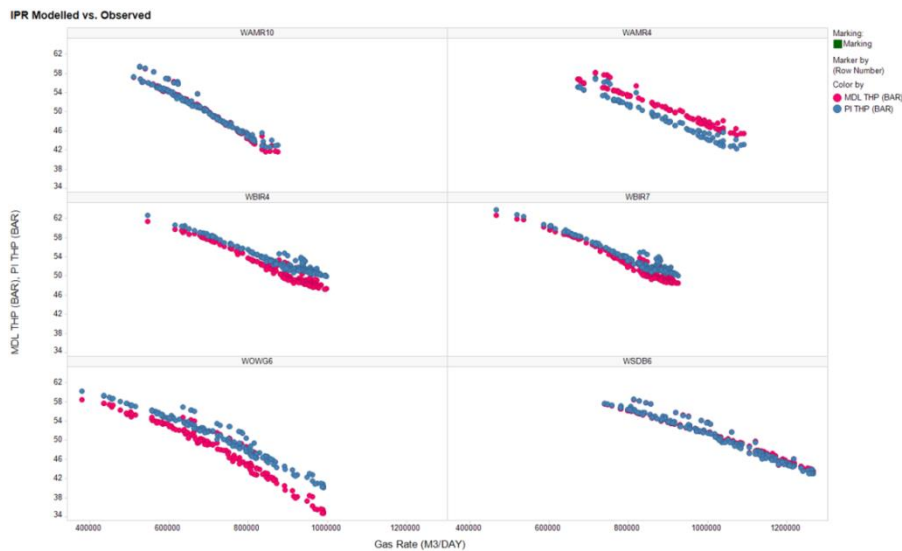


Figure 109 Examples of PQ match on data from January-July 2014 where the matching was done on 2012 data

Since capacity matching is a local tuning of well performance (and does not affect the overall model history match), the tuning parameters should be updated on e.g. an annual basis as new production data is integrated into the model. At the time of writing, 2015 data with associated THP was not available. In Figure 110 the predicted capacities (THP<sub>20</sub>)<sup>6</sup> at the start of 2014 are shown. The comparison is between the 2012 capacity match and a match that is updated to the 2014 data. The overall predicted field capacities (THP<sub>20</sub>) are 338 vs 343 million Nm<sup>3</sup>/day respectively.

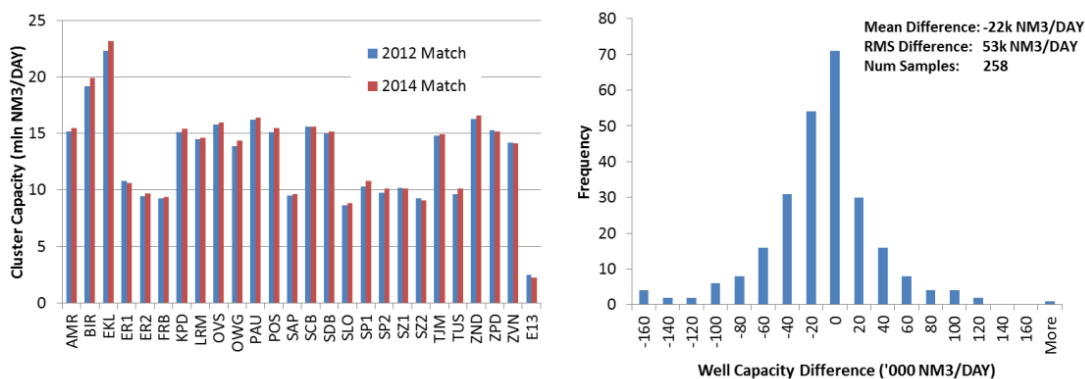


Figure 110 Comparison of cluster and well capacities (THP<sub>20</sub>) at the start of 2014. Comparison between 2012 capacity match and one updated to 2014 data

## 7.5. Areas for Improvement

While the capacity matched model is a major improvement over a model without any form of tuning, there are still areas for improvement.

- The dataset used for the capacity match is generated in SAS/Wikker by applying a collection of rules that define a set of filters that are applied to the THP and gas rate values recorded by PI. The main challenge is to generate enough data over a relatively short time period such that reliable PQ matches can be formed. While this is not a problem for the high permeable clusters that are high on the start-up list (e.g. Leermens prior to production caps), it is a challenge for some of the southern clusters like De Eeker. Work will continue to refine filters with respect to, for example, minimum flow period, maximum daily variation and number of daily well start/stops.
- The tuning factors defined (Kh multiplier, pump height and rate dependent skin) are all mostly affecting the subsurface inflow. A major uncertainty when predicting THP is tubing frictional pressure loss. As long as the inflow pressure loss is of comparable size, minor errors in the tubing friction factor can be corrected with the current set of tuning parameters. The default tubing friction factor used for Groningen wells are 0.015mm. For wells that have flow coating installed (e.g. ZND-7) this seems too conservative. Combined with small drawdown due to high permeability, this makes PQ matching for such wells difficult. Reducing the friction factor to 0.005mm increases the hydraulic performance of the well with about 100k Nm<sup>3</sup>/day. This is consistent with observed data (61). Ensuring all wells with flow coating installed are modelled with appropriate friction factor, would minimize the need for unrealistic PQ tuning parameters.

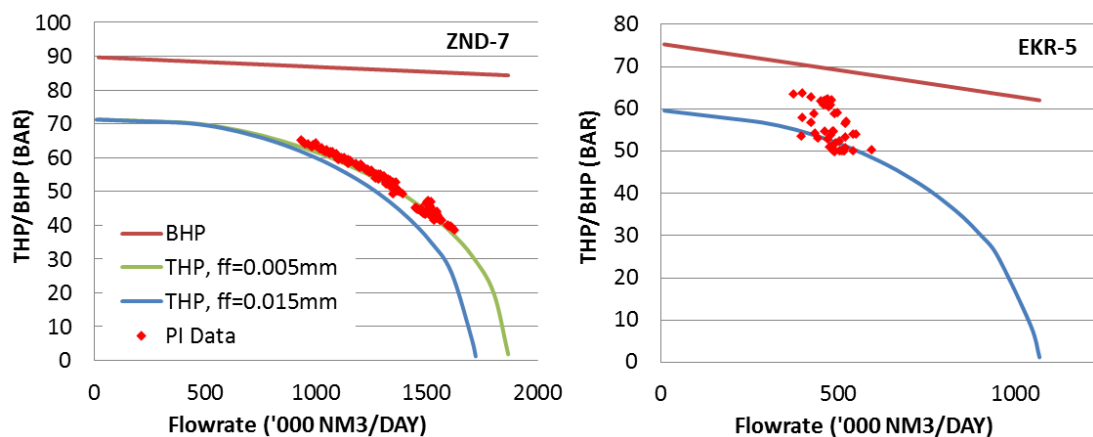


Figure 111 PQ curves for ZND-7 and EKR-5 in terms of both THP and BHP

- The current strategy for SPTG surveys is once every 5 years for each cluster (62). This is relatively infrequent to ensure that there is no drift in the history match of reservoir pressure. While any error in reservoir pressure is accounted for in the PQ matching process, any drift in this error can quite quickly result in significant capacity errors, as seen in Figure 110 or Figure 111. While more frequent surveys are one option, another would be to augment high quality downhole SPTG surveys with lower quality, but more readily available, surface THP data converted to downhole.

## **8. Recommendations for further work**

Based on the Groningen field review and the resulting history matched models and gained insights a few recommendations for further work are made in this section. These recommendations will be part of the full text of the Groningen field review and are mentioned here first because of the fit in this section. The critical gas story introduces new data which has not been taken into account in the current workflow but it results from the insights and matching results.

### **8.1. Investigate gas saturation in the Aquifer**

There may be gas beneath the gas water contacts of the Groningen field close to the critical gas saturation, with an unknown extent and distribution. The origin of this gas saturation is uncertain. It could possibly be explained by paleo contact movements or by gas staying behind during migration, or a combination or other.

Multiple disciplines have implicit proof for this gas. In the seismic inversion study the geophysicist need a gas saturation below the aquifer to obtain a model based match. Without the gas a clear contact would be visible in the seismic data, however such a contact is not at all visible.

In a petrophysical reservoir properties study in 2003 the gas saturations below the gas-water contact were already observed. These gas saturations are not in the models because the gas saturation was set to zero below the gas water contact. After reviewing the open-hole saturations which were calculated based on GFR2003 log saturation model, which remained unchanged in GFR2012, the average gas saturations for the zone below the gas-water contact were calculated and displayed for the selected wells in Figure 112. This is not a local observation, gas below the contact can be seen through the whole field with varying amounts.

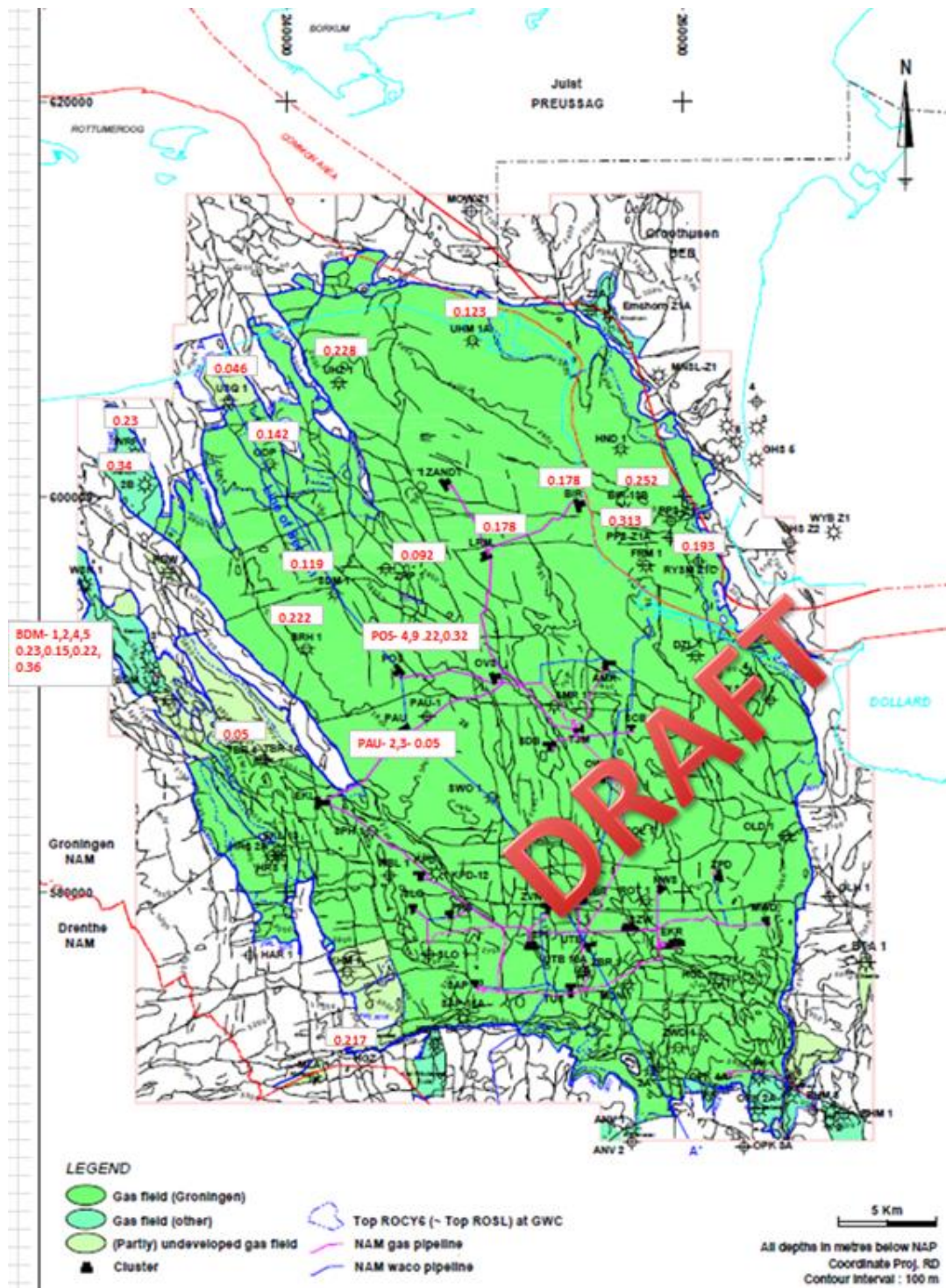
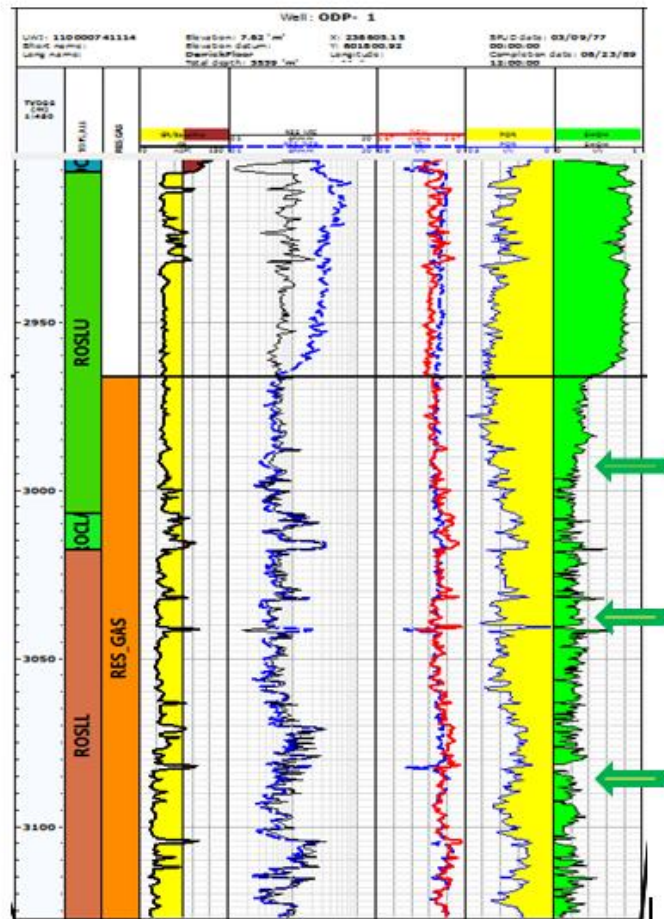


Figure 112 Average gas saturation below the gas water contact as determined by a preliminary review of the open hole logs, note that these values are based on a first investigation and should not be used in future studies.

For instance the logs of UHZ-1 clearly show a gas saturation whilst the proximal UHM-1 shows hardly any gas below the contact. An example of gas saturation below the gas water contact displayed in Figure 113.



**Figure 113 Example of miniplot with the gas saturation below the gas water contact**

There are four indications that could be explained by gas in the aquifer from a reservoir engineering perspective. Firstly, in GFR2012 the following statement was made: “*When we plot the P/Z of these clusters [referring to BIR, ZND in the North of the field], there are indications of slow gas coming into these clusters. It is not entirely clear whether it is due to transient effects, lower Slochteren being behind in pressure, or perhaps aquifer.*” This slow gas could also be explained by the gas saturation which is initially immobile. When the pressure drops below a threshold value the saturation of gas increases to a critical saturation due to expansion of the gas to become mobile, at this stage inflow of gas into the reservoir will happen. Secondly, the history matching work shows that the aquifers surrounding Groningen should not deplete in pressure. A very low permeability will prevent a pressure drop in the aquifers. Faults disconnecting the aquifers from the Groningen field will prevent a pressure drop. And the gas saturation in the aquifer could also support pressure for this region of the field.

Thirdly, when the model is initialized with a gas saturation in the aquifer, the GBV multiplier is not needed to achieve a good match in the main area of the field. Fourthly, when this gas is modelled the match of the RFT well in UHZ-1 the match improves dramatically for the underwater part of the measurements, see Figure 114. Other methods of improving this match were not successful, such as a decrease of the permeability.

Currently the history matched model does not take gas in the aquifer into account. A more detailed knowledge of where the gas is located in the aquifer will be needed to test the impact in

the entire field. A detailed microscopic pore-scale study would be needed to investigate critical gas saturation required for percolation and possible re-mobilization due to pressure depletion.

It is recommended to further investigate the residual gas saturation and the critical gas saturation to improve the history match for the pressure under the contact and with that the subsidence match. This would require a multi-disciplinary approach involving at least geosciences, petrophysics and reservoir engineering.

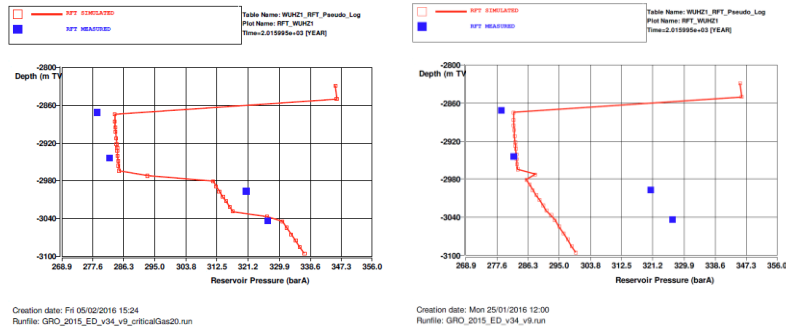


**Figure 114 comparison between two identical model with the exception of a model with 20% gas saturation in the aquifer and no GBV multiplier on the Slochteren (left) and one without gas saturation in the aquifer and with a GBV multiplier of 1.05 on the Slochteren (right).**

### 8.2. THP history matching

It is recommended to use tubing head pressures converted to bottom hole pressures as another quantifier in the history matching process. In recent years the density in SPG measurements over time has decreased significantly with respect to the 1960-1990 measurements, see Figure 115. To complement the SPG data set it is possible to use tubing head pressures. Tubing head pressure data is available since the completion of the Groningen Long Term project as of 2007. Work needs to be done on the correct conversion factor from static tubing head pressure to static bottom hole pressure and the associated uncertainty. It is recommended to continue SPG measurements since converted static tubing head pressures have a higher uncertainty.

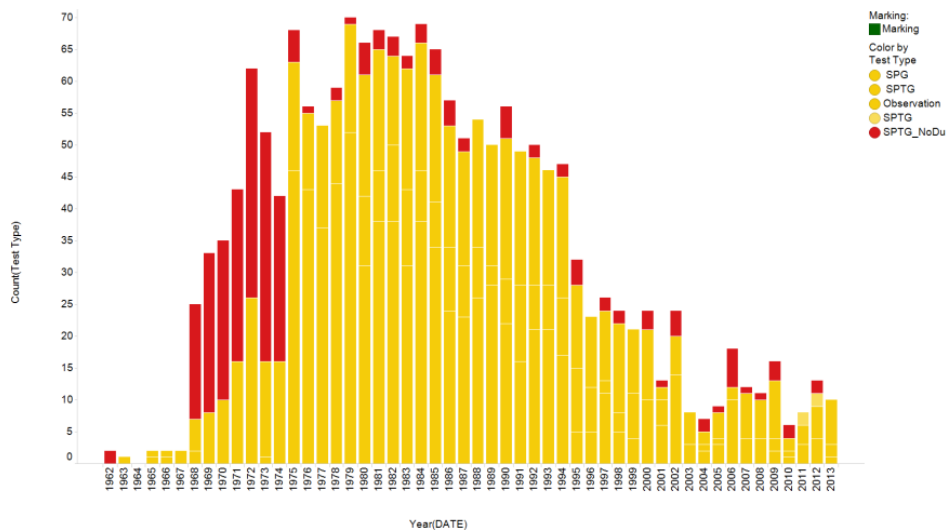


**Figure 115 1771 SPG measurements from the Groningen and peripheral fields and the annual measurement frequency showing tests without and with recorded shut-in time.**

### 8.3. Apply “closed-loop” to $C_m$ porosity relationship

The Geomechanicist applied inversion to match the geomechanical model to subsidence data.

The inversion results can be used to obtain an improved compressibility function for the subsidence proxy. Currently the polynomial reflects the low side of the acquired data and the results from the seismic inversion, see Figure 116. An update of our compressibility and porosity relationship could improve the match to subsidence.

**$C_m$  vs Porosity, 1st cycle coreplug experiments and calibration to measured subsidence**

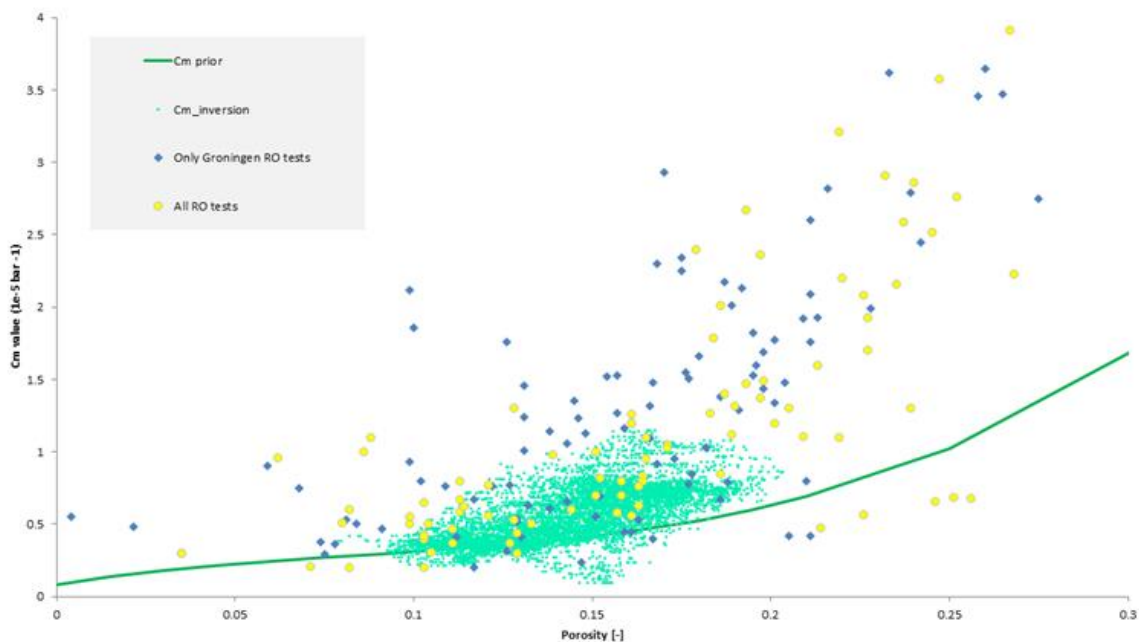


**Figure 116 Comparison between a prior polygon shown in Figure 39, and the  $C_m$  vs porosity from inversion, all compared to core data.**

### 8.4. CMI history matching

Some wells in Groningen are equipped with radioactive bullets. Periodical monitoring of the distance between these bullets will give a measure for the compaction at the location of the wellbore. These measurements are not used in the history matching yet, however it is possible to generate a proxy of compaction along a well trajectory. This compaction output can then be used to compare to all available CMI measurements as a history match quantifier.

### 8.5. Central area high permeability investigation

In the history matching workflow a permeability multiplier is needed in the central region of improve the pressure match during 1970-1990. Further studies could explain this behaviour. In the south of the field our model currently under predicts subsidence in the same region. There are ideas that could explain these early pressures, such as high permeability streaks. However the loop in this has not been closed. Work is needed to further improve the understanding of the dynamic behaviour and subsidence in the south of the field.

### 8.6. Apply Gravity survey into AHM workflow

Four gravity surveys have been taken for the Groningen field. The results of these studies can be used to explain reservoir behaviours that cause mass changes in the subsurface, such as the

depletion of gas (density reduction) or the encroachment of water (density increase), see as an example Figure 117. The current model has not been constrained to results of the gravity surveys. It is suggested to investigate the possibility of applying results of the gravity surveys in the history matching workflow, either qualitatively or quantitatively when it is possible to invert the results to dynamic properties, such as saturation changes.

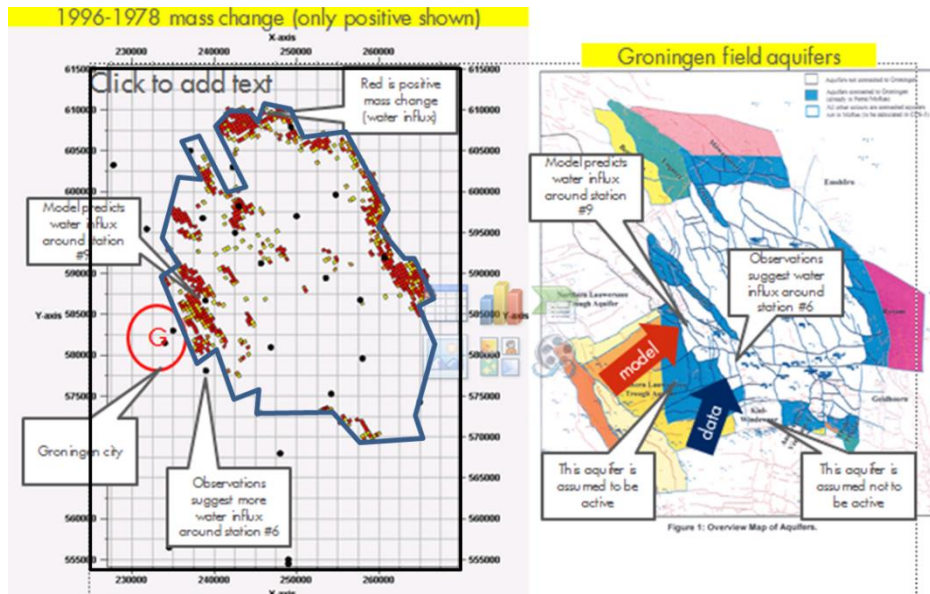


Figure 117 Gravity survey to be used in AHM

### 8.7. Additional pressure point on model area only constrained by Subsidence

Nothing but a good match to subsidence data is currently constraining the modelled pressures in the aquifers to the west of the Groningen field. A pressure data point in either the Rodewold aquifer or the Lauwerszee Through Aquifer could confirm this behaviour. The only way to obtain this pressure is to drill a dedicated well.

## References

1. **Mar-Or, A.** *The GFR2012 Integrated Production-System Model (IPSM)*. Assen : NAM b.v., 2013. EP201304231761.
2. **Evans, S and Bandiziol, D.** *Independent Review of Groningen Subsurface Modelling*. s.l. : SGS Horizon, 2013. OGC/NL/HAG/2013/NL30H-NAM-005-02.
3. **Kole, Pepijn.** *Review of the saturation height function in Groningen*. Assen : NAM, 2015. EP201510212360.
4. **Benten.** *Countercurrent Imbibition and Hysteresis Air/Mercury capillary pressure curve measurements of core samples from various Groningen wells*. Rijswijk : SIEP, 1988. RKER 88.057.
5. **Gijp, K.H. van der.** *Oil/Water Relative Permeability Measurements on Three Groningen Wells*. Assen : NAM, 1990. RKER.89.211.
6. **Berre, J.E.** *Special Core Analysis Review, Groningen Field*. Assen : NAM, 1990. NAM.18.272.
7. **Vermolen, E.** *Groningen SCAL data Review*. Assen : NAM, 2014. EP201504200615.
8. **Warnes, C.D.** *Groningen Reservoir Studies: Full Field Model Construction and History Matching Phase*. Assen : NAM, 1995.
9. **Gasunie.** *Groningen Gas Density Data at 50 bar and 15 degrees celcius flashed back to initial reservoir conditions*.
10. **Kuzan, J.D., Pozzi, A.L. and Shilkun, K.F.** *Groningen Field Special Core Analysis Phase 3*. Houston : Exxon Production Research Company, 1991. NAM20026.
11. **Masalmeh, S.K. and Jing, X.D.** *Improved Characterisation and modelling of Carbonate Reservoirs for predicting Waterflood performance*. Dubai : IPTC, 2007. IPTC 11722-PP.
12. **Scherpenisse, W.** *Gas/Water Interfacial Tension Measurements for the Groningen Gas Field (The Netherlands)*. Rijswijk : Koninklijke/Shell Exploratie en productie laboratorium, 1990. RKGR.90.048.
13. **Arnold, R.** *Advanced Rock Properties Well: Norg-4*. Rijswijk : Western Atlas International, 1991. 221-90115.
14. **de Loos, J.M.** *Groningen Gas Properties*. Assen : NAM Report no. 5890, 1975.
15. **Vos, L.L.** *Estimate of the Uncertainties of PVT properties of Groningen Gas due to Gas Compositional Variation*. Assen : NAM, 2002. NAM200203100465.
16. **Zeelenberg, J.P.W.** *PVT Analysis of Gas/Condensate reservoir fluid from well Harkstede-2*. Rijswijk : Koninklijke/Shell exploratie en productie laboratorium, 1982. RKTR82.033.
17. **Otten, G.L.** *PVT Analysis of Gas/Condensate from well Annerveen-Wildervank-1*. Rijswijk : Shell Research N.V., 1968. EP39247.
18. **Pekela, Oude.** *Accepted Reservoir Compositions/Properties OPK-RO*. s.l. : NAM, 5-Oct-1998. 1948.
19. **Beek, R van.** *Compositional Analysis and Gas-deviation factors of a gas/condensate sample from well Bedum-1, the Netherlands*. Assen : NAM, 1979. RKTR.0012.79.
20. **NAM.** *Analysis of Oldorp Gas Sample*. 20-04-1979.
21. **Vos, L.L.** *Groningen Field Review 2003 - volume 5 Dynamic Modelling and Technical Ultimate Recovery Factor*. Assen : NAM, 2003. NAM200308000870.
22. **Jaarsveld, J van.** *Groningen Field Review 2012*. Assen : EP201202215894, 2012.
23. **Büker, C.** *Groningen Field Basin Modelling*. Assen : NAM, 2002. NAM200212000141.

24. *The East Groningen Massif - Detection of an intrusive body by means of coalification.* **Kettel, D.** 203-210, The Hague : Geology en Mijnbouw, 1983, Vol. 62.
25. **Wong, T. E., Batjes, D.A.J. and De Jager, J.** *Geology of the Netherlands.* s.l. : Edita-KNAW, 2008.
26. **Stevanovic, Snezana.** *Updated Groningen Basin Model.* [Powerpoint presentation] Rijswijk : SIEP, Aug-2012. <https://sww-knowledge-epe.shell.com/teamepns/livellink.exe?func=ll&objId=56719248&objAction=browse&sort=n>.
27. *DREAM.* [Online] [Cited: 24 04 2015.] <https://wrfm-ssw-uic.sharing.shell.com/App/Dream/Home.aspx#>.
28. **Whitson, C.H. and Brule, M.R.** *Phase Behavior.* Richardson, TX : SPE, 2000. Monograph Volume 20.
29. **Trompert, R.A.** *Formation water composition of the Groningen field.* Assen : NAM, 2002. NAM200209100650.
30. **Marcelis, F.** *Well: Zeerijp-3A NAM (ZRP-3A) in-situ brine composition.* Rijswijk : SIEP, 2015. NF 2015-003.
31. **Handbook, Shell Production.** *Volume 4 Reservoir Engineering.* The Hague : Shell Internationale Petroleum Maatschappij, 1991.
32. **Vink and Hofsteenge.** *Review of Groningen CGR for BP2007 and ARPR01.01.2008.* Assen : NAM, 2007. EP200703210997.
33. **Vink.** *Review of Groningen CGR for ARPR 01.01.2007.* Assen : NAM, 2006. EP200611203328.
34. **van Oeveren, H.E.J.** *Groningen Model Update 2015: PVT Section.* Assen : NAM, 2015. EP201511214419.
35. **van Oeveren, Henk.** *Groningen Model Update 2015: PVT section.* EP201511214419.
36. **van Oeveren, Henk.** *Groningen Model Update 2015: Saturation Functions section.* EP201511214433.
37. **Vos, L.** *Basis for FWL Data in MoReS.* NAM200304001853.
38. **Schrama, J.M.** *Groningen Field Review 2015; GFR2015 "Clean-sheet" Dynamic Model.* SR.15.13479.
39. **Bierman, S.M., Kraaijeveld, F. and Bourne, S.J.** *Regularised direct inversion to compaction in the Groningen reservoir using measurements from optical levelling campaigns.* Rijswijk : SIEP, 2015.
40. *Land Subsidence Above Compacting Oil and Gas Reservoirs.* **Geertsma, J.** Journal of Petroleum Technology, Rijswijk : Koninklijke/Shell Exploratie en Productie Laboratorium, 1973, Vol. June 1973. SPE3730.
41. **Smits, R.M.M.** *Analytical Calculation of the Subsidence Above the Centre of a Disc-shaped Reservoir Underlain by a Rigid Basement.* Rijswijk : SIEP, 1987. RKGR.87.032.
42. **Geertsma, J. and van Opstal, G.** *A Numerical Technique for Predicting Subsidence above Compacting Reservoirs, based on the Nucleus of Strain Concept.* Rijswijk : Koninklijke/Shell Exploratie en Productie Laboratorium, 1972. Publication 405.
43. **van Opstal, G.** *The Effect of Base-rock rigidity on subsidence due to compaction.* Rijswijk : SIPM-EP, 1972. RKOR.0039.72.
44. **Handbook, Shell Production.** *Volume 3 and Chapter 9.* 1991.
45. **Vos, L.L.** *Groningen Field Review 2003 - volume 5 Dynamic Modelling and Technical Ultimate Recovery Factor.* Assen : NAM, 2003. NAM200308000870.

46. **Groningen Asset Leadership Team.** *Groningen Asset Reference Plan 2014.* Assen : NAM, 2014.
47. **Naus, Marc.** *Validation of the Groningen well test data and a study on the pressure behaviour in the Southwest peripheral blocks.* Assen : NAM, 2002. NAM200207003766.
48. **Schrama, J.M.** *GFR2015 "clean sheet" Model Report.* Assen : NAM, 2015. SR.15.13479.
49. **Schlumberger.** *Memory PS Platform Production Services.* www.slb.com/welltesting : Schlumberger, 2008. 07-WT163.
50. **van Oeveren, H.E.J.** *GFR2015: Saturation Functions section.* Assen : NAM, 2015. EP201511214433.
51. **Vos, L.L.** *Groningen Field RFT and FIT Data & Information on Limburg Connectivity.* Assen : NAM, 2002. NAM Doc. No: 200301000527.
52. **van Oeveren, H.E.J.** *Production Forecast Pop-up blocks Kooijpolder and Froombosch.* Assen : NAM, 2015. EP20150321994.
53. **van Kersbergen, E.** *SSM\_2a well test interpretation.* Assen : NAM, 2006. EP200612205742.
54. **Sleeboos, D.** *KWR1 -27-07-2004 Gas Well Test Evaluation Sheet.* Assen : NAM, 2004. EP200409220739.
55. **Bosman, G.** *Usquert Field - Volume Evaluation of the Rotliegend Reservoirs.* Assen : NAM, 2008. EP2008-----.
56. **Ponte, W.** *RCCN Bedum.* Assen : NAM, September 2014.
57. **NAM.** *ARPR2015 Recourse Change Control Note Midlaren.* Assen : NAM, 2015.
58. **van Heeswijk, V.** *OPK-4 Reservoir engineering handover note (RFT+reserves).* Assen : NAM, 2006.
59. **Steenbrink, J.** *Re-evaluation of static GIP of Zuidwending East (OPK-4).* Assen : NAM, 2009. EP200901205065.
60. **Tijdhof, Jan.** *Functional Specification; Well Pressure Flow data (PQ) for Pressure Calibration MORES model.*
61. **Kam, Fredrik.** *EP201309204177; Tubing coating evaluation Groningen field 2013.*
62. **Groningen.** *EP201102208019; Wells, Reservoir and Facilities Strategy.*
63. **GDP/12.** *GWC discrepancies in the Warffum field.* Assen : NAM, 1997. NAM980130038.

**Bibliographic information**

Classification	Restricted
Report Number	SR.16.
Title	Groningen Field Review 2015
Sub title	Subsurface Dynamic Modelling Report
Author(s)	Burkitov, Ulan (NAM-UPO/T/DL) Van Oeveren, Henk (NAM-UPO/T/DL) Valvatne, Per (NAM-UPO/T/DL)
Keywords	GFR2015, Groningen, Dynamic Modelling
Date of Issue	March 2016
US Export Control	Non US - Public Domain
Reviewed by	Burkitov, Ulan (NAM-UPO/T/DL) Geurtsen, Leendert (NAM-UPO/T/DL) Eikmans, Dick (GSNL-PTT/SPI) Wesenborn, Toon (NAM-UPO/T/DO)
Approved by	Jelgersma, Frank (NAM-UPO/T/DL) Pardoel, Frank (NAM-UPO/T/DG) Kelder, Oscar (NAM-UPO/T/DL) Van Boom, Ruud (NAM-UPO/T/DL) Svendsen, Grete (NAM-UPO/T/GW) Doornhof, Dirk (NAM-PTU/E/Q)
Sponsoring Company / Customer	Nederlandse Aardolie Maatschappij b.v.
Spons./Cust. Address	Schepersmaat 2, Assen, 9405TA, The Netherlands
Issuing Company	Nederlandse Aardolie Maatschappij b.v.

**Report distribution****Electronic distribution (PDF)**

*Name, Company, Ref. Ind.*

*PDF*

PT Information Services, PTT/TIKE, [PT-Information-Services@Shell.com](mailto:PT-Information-Services@Shell.com)

**Paper copy distribution**

*Name, Company, Ref. Ind.*

*No. of copies*

## Appendix 1. Model repository

The models used in the workflow are located in the network drive:

[\\europe.shell.com\tcs\ams\ui.nam\field\epe\\_re\\_08\ groningen\GFR\\_Model\\_2015\](\\europe.shell.com\tcs\ams\ui.nam\field\epe_re_08\ groningen\GFR_Model_2015\)

The folder structure has been kept simple, see Figure 118.



**Figure 118 Folder structure**

Additional information can be found in the model inventory which is kept in the file: /glb/eu/epe/field/groningen/RunInfo.xlsx. The structure in the excel file mirrors the folders on the Unix drive. The following sections will describe the content of the main folders.

### A1.1. 00\_Petrel

In the 00\_Petrel folder the rescue files exported from the static GFR2015 Petrel model are kept. The static model version used for the Winningsplan 2016 is called v2.5 is 01\_Base/150903\_GFR/150903\_GFR/150903\_GFR.bin. This work only used a base case petrel model and there are neither low and high cases available nor used in the workflow, these folders are empty, see Figure 119.

### A1.2. 10\_RPP

Under the 10\_RPP folder there are all the Reduce++ input and include files. Also the outputs of the Reduce runs are kept here. The Reduce++ runfile used for the winningsplan is called GRO\_2015v13\_Mrs\_4X\_4Y\_8uZ\_4lZ. The reduce files are also imported back into Petrel for quality control and the creation of certain maps. These exports can be found in subfolders within the 10\_RPP folder, see Figure 119.

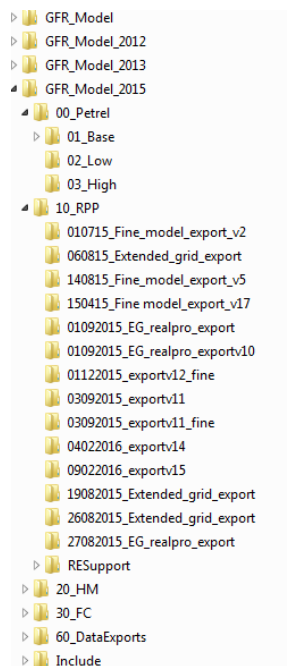


**Figure 119 GFR2015 folder structure (Petrel and Reduce ++)**

### A1.3. 20\_HM

MoReS history match models are store in folder 20\_HM. The reference model is an upscaled model with a reasonable history match.

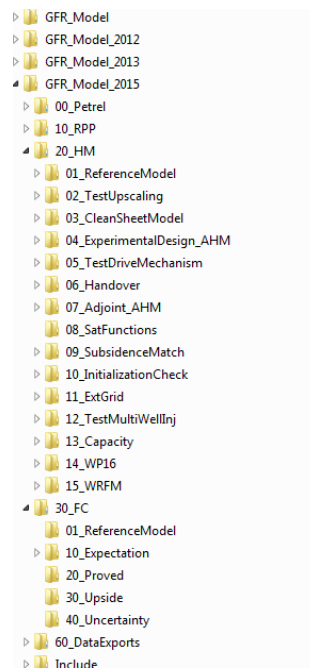


**Figure 120 GFR2015 folder structure (History Match and Forecast)**

All MoReS runs are linked by a system link to the correct reduce++ runfile. And a description of the project name, the scenario, the version and the used reduce run can be found on the top of all runs and can be used as a reference, see Figure 121 Top of all MoReS input decks showing references.

```

!-----
! Specify ProjectName
!-----
PRJDICT BEGIN

    VARIABLE STRING ProjectName Scenario Version rpp_model Syslink
    ProjectName      = "GRO_2015";
    Scenario         = "ED";
    Version          = "34_v9" ! As v8 cleandeck but now with PQ match, with upscaled well models
    rpp_model        = "GRO_2015v13_Mrs_4X_4Y_8uZ_41Z"; ! reduce model name without .run
    Syslink          = ("ln -s /glb/eu/epe/field/groningen/GFR_Model_2015/10_RPP/" + rpp_model + ".run");
    SYSTEM(Syslink) ;

PRJDICT END

PROJECT DYNASHELL $(ProjectName+"_"+Scenario+"_v"+Version+"_dys.run");
ENDPROJ

```

**Figure 121 Top of all MoReS input decks showing references**

To open the models without having to set the environment folders interactively in Dynamo the FERUNINPATH is given below. In the Unix profile `custom` file this needs to be one long line starting with “export”. Copy the following to the custom file:

```

# groningen paths for GFR_2012, GFR_2013 and GFR2015 (June 2015)
export
FERUNINPATH=%N:/glb/eu/epe/field/groningen/GFR_Model_2015/20_HM/02_TestUpscaling/%N:/glb/eu/epe/field/groningen/GFR_Model_2013/20_MoReS/00_StartRuns/%

```

N:/glb/eu/epe/field/groningen/GFR\_Model\_2013/20\_MoReS/10\_BP14/2P\_HM/%N:/glb/eu/epe/field/groningen/GFR\_Model\_2013/30\_IPSM/00\_StartRuns/%N:/glb/eu/epe/field/groningen/GFR\_Model\_2012/20\_MoReS\_HM/00\_StartRuns/%N:/glb/eu/epe/field/groningen/GFR\_Model\_2013/20\_MoReS/01\_ReferenceModel/00\_ModelEvolution\_2015/%N

### *20\_HM/01\_ReferenceModel*

Upon approval of the work this folder will have the Groningen\_ED\_v34\_v9 and the p10 and p90 models from the uncertainty analysis for ultimate recovery as reference models. The reference models will be kept evergreen by refreshing the content of this folder by the latest set of reference models.

### *20\_HM/02\_TestUpscaling*

This runs in this folder are used for testing the upscaling on the model. Details on this work can be found in the GFR2015 “CleanSheet” model report (48).

### *20\_HM/03\_CleanSheetModel*

This runs in this folder are used for testing the subsidence proxy and a cleansheet model. Details on this work can be found in the GFR2015 “CleanSheet” model report (48). MoReS clean-sheet model: use the upscaling from variogram (NX=120, NY=153, NZ=35) and “high” case faults. Removed all multipliers por, perm, faulttransmissibility and use reviewed inputs (redefined dynamic compartment, aquifer assignment, saturation functions, history matching monitor ...) with subsidence proxy calculations for the “2D” and “3D” at 31/12/2012 with the cm as function of porosity (fit function same as used for GFR2012)

### *20\_HM/04\_ExperimentalDesign\_AHM*

The 04\_ExperimentalDesign\_AHM contains the work done for the history match and uncertainty analysis. All the modelling work done for the assisted history matching and the forecast uncertainty analysis has a current size of 379 GB. Folders that are out of use have been cleaned up. The run files have been deleted but the input files are still available in case rework is required. The folder with the different models is shown in

Figure 122. Every folder consists of an input deck with a .INP extension for the dynamic model and for the experimental design exercises an input deck with a MRN\_ precursor and a .INP extension.

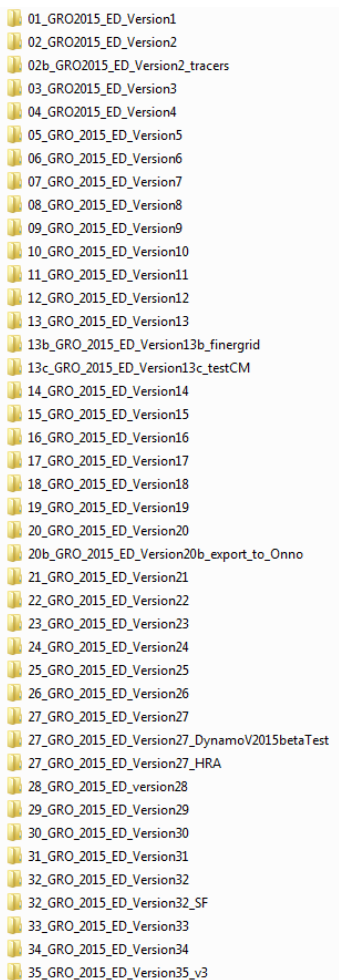


**Figure 122 Structure of the experimental design folder**

A summarized description of the runs and the changes with respect to other runs can be found in the RunInfo.xlsx document, which is stored in the following folder:

[\\europe.shell.com\tcs\ams\ui.nam\field\epe\\_re\\_08\ groningen\](\\europe.shell.com\tcs\ams\ui.nam\field\epe_re_08\ groningen\)

The text from the RunInfo for this work has also been copied for completeness, see Table 15.

**Table 15 RunInfo of the 04\_ExperimentalDesign\_AHM folder**

Folder name/Model name	Description of the model or the model versions
\\01_GRO2015_ED_Version1\GRO_2015_ED_v1.INP	Multirun Deck and corresponding worker deck for Experimental Design for the Groningen model update 2015. Includes use of mismatch functions to PNL, SPG and RFT. And updated PVT model. Varmodel is largely based on global matching parameters used for GFR2013, it does not have fault multipliers initially
\\02_GRO2015_ED_Version2\GRO_2015_ED_v2.INP	as v1; including updated saturation functions and aquifer function and importing historical data from /SurveillanceData folder.
\\02b_GRO2015_ED_Version2tracers\GRO_2015_ED_v2tracers.INP	as v2; added tracers for aquifers
\\03_GRO2015_ED_Version3\GRO_2015_ED_v3.INP	as v2; addition of fault seal factors USQ,ODP,RDW,ZWD,ZRP,BIR,Rys,Popups,TBR,SDBtoSZWtoEKR,SPHWest,KHMTrough,EKL West,Harkstede,based on GFR2012 matching parameters to match wells to SPTG, RFT and PNL data
\\04_GRO2015_ED_Version4\GRO_2015_ED_v4.INP	as v3; addition of big lift tables, OPK historical data, and additional matching parameters for HM: permeability multipliers for OPK4 and NE, and added 3 new fault: HGZ, PosPauTjm,SDM
\\05_GRO2015_ED_Version5\GRO_2015_ED_v5.INP	as v4; addition of production data up to August 2015; Attempt to match central region with porosity multiplier; added ODP permeability multiplier to control inflow of water;
\\06_GRO2015_ED_Version6\GRO_2015_ED_v6.INP	as v5; integrated subsidence workflow; no geomodel update;
\\07_GRO2015_ED_Version7\GRO_2015_ED_v7.INP	as v6;executed tornado design to investigate matching parameter sensitivity; added underwater permeability multiplier to improve subsidence match

\08_GRO2015_ED_Version8\GRO_2015_ED_v8.INP	as v7; updated base case matching parameters based on tornado, execute space filling design test, 50 runs; added local subsidence mismatch regions (NW, USQ, NE)
\09_GRO2015_ED_Version9\GRO_2015_ED_v9.INP	as v8; updated well list, aquiferv2, varmodel on tornado result, spacefilling 1000*; added more regions to the underwater multiplier (SW, EKL, KHM)
\10_GRO2015_ED_Version10\GRO_2015_ED_v10.I NP	from v9 sf, top 10 results, 1000th run and base case compared in PNL,RFT,SPTG and Subs; new aquifer function
\11_GRO2015_ED_Version11\GRO_2015_ED_v11.I NP	as v9, changed matching parameter ranges based on sf results, spacefilling 1000*
\12_GRO2015_ED_Version12\GRO_2015_ED_v12.I NP	as v9, manual investigation of impact of poissonration and cm multiplier on subsidence proxy on best run 661 of v9.
\13_GRO2015_ED_Version13\GRO_2015_ED_v13.I NP	as v9, changed to large grid including land fields; manually updated the vartable to increase first fit to new model; redefined compartments; added porosity multipliers ZWDEast and Bedum; Added underwater Permeability multipliers; Introduced Utube structure in Usquer by changeing permeability of cells in between ODP and USQ. Reorganised and added to fault groups: USQ, RDW,Annerveen, NE,BIR,RysumAquifer,KPD,TBR,SDBtoEKR,EKL, HRS, OPK4, MLA, KielWindeweer, BDM and SSM. Also created new PVT file for the new land fields; A new initialisation files with new regions; Redefinition of aquifers and renaming of aquifers; and new free water levels; Manually shifted SSM2A to be in the actual block, this was missed due to upscaling; updated well function and added new land wells with perforations; Included land fields historical data rates and measurements; Calculate subsidence at end 2014 (previously at end 2012);
\13_GRO2015_ED_Version13\GRO_2015_ED_v13b finergrid.INP	test of the v13 model with a finer grid
\13_GRO2015_ED_Version13\GRO_2015_ED_v13c _testCM.INP	manual test of the v13 model for different values of nu and cm
\14_GRO2015_ED_Version14\GRO_2015_ED_v14.I NP	incorporate learnings from SF v11, also attempt to merge HFPT deck with MoReS deck; changed matching parameter values ; reduced phi mult on opk4 and bdm; fewer underwater mults; no USQ utube; changed HRS faults; closed of SSM based on subsidence results;
\15_GRO2015_ED_Version15\GRO_2015_ED_v15.I NP	as v14, sf 300; added Phi mult for central and opk4; added faults to RDW to seal the aquifer; added faults to annerveen; changed faults near HRS; close of SSM; changed subsidence input file from v2 to v5 to incorporate poissonratio to uz,
\16_GRO2015_ED_Version16\GRO_2015_ED_v16.I NP	as v14, sf 1000; added BDM porosity multiplier; Added NE beyond the field underwater multiplier to improve subsidence and BDM match; added BIR faults; and Rys aquifer faults to try to funnel water into BIR;
\17_GRO2015_ED_Version17\GRO_2015_ED_v17.I NP	based on results v16 manual HM in versions a - s brining version l forward to next sf; added NE por mult; added KWRpor mult; added TBR4logkvmult to reduce water influx; added underwater k mult sw; added BDM faults based on Land RE's model; changed aquifer lengthh; changed underwater aquifer also land fields; PVT v05; actually fixed SSM2A; improved output plots to v14;
\18_GRO2015_ED_Version18\GRO_2015_ED_v18.I NP	as 17l sf 400
\19_GRO2015_ED_Version19\GRO_2015_ED_v19.I NP	replot best candidates of v18
\20_GRO2015_ED_Version20\GRO_2015_ED_v20.I NP	sf400 based on v18 insights; changed varmodel; more underwater aquifer reduction; base case 20b exported to Onno
\21_GRO2015_ED_Version21\GRO_2015_ED_v21.I NP	manual history matching based on sf results v20, best case v21_v2b brought forward; Added feerwerd porosity multiplier; added underwater k for BDM,SSM,WRF; additional faults for BDMS; changed BIR faults; changed RYS faults; add BDM4 faults;
\22_GRO2015_ED_Version22\GRO_2015_ED_v22.I NP	small sf based on v21; changed vartablevalues;
\23_GRO2015_ED_Version23\GRO_2015_ED_v23.I NP	big spacefilling1000, based on v21
\24_GRO2015_ED_Version24\GRO_2015_ED_v24.I NP	sf as v23, search of best model in /BestModelattemp, based on sf of v24, result v24_v2_brw2b. Changed all Porosity multipliers to GBV multipliers. This is based on erronic compressibilities results that lead back to the porosity multipliers used in GFR2013. GBV does not affect cr nor kr. Feerwerd GBV added. Added kielwindeweer permeability multiplier. Compressibility function v05.INC instead of v02.INC. Including BRW fault-set, changed RDW faults, changed NE boundary fault, added one Rysum fault, added faults west of TBR separating BDM from GRO, added KWR faults added WRF faults. Subsidence calculation v6 instead of v5.
\25_GRO2015_ED_Version25\GRO_2015_ED_v25.I NP	sf based on best model of v24, uses compressibility function v02.INC. No special underwater multiplier for BDM. Changed the layout of the Birum faults, to ensure water reaches the cluster at the right time. This needed change of some petrel faults by means of reservoir engineering faults (mFS6_Fault_1, INT6). Subsidence calculation v5 instead of v6.
\26_GRO2015_ED_Version26\GRO_2015_ED_v26.I NP	sf based on best model of v25, changed varmodel ranges. Without BIR fault setup, changed to Rysum faults.
\27_GRO2015_ED_Version27\GRO_2015_ED_v27.I NP	HRA2015 model: v27 best model attempt based on v24 sf and v25 sf (attempt different BRW settings in v1, but v1 not used) v27 is exported to Onno for subsidence work. Data updated until end of august.
\28_GRO2015_ED_Version28\GRO_2015_ED_v28.I NP	sf with varspace same as v27 but adapted ranges to scan solution space.

\29_GRO2015_ED_Version29\GRO_2015_ED_v29.I NP	manual history matching of 29 steps based on v27, improving on BDM in /01BDM, multiple versions. First step is to get rid of underwater multipliers which were deemed unphysical(v2), then getting rid of all other field wide multipliers except for ameland (v3), reduce feerwerd (v4), focus on RDW match and SAU based on subsidence match (v5), close SAU, open RDW, close LAU_AQF to improve SW aquifer subsidence match, close NE, added SPH res_fit (v6), decrease HRS size and fault, slightly adjusted LAU_AQF faults, added WRF fault(v7), split SAU_BDM4 fault and added WRF1 fit, added initial pressure correction to blocks (v8), changed LAU_AQF fault setup, closed RDW aqf from GRO main, closed WRF more (v9), new subsidence delta function v03 insted of v01, closed LAU aqf off, slightly changed WRF, close BDM and fix ODP fault, deleted unused underwater multipliers from deck (v10), fixed USQ RE fault, changed LAU aqfs again to improve subsidence match, opened TenPostwest, BRWDifferent faults and changed HRS faults added possibility to see compaction in model (v11), added RNM and BDM fault set based on land RE setting (v12), added RDWs, and hydraulic fracture for KWR1A(v13), Added Annerveen&TBR1 match by Ulan, including BDM setup based on Wuilmers model including splitting of faults, slightly changed LAU setup (v15), changed BDM fault settings (v16), SDM faults changed, improved KHM faults, renamed BDM/SAU faults, decrease LAU(v17), Applying ATLAS-deck approach to split extensive faults' seal factors (v18), extended pop-up fault group, and SDBtoEKR fault and EKL cluster fault to match SW and S wells better (v19), split EKLwest to improve KHM match (v20), slight changes to BDM seal factors (v21), changed BIR faults by splitting them(v22), low permeability in feerwerd, kolham fault to M28, open SPH-west, BMD faults lower sealing and GBV to BDM south, RDM connects to Groningen, changed GBV feerwerd and KWR (v23), fixed lower Feerwerd Perm increased its volume (ARPR volumes), KWR lower permz and slightly larger (ARPR volumes), changed EKL cluster fits, lower BRW fault, added BRW5 fit, decreased initial pressure in BDM, KWR and WRF(v25), Add fault through EKL cluster (v26) new RPP model with permz reduction according to geological model, added kv multiplier in the North to improve RFT data(v27) underwater kh multiplier in the North(v28), accidentally used RPP model without permz again, added skins for feerwerd and open hole completion, changed lauwerszee, changed pressure reduction to lower water gradient from documents, also set data of subsidence match correctly to 10-2013, and subsidence data to stable points (v29)
\30_GRO2015_ED_Version30\GRO_2015_ED_v30.I NP	as v29v29, Uncertainty analysis of the forecast tornado design
\31_GRO2015_ED_Version31\GRO_2015_ED_v31.I NP	as v30, uncertainty analysis of the forecast tornado design now with GBV taken into the design
\32_GRO2015_ED_Version32\GRO_2015_ED_v32.I NP	as v31, changed ranges in the varmodel. Applied 1 sgr matching parameter instead of 2 depending matching parameters sgr_slope, added hydraulic fractures for BRW, HM v03 and SPG match v7, submatchtable v08
\33_GRO2015_ED_Version33\GRO_2015_ED_v33.I NP	not used
\34_GRO2015_ED_Version34\GRO_2015_ED_v34.I NP	as v32, first test the impact of low permeability below the water contact to improve the RFT match, no satisfactory match obtained (v1), changed base case parameters on v32 results built in functionality to look at Groningen (excluding land) results (v2) repeated run v2 with a very fine model +3 million cells, to see the effect of this (v2_fine), attempt to set gas in the aquifer to improve RFT match in the North of the field, successful for certain gas saturations, also added switch to run standalone forecast (v3). In a separate folder SF to investigate impact of gas in the aquifer (v5). Using the correct RPP model, v12, with reduction of PERMZ again, changed base case parameters based on spacefilling results also copied information out of dynashell to MoRes(v6), further improved base case parameters based on spacefilling and manual match improvement, replaced the usquert utube for a fault that has higher sealing to gas than to water (v7). Cleaning up unused matching parameters from the deck, set KHM fault back to M28, matched WGR to historical data, applied water gradients based on reports for Bedum, Midlaren and Warffun, included historical production up to end of 2015 (v8_cleandeck), new RPP include model v13 with well indices upscaled from petrel, PQ match on wells added(v9).

#### A1.4. 30\_FC

This folder contains the forecasting work done for the GFR2015. The folder has the following structure, see Figure 120.

#### A1.5. 60\_DataExports

Data exports of GFR2015 files are all prepared and stored in this folder with the name of the subfolder indicative of the recipient of the model.

## A1.6. Include

The dynamic model include files are all stored in the folder “Include” with a few subfolders. In the input deck multiple include files are used. All include files have a .INC extension and contain data or functions used by the model. The applied include files can be found in the include folder:

[\\europe.shell.com\tcs\ams\ui.nam\field\epere\\_08\ groningen\GFR\\_Model\\_2015\Include](\\europe.shell.com\tcs\ams\ui.nam\field\epere_08\ groningen\GFR_Model_2015\Include)

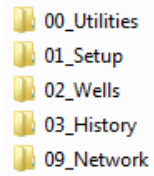


**Figure 123 Structure of the include folder**

## Appendix 2. Matching Parameter ranges

Below is the list of matching parameters as they are used for the uncertainty analysis of the ultimate recovery. During the workflow 96 matching parameters have been used. All parameters are shown in Table 16. The Base case model represents the best achieved match. The ranges are determined to be physically plausible and covering the solution space broadly not to exclude outlying possibilities.

**Table 16 Uniformly distributed parameters used for history matching and forecast uncertainty analysis**

Matching Parameter Name	Base	Low	High
<b>Gross Bulk Volume Multipliers</b>			
TenBoerGBVMult	1.00	0.95	1.05
SlochterenGBVMult	1.05	1.03	1.06
LocalGBVMultHarkstedeBlock	1.17	1.05	1.20
LocalGBVMultTBR4EKLArea	1.01	0.95	1.05
LocalNEGBVMult	1.00	0.95	1.05
LocalOPK4GBVMult	1.05	1.03	1.06
LocalBDMFieldGBVMult	1.17	1.05	1.20
LocalKWRGBVMult	1.01	0.95	1.05
LocalFeerwerdGBVMult	0.96	0.95	1.05
LocalWarffumGBVMult	1.55	1.50	1.60
LocalAnnerveenGBV	0.85	0.70	1.00
<b>Permeability Multipliers</b>			
TenBoerlog_k_h_Mult	-1.5	-3	0
TenBoerlog_k_v_Mult	-1.5	-3	0
RSLUlog_k_h_Mult	-0.05	-0.11	0.11
Het_SLUlog_k_v_Mult	-2	-4	0
Amelandlog_k_v_Mult	-2.6	-3	-2
RSLlog_k_h_Mult	0	-1	0
RSLlog_k_v_Mult	0	-3	0
Het_SLLlog_k_v_Mult	-2	-4	0
Central_k_h_Mult	0.4	0.2	0.8
KWRLog_k_Mult	-5	-1.5	-0.5
Feerwerd_k_Mult	-1.93	-3	-1.6
UtubeUSQ_k_mult	-1.6	-2	-1.2
<b>Fault Seal Factors</b>			
LogFaultSeal_USQ	-0.45	-0.5	-0.0
LogFaultSeal_USQgas	-1.9	-3	-1
LogFaultSeal_ODP	-0.5	-1.4	-0.4
LogFaultSeal_RWD	-0.1	-1	0
LogFaultSeal_RWDS	-0.5	-2.5	0
LogFaultSeal_RDWN	-2.0	-3.5	0
LogFaultSeal_ZWDNorth	-0.1	-0.2	0
LogFaultSeal_NE	-1	-3	-1
LogFaultSeal_BIRSouth	-0.6	-2	0
LogFaultSeal_RysAquifer	-1.9	-3	-1
LogFaultSeal_RysAquiferNorth	0	-1	0
LogFaultSeal_BRW5	-1.55	-1.6	0
LogFaultSeal_AMR_LRM	-0.5	-1	0
LogFaultSeal_PopUps	-0.0	-1	0
LogFaultSeal_TBR	-1.4	-2	-1
LogFaultSeal_SDBtoSZWtoEKR	-6	-1	0
LogFaultSeal_SPHWest	-0.8	-2	0
LogFaultSeal_KHMTrough	-2.5	-3	-1
LogFaultSeal_EKLWest	-2.0	-3	-1
LogFaultSeal_Harkstede	-2.5	-3	-2
LogFaultSealHRS_AQF	-1.5	-3	0

LogFaultSeal_HGZ	-1.0	-1.3	-0.9
LogFaultSeal_PosPauTjm	-0.2	-0.4	0
LogFaultSeal_SDM	-1.8	-2	0
LogFaultSeal_OPK4	-0.72	-1	-0.5
LogFaultSeal_MLA	-1.2	-1.4	-1
LogFaultSeal_BDM	-7.5	-10	-5
LogFaultSeal_BDM3	-2.9	-3.3	-2.5
LogFaultSeal_BDM4	-1.7	-2	-1
LogFaultSeal_BDM5	-2.65	-2.8	0
LogFaultSeal_BDM5b	-3	-3.5	-2.5
LogFaultSeal_RNM1	-3.3	-4	-2.5
LogFaultSeal_LAU	-1.5	-4.0	-1
LogFaultSeal_WRF	-4	-4	-2
LogFaultSeal_WRF1	-0	-1	-0
LogFaultSeal_ANV	-3	-4	-2
LogFaultSeal_ANV_N	-0.3	-1	0
Hydraulic Fractures			
Skin_KWR1A	-4	-4	-2
Skin_SSM2A	-1.6	-4	0
Skin_SSM4	-4	-4	0
Aquifers			
AqfLength_AnnerveenVeendam	1500	0	3000
AqfLength_Lauwersee1	6000	4000	8000
AqfLength_Lauwersee2	1000	0	2000
AqfLength_Lauwersee3	1000	0	2000
AqfLength_Lauwersee4	3000	0	6000
AqfLength_Moewensteert	35000	10000	35898
AqfLength_Rodewolt	10000	0	30000
AqfLength_Rysum	5000	0	30321
AqfLength_Usquert	1000	0	15000
AqfVsc	1	0.5	1.5
Saturation functions			
Sw_unc	0	-0.13	0.13
density_gas	197	195	199
density_water	1172	1171	1173
Srg_slope	0.0035	0	0.007
Krw_at_Srg	0.13	0.03	0.23
Krg_at_Swc	0.86	0.83	0.89
Nw	3	2.7	4.0
Ng	1.7	1.4	2.0
PhiMin	0.06	0.02	0.08
Free Water Levels			
FWL_Groningen_Central	2992	2972	3012
FWL_Groningen_E	2972	2970	2972
FWL_Groningen_NE	2978	2970	2982
FWL_Groningen_NW	2984	2982	2984
FWL_Groningen_SE	3006	3003	3015
FWL_Groningen_SW	2995	2984	3006
FWL_Gron_Emskanaal	2996	2993	2997
FWL_Gron_Ellerhuizen	2997	2970	3040
FWL_Gron_Harkstede	3016	3014	3018
FWL_Gron_Hoogezand	3030	3016	3030
FWL_Gron_Oldorp	2967	2966	2988
FWL_Gron_Zuidwending	3017	3006	3028
Subsidence data			
Compress_rock_mult	0.58	0.50	0.6
PoissonRatio	0.25	0.24	0.26